DYNAMICS OF TERRESTRIAL WATER BUDGET OVER AMAZON AND MISSISSIPPI BASINS USING SATELLITE DATA

by

Marzieh Azarderakhsh

A dissertation submitted to the Graduate Faculty in Civil Engineering in partial fulfillment of the Requirements of the degree of Doctor of Philosophy.

The City University of New York

2012

© 2012

MARZIEH AZARDERAKHSH

All Rights Reserved

This manuscript has been read and accepted for the Graduate Faculty in Engineering in satisfaction of the dissertation requirement for the degree of the Doctor of Philosophy.

Date	Dr. Reza Khanbilvardi Professor of Civil Engineering and Chair of Examining Committee
Date	Dean. Mumtaz K. Kassir Executive Officer

Supervisory Committee:

Dr. Amir Aghakouchak

Dr. Reza Khanbilvardi

Dr. Shayesteh Mahani

Dr. William B. Rossow

Dr. Marouane Temimi

THE CITY UNIVERSITY OF NEW YORK

ABSTRACT

DYNAMICS OF TERRESTRIAL WATER BUDGET OVER AMAZON AND MISSISSIPPI BASINS USING SATELLITE DATA

by

Marzieh Azarderakhsh

Advisors: Drs. William B. Rossow and Reza Khanbilvardi

The components of the water budget and their spatio-temporal variability are diagnosed using monthly-averaged remote sensing-based data products over the Amazon and Mississippi basins. These two large basins are divided into 14 and 12 smaller sub-basins (SB) respectively, and for each of these SBs, fresh water discharge is estimated from the water balance equation using satellite data products. The purpose of this study is to learn how to apply satellite data with global coverage over the large tropical and mid-latitude regions; therefore several combinations of remote sensing estimates including total water storage changes, precipitation and evapotranspiration. The results are compared to gauge-based measurements and the best spatio-temporal agreement between estimated and observed runoff is within 1 mm/d for the combination of precipitation from the GPCP and the Montana evapotranspiration product. Mean annual precipitation, evapotranspiration and runoff for the whole basin are estimated to be 6.1, 2.2 and 3.0

mm/d respectively but also show large spatial and temporal variations at SB scale. Using the most consistent data combination, the seasonal dynamics of the water budget within the Amazon system are examined. Agreement between satellite based and in-situ runoff is improved when lag-times between SBs are accounted (RMSE from 0.98 to 0.61 mm/d). We estimate these lag times based on satellite inferred inundation extents. The results reveal not only variations of the basin forcing but also the complex response of the inter-connected SB water budgets. Inter-annual and inter-sub basin variation of the water components are investigated and show large anomalies in north-western and eastern downstream SBs; aggregate behavior of the whole Amazon is more complex than can be represented by a simple integral of the forcing over the whole river system. Moreover, the same approach proposed for Amazon for estimating the runoff is applied to large Mississippi basin. The results show that applying the proposed method can improve the estimation of runoff using the satellite information. Some limitations exist in this basin that will decrease the reliability of the results, as the uncertainty of estimated runoff is greater that the magnitude of runoff due to existence of dams, and smaller precipitation rate compared to Amazon basin.

ACKNOWLEDGEMENTS

Foremost, I would like to express my sincere gratitude to my advisor Prof. William Rossow for the continuous support of my Ph.D study and research, for his patience, motivation, enthusiasm, and immense knowledge. His guidance helped me in all the time of research and writing of this thesis. I could not have imagined having a better advisor and mentor for my Ph.D study. I specially want to thank Prof. Reza Khanbilvardi for all his support during these four years. He introduced me to the interesting research activities in NOAA-CREST and helped me to choose my path. Besides my advisors, I would like to thank the rest of my thesis committee: Prof. Mahani, Dr. Aghakouchak and Dr. Temimi for their encouragement, insightful comments, and hard questions. I am indebted to Remote Sensing of Climate group lab director, Cindy Pearl, for patiently helping me in technical issues, my fellow lab-mates, Narges Shahroudi and Dr. Ademe Mekonnen for providing a stimulating and fun environment in which to learn and grow. My sincere thanks also go to Dr. Fabrice Papa, for his kind assistance and wise advice. Besides my research, Dr. Shakila Merchant, helped me to practice to present my findings professionally in fruitful seminars and conferences. Last but not the least, I would like to thank my family: my husband, colleague and best friend Hamidreza Norouzi, and my parents by supporting me spiritually throughout my life; to them I dedicate this dissertation; and my son, Ryan for being joy and fun in my life.

Table of Content

LIST OF FIGURES:

LIST OF TABLES

CHAPTER 1: INTRODUCTION

The hydrological cycle can be considered as an integrated product of the climate and of the bio-geophysical attributes of the surface. It exerts an influence on climate and the interaction between the atmospheric moisture, rainfall and runoff. A better understanding of the components of the hydrological cycle in a basin and their variability will depend on the knowledge of physical mechanisms related to regional and large scale atmospheric-oceanic-biospheric forcing, that at the end modulate temporal and spatial variability of the hydrometeorology of the basin.

To better understand the dynamics of each water budget component in hydrologic and climate studies, several ground measurements are available. However, these observations are very limited spatially and temporally. Even the operation costs of these instruments are very expensive, and political decisions may affect the availability and continual coverage of the observations. Remote sensing measurements could be an alternative in variety of geophysical, hydrological, and hydroclimate studies. Several applications have been attempted. Several water budget components have been estimated using these remotely-sensed observations. More detail of some these components are presented throughout this dissertation. Some significant differences are seen in some these products. In validation and evaluation of these products, only the estimates are compared with other estimates. However, most of them are not being tested and

evaluated based on other water budget components in specific applications. For instance, precipitation estimates are evaluated with other estimates and ground observations. One should note that the main objective of production of these products is to use them in particular application. Therefore, the estimated precipitation has to be consistent with other water budget components. It means their interannual variations should be consistent with other components.

This research study aims to examine and use different components of the water budget together, and find the potentials and limitations of these products. Large tropical basin of Amazon will be studied first, and then the technique will be expanded to large mid-latitude Mississippi basin. These large basins have great impact in climate and hyroclimate regimes.

The Amazon River system is the single, largest source of freshwater on Earth and its flow regime is subject to interannual and long-term variability represented as large variations in downstream hydrographs. The flow regime of this river system is relatively un-impacted by humans, and is subject to interannual and long-term variability in tropical precipitation, that ultimately is translated into large variations in downstream hydrographs. This river drains an area of 6.2×10^6 km2 and discharges an average of 6300 km^3 of water to the Atlantic Ocean annually.

The Mississippi River is the largest river system in North America. This river rises in western Minnesota and meanders slowly southwards for 2,320 miles (3,730 km)[5] to the Mississippi River Delta at the Gulf of Mexico. The Mississippi ranks fourth longest and tenth largest among the world's rivers. The Mississippi River drainage

basin is the world's second largest, draining 4.76 million square kilometers, including tributaries from thirty-two U.S. states and two Canadian provinces. The flow regime of this basin is highly impacted by human, and therefore its underground and surface water storage variability is different than natural systems. Its climate also different than Amazon, exhibiting large seasonal variation in ET than P and R.

The dissertation is structured as follows. In this chapter, some detail introduction about water budget studies using remote sensing information is presented. The previous studies are highlighted and difficulties in these applications are mentioned. Chapter 2 introduces available remote sensing and gauge data sets that will be used in this study. In Chapter 3, Water budget analysis and comparison of different data sets over Amazon basin is explained. Then the lagging method is introduced in this study to make the gridded data consistent with the pointed integrated discharge at mouth of the Amazon basin.

Chapter 4. Explains the analysis of the seasonal and inter-annual dynamics of water over Amazon after applying lagging to the discharge data. To test the application of the proposed method in another large-scale basin, Mississippi basin, which is also instrumented well with discharge gauges, is studied in Chapter 5. Chapter 6 compares the results over the two basins and concludes explaining the capability of the proposed method and its limitations to study the dynamics and climatology of the other large-scale basins.

1.1. Background and Literature review

The water balance of the Amazon basin is difficult to assess due to the lack of basic hydro-meteorological observational data systematically collected over time and space. Using existing data some attempts have been made to quantify the water fluxes involved on this cycle. Earlier studies have used river discharge data, rainfall and upper air information from few stations in Amazon, while present studies use data from more comprehensive but still sparse networks of rainfall and river data, as well as some data from flux towers from some field experiments implemented in Amazon since the 1990's. The availability of gridded rainfall and evaporation data sets and the global reanalysis has allowed basin scale studies on the components of the hydrological cycle, even though some uncertainties have been ascribed to these estimates. Some studies have been done on water budget components in different large basins, i.e. Amazon, Mississippi, Sacramento using land surface, atmosphere and coupled land-atmosphere water balance approaches [*Marengo*, 2005; *Rodell et al*., 2004a; *Sheffield et al*., 2009b; *Syed et al*., 2009; *Syed et al*., 2005; *Zeng*, 1999]. The outcome of these studies shows that it is possible to estimate closure with some accuracy limit (error, uncertainty) at annual and interannual scales using remote sensing or reanalysis data of precipitation, evaporation and water storage changes. Figure 1-1 applies atmospheric balance and estimates different component (p, precipitation, E, evapotranspiration; C, vertical moisture convergence; R, runoff) using rain gauge data and NCEP/NCAR reanalysis for

evaporation and moisture convergence and total precipitable water. Of course the unclosure of 50% implies the failure of reanalysis to estimate moisture convergence term over the Amazon basin [*Marengo*, 2005]. Figure 1-2 and 1-3 are also other applications of coupling land-atmosphere since there was no evapotranspiration data available to use in land surface balance although they have not neglected land water storage changes by using GRACE measurements. Yirdaw et al [*Yirdaw et al*., 2008] (figure 1-2) used atmospheric balance approach to estimate storage changes over Canada and compared the Storage values with GRACE measurements, concluding better ability of GRACE in detecting total water storage. [*Syed et al*., 2005; *Yirdaw et al*., 2008] estimated the closure of the annual water budget within 23% and 27% for the Amazon and Mississippi basins respectively seeing a phase lag in interannual cycle and underestimation in low flows (Figure 1-3a.b). With releasing global evaporation estimates, [*Sheffield et al*., 2009b] used this new information in land water balance for the first time and saw high uncertainties in estimate due to mainly remote sensing based precipitation data (figure 1-4). Therefore, further study is necessary to reduce these uncertainties by analyzing different data in order to be able to integrate the components of the hydrological cycle of the basins.

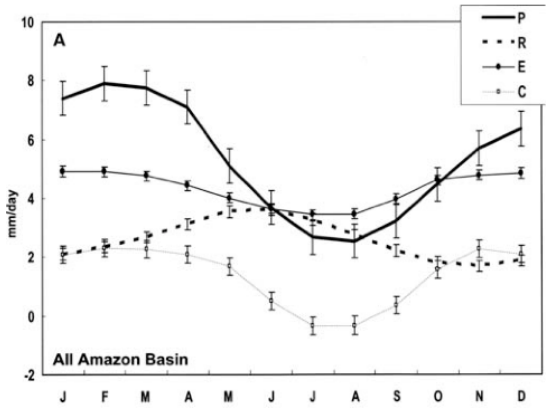

Figure 1- 1:surface water budget components of Amazon from the study of [*Marengo*, 2005]

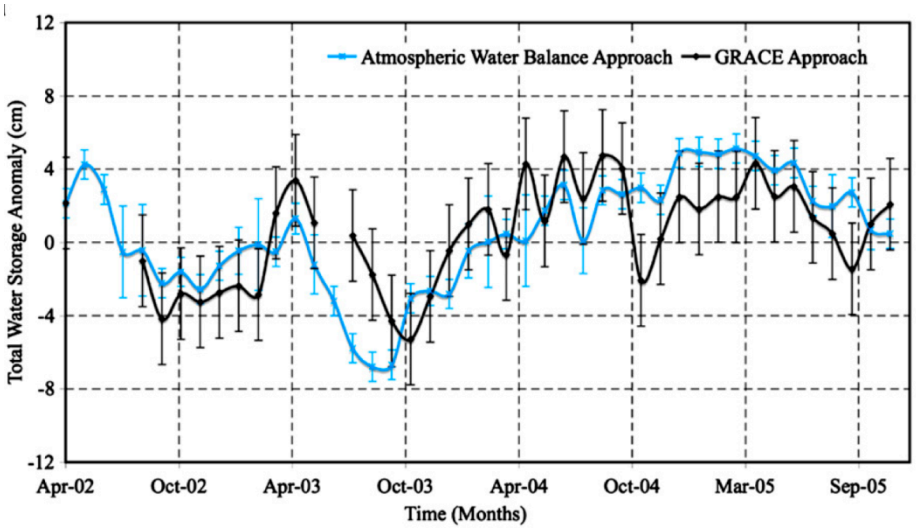

Figure 1- 2:Total water storage estimates for the Canadian Prairie from GRACE and atmospheric water balance [*Yirdaw et al.*, 2008]

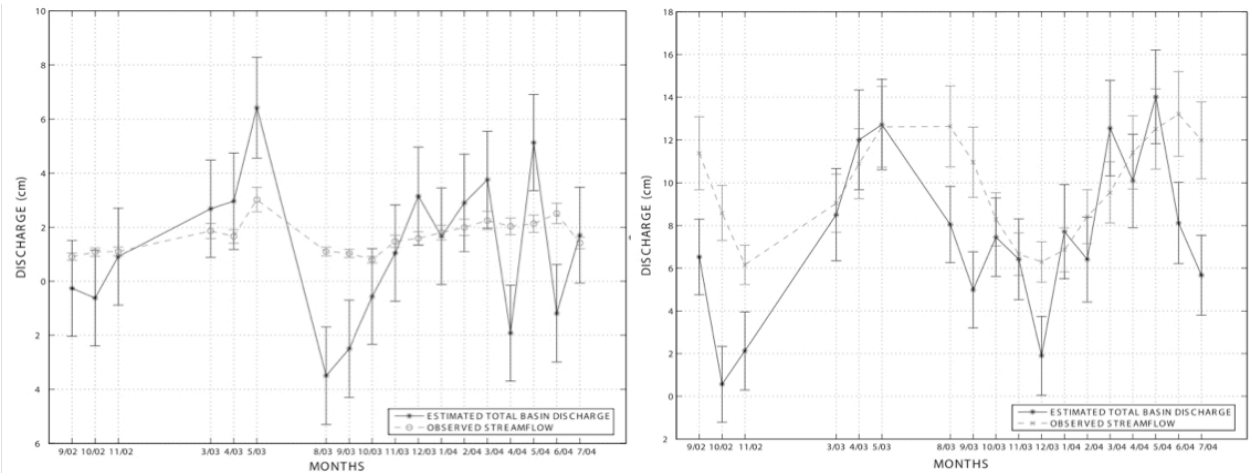

Figure 1- 3:Estimated and observed runoff for the a) Mississippi b) Amazon Basin [*Syed et al.*, 2005]

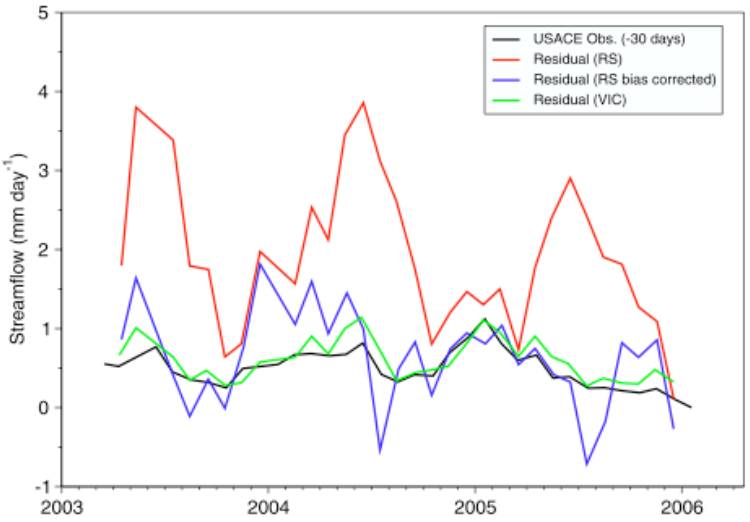

Figure 1- 4: Estimated vs. observed discharge for the Mississippi basin [*Sheffield et al.*, 2009a]

1.1.1. Studies on the components of the hydrological cycle for the Amazon Basin

Since the middle 1970's, large-scale water budget studies have been conducted in the Amazon region. [*Salati et al*., 1978] attempted to quantify the components of the water balance and moisture recycling by combining observations of few upper-air stations in the Brazilian Amazonia, as well as water balance models. Later studies using a variety of observational data sets varying from radiosondes to the global reanalysis, or a combination of both as well as climate models [*Costa and Foley*, 1999; *Eltahir and Bras*, 1994; *Labraga et al*., 2000; *Leopoldo et al*., 1987; *Marengo*, 2005; *Matsuyama*, 1992; *J Roads et al*., 2002; *Salati et al*., 1978; *Vorosmarty et al*., 1996; *Zeng*, 1999]; have quantified estimates of the hydrological cycle, its variability in various time scales, and the impacts of remote atmospheric or local forcing on the variability of the components of the water balance, as well as the closure of the water balance for the entire Amazon.

The lack of continuous precipitation and evaporation measurements across the entire Basin and of measurements of river discharge along the Amazon River main channel and its main tributaries has forced many scientists to use indirect methods for determining the water balance for the region. Estimates of the components of the water cycle have been derived using gridded moisture and circulation data from the global reanalysis produced by some meteorological centers in the US and Europe. The National Centers for Environmental Prediction (NCEP), National Aeronautics and Space Administration/Data Assimilation Office (NASA/DAO) and the European Center for Medium Range Weather Forecast (ECMWF) have carried out retrospective analysis (re-

analyses) projects over the last decade using a single model and data assimilation to represent climate evolution since as early as World War II. Several papers can be referred as using the ECMWF, NASA/DAO and NCEP reanalysis for hydrological studies in Amazonia:[*A. K. Betts*, 2007; *Costa and Foley*, 1999; *Dai and Trenberth*, 2002; *Marengo*, 2005; *Rao et al*., 1996; *J Roads et al*., 2002; *Zeng*, 1999] among others. These reanalysis can highlight characteristic features of the circulation and water balance. However, while data assimilation should in principle provide for a description of the water flux field, there are no guarantees that this description will be superior to that obtained from objective analysis and radiosonde observations alone, especially over continental regions, and there is a need for the level of uncertainty to be identified in the measurement or estimation of the components of the water budget. Results of previous studies of the annual water budget in Amazonia are listed in Table 1-1. Main differences in results are due to the different areas considered for the basin that translate to different discharge and derived runoff: different precipitation networks and methods of assessment (mostly based on gridded rainfall data or from rain gauge distributed irregularly in the basin); the methods used to determine the annual water balance, where evapotranspiration ET is estimated as residual of precipitation P and discharge R; and the length of the time series used, spanning sometimes different periods. Assuming that P = ET + R does not guarantee accurate estimates of the possible role of the tropical forest on recycling of moisture for rainfall.

Table 1- 1: The annual water budget of the Amazon basin. P indicates precipitation, ET indicates Evapotranspiration, and R indicates streamflow, all in mm y-1. In here the water balance equation ET = P – R is used. P and R are measured, and ET is obtained as a residual. Marengo (2005) used the water balance equation that considers the non-closure of the Amazon Basin (Sources: Salati, 1987; Marengo and Nobre, 2001; Marengo, 2005).

Study	P	ET	R
Baumgartner and Reichel (1975)	2170	1185	985
Molion (1975)	2379	1146	1233
Villa Nova et al. (1976)	2000	1080	920
Jordan and Heuveldop (1981)	3664	1905	1759
DMET (1978)	2207	1452	755
Leopoldo et al. (1982)	2089	1542	541
Leopold (2000)	2076	1676	400
Franken and Leopoldo (1984)	2510	1641	869
Marques et al. (1980)	2328	1260	1068
Shuttleworth (1988)	2636	992	1320
Vörösmarty et al. (1989)	2260	1250	1010
Russell and Miller (1989)	2010	1620	380
Nizhizawa and Koike (1992)	2300	1451	849
Matsuyama (1992)	2153	1139	849
Marengo et al. (1994)	2888	1616	1272
Zeng (1999)	2044	1679	1095
Costa and Foley (2000)	2166	1366	1800
Marengo (2005)	2117	1570	1050

- **Recycling**

The ratio of how much precipitation comes from a local region through evaporation versus how much comes from advection into the region is known as the "recycling" ratio, and has been matter of studies since the middle 1970's by [*Molion*, 1990; *Salati et al.*, 1978; *Salati et al.*, 1979]. This ratio varies substantially from lower values in winter to higher values in summer, when the large-scale transports diminish in importance. Precipitation recycling is the contribution of evaporation within a region to precipitation in that same region. The recycling rate is a diagnostic measure of the potential for interactions between land surface hydrology and regional climate. The recycling of local evaporation and precipitation by the forest accounts for a sizable

portion of the regional water budget, and as large areas of the basin is sensible to active deforestation there is grave concern about how such land surface disruptions may affect the water cycle in the tropics.[*Brubaker et al.*, 1993; *Eltahir and Bras*, 1994], and [*Costa and Foley*, 1999] among others have estimated an annual mean recycle rate of about 20% to 35% that are lower than the previous estimates by Molion. Climate variability and change, due both to natural climate variability or to the increase in the concentration of greenhouse gases in the atmosphere of anthropogenic origin may have a potential to accelerate the hydrologic cycle, and the Amazon region would be one of the most affected regions. Changes in land use patterns due to deforestation might produce changes in latent heat and can ultimately influence precipitation in two important ways. First, an increase in evapotranspiration adds moisture to the atmosphere, which, if recycled, directly increases rainfall. Second, increased latent heating associated with this increased rainfall can drive an intensified circulation (e.g., the Hadley cell), resulting in changes to the moisture convergence from remote sources. Land-use practices, such as agriculture or urbanization often disrupt the supply of fresh water through changes in the surface water balance and the partitioning of precipitation into evapotranspiration, runoff and groundwater flow. This basin constitutes a source of atmospheric moisture for other regions in the continent. Moisture transport in and out of the Amazon basin has also been studied since the 1990's using a variety of upper air and global reanalysis data sets as well as from climate model simulations.

- **River discharge**

  The Amazon River drains an area of 6.2×10^6 km2 and discharges an average of

about 200,000 m3 sec-1 to the Atlantic Ocean annually. In Brazil, the term *Amazonia Legal* refers to the Brazilian Amazonia, with an extension of about 5.8 x 10^6 km^2. Figure 1-5 shows the boundaries of the Amazon basin and its tributaries. The different estimates of areas of the Amazon Basin by different authors have led to a wide range of computed discharges of the Amazon River during the last 25 years generating uncertainty in the estimation of this quantity. Most of these estimates are based on the records of the Amazon in Obidos (Table 1-2) peak in May-July. The discharge measured at Obidos (01° 55'S, 55° 28'W) of 175,000 m^3sec^{-1} (or 2.5 mm/d) does not represent the real conditions of water that reaches the mouth of the Amazon, since it does not include the waters of the Xingu and Tocantins Rivers [*Marengo*, 2005]. [*Perry et al.*, 1996] listed the Amazon with a mean flow rate of 193,000 m^3sec^{-1} based on 11 different sources. Perry's estimates are about 10% lower than the estimate of Amazon mouth flow of 217,000 m^3 sec^{-1} from [*Dai and Trenberth*, 2002]. The observed R at the mouth of the Amazon River has been estimated as 2.9 mm/day (or 210,000 m3 sec-1) for a basin area of 6.11 x 10^6 km^2, and this represents the combination of the Amazon River discharges at Obidos with the discharges of the Xingu and Tocantins Rivers [*Marengo*, 2005]. This value was obtained after corrections by the Brazilian National Water Authority ANA, Obidos, the farthest downstream station available for the Amazon, is 750 km away from the mouth.

Figure 1- 5. Amazon River and its main tributaries.

As indicated before, the mean discharge at the Obidos gauging station is 175,000 m^3 s^{-1} (or 2.5 mm/d), while the corrected values at the mouth of the Amazon reach 210,000 m^3s^{-1} (or 2.9 mm/d). [*J Roads et al.*, 2002; *Zeng*, 1999] have used 2.9 and 3.1 mm/d, respectively for R for the Amazon basin, which are closer to the corrected value. In comparison, the discharge derived from the GRDC (Global Runoff Data Centre) for Amazonia is 3.2 mm/d ([*Fekete et al.*, 1999; *J Roads et al.*, 2002]). Table 1-3 lists estimated runoff for the mentioned studies.

Table 1-1: Comparison of different studies on annual runoff for the Amazon basin

Study	mm/d	Study	mm/d
Leopold (1962)	.69	Marengo et al. (1994)	2.99
UNESCO(1971)	2.25	Perry et al. (1996)	2.51
Nace(1972)	2.61	Costa and Foley (1998)	2.41
UNESCO(1974)	2.58	Zeng (1999)	3.05
Baumgartner and Reichel(1975)	2.34	Leopoldo (2000 a)	2.38
Villa Nova et al. (1976)	2.34	Leopoldo (2000b)	2.98
Miliman and Meade (1983)	2.97	Roads et al. (2002)	3.33
Oki et al. (1992)	2.3	Dai and Trenberth (2002)	3.23
Matsuyama (1992)	2.3	Marengo (2005a)	2.605
Russel and Miller (1990)	2.98	Marengo (2005b)	3.12
Vorosmarty et al. (1989)	2.53	Sausen et al. (1994)	2.98

- **Evaporation (Evapotranspiration)**

Estimates of evaporation (or evapotranspiration) ET from [*Marengo*, 2005] derived from the NCEP reanalysis latent heat reach an annual mean of near 4.3 mm/d, which is close to the 4.6 mm/d obtained by [*Zeng*, 1999] derived from the NASA/DAO reanalysis. Estimates based on the ECMWF reanalysis of ET are ~3.7 mm/d, [*Marengo*, 2005] whereas Rocha, 2004 ([*Marengo*, 2006]) obtained ET as high as 4.0 mm/d from a different period of the ECMWF reanalysis. These estimates are larger than some estimates reported on the literature: 3.1 mm/d derived using the climatologic model by Molin ([*Marengo*, 2006]), 3.2 mm/d using Penman method [*Marengo*, 2006], 3.5 mm/d

using atmospheric water balance (Marques et al., 1980), 3.1 mm/d using ECMWF data [*Eltahir and Bras*, 1994; *Matsuyama*, 1992], 3.3 mm/d using Thronthwaithe method [*Vorosmarty et al*., 1996; *Willmott et al*., 1985], and 3.8 mm/d using the NCEP/NCAR reanalysis after correction by [*Costa and Foley*, 1999]. Direct measurements of ET are not made continuously all around the basin, and the estimation of this quantity requires high frequency surface observations. Few ET measurements derived from latent heat observations during the Anglo Brazilian Climate Observational Study (ABRACOS) field experiment during the 1990's (Rocha, 1996 [*Marengo*, 2006]) yield 3.9 mm/d in the eastern Amazon region and 3.7 mm/d at sites in central and southern regions, and few available observations at Manaus in the central Amazon section (Shuttleworth, 1988 [*Marengo*, 2006]) exhibit values of 3.6 mm/d. The mean of these observations (~3.8 mm day $^{-1}$) suggests that the ET derived from the global reanalysis in general may be about 10% higher than observations. [*Bruno et al*., 2006] used frequency-domain reflectometry to make continuous, high-resolution measurements for 22 months of the soil moisture to a depth of 10 m in the Amazonian rain forest at Santarem, where the mean annual precipitation is over 1900 mm. In the 4-month dry season, ET is about 150 mm/month, much higher than precipitation, which averages about 60 mm mo $^{-1}$. Thus, the forest at the site was well adapted to the normal cycle of wet and dry seasons; and the dry season had only a small effect on ET, because of the very large available water storage.

- **Precipitation and integrated moisture convergence**

An all-Amazonia rainfall P estimate based on rain gauge stations (Marengo 2005) is 5.8 mm/d that is closer to various other estimates obtained from several other studies

based on rainfall stations or gridded data from CMAP (Climate Prediction Center Merged Analysis Precipitation), CRU (Climate Research Unit), and GPCP (Global Precipitation Climatology Project). These CRU, CMAP and GPCP derived rainfall as well as the station rainfall values are lower than the [*T C Chen et al*., 2001] value of 8.1 mm/d derived from the GHCN (Global Historical Climatology Network), and from the NCEP/NCAR reanalysis derived rainfall. The value derived from GPCP by [*J Roads et al*., 2002] reaches 5.1 mm/d. The integrated moisture convergence C value derived from [*Marengo*, 2005] using the NCEP/NCAR are 1.4 mm day $^{-1}$ and is closer to the 1.3 mm/d derived by [*Rao et al*., 1996] using 5 years of the ECMWF reanalysis (1985-88). [*Zeng*, 1999] obtained 0.8 mm/d from NASA/ DAO reanalysis for 1985-93. Furthermore, this value is lower than that derived by [*Eltahir and Bras*, 1994] using 6 years of the ECMWF analyses (1985-90) of approximately 1.9 mm/d, and much smaller than the 2.5 mm/d obtained by [*Costa and Foley*, 1999]. [*J Roads et al*., 2002] derived 1.7 mm/d from the NCEP reanalysis during 1988-99. Taking in consideration all the components of the water balance, Figure 1-6 a-d shows a summary of the estimates of the balance from four different studies for the entire Amazon basin. These studies use either the global reanalysis, or a combination of the reanalysis and observations (gridded or station data). In the long–term, the basin average precipitation P assumed to be balanced by ET+R, and C=R. The studies from [*Zeng*, 1999] using the NASA-GEOS reanalysis and [*Costa and Foley*, 1999] using the NCEP reanalysis shows high difference between C and R, is much smaller in Costa and Foley, suggesting a source of water inside the basin "which could have been artificially added during the reanalysis process, as suggested by the authors".

The studies by [*J Roads et al*., 2002] and [*Marengo*, 2005] use a combination of NCEP reanalysis and observations (gridded or station data). Since the NCEP reanalysis parameterized processes like precipitation, evaporation, and runoff are likely to have larger errors than obserced and it, therefore, makes some sense to compare the reanalysis precipitation, evaporation, moisture convergence, and runoff with the currently "observed" precipitation, runoff, and evaporation. In these two studies, C is different from R in almost 50% indicating a large imbalance[*Marengo*, 2006]. This imbalance may be due to large uncertainties detected in the evaporation and moisture convergence. It is also because of the uncertainties in the observation of precipitation, sampling problems and interpolation techniques. The same can be said for streamflow estimates, since these estimates vary almost 10% among them considering the measurements at the gauging site or at the mouth of the River. In fact, for the Amazon region, the errors can be almost as large as the associated runoff. In addition, error in the moisture convergence is almost as large as the error in the evaporation. There are some differences in P, which depend on the source of data (reanalyzes, observations) and the period of time considered. The imbalance is larger over the southern Amazon region than over the northern region and it also exhibits interannual variability.

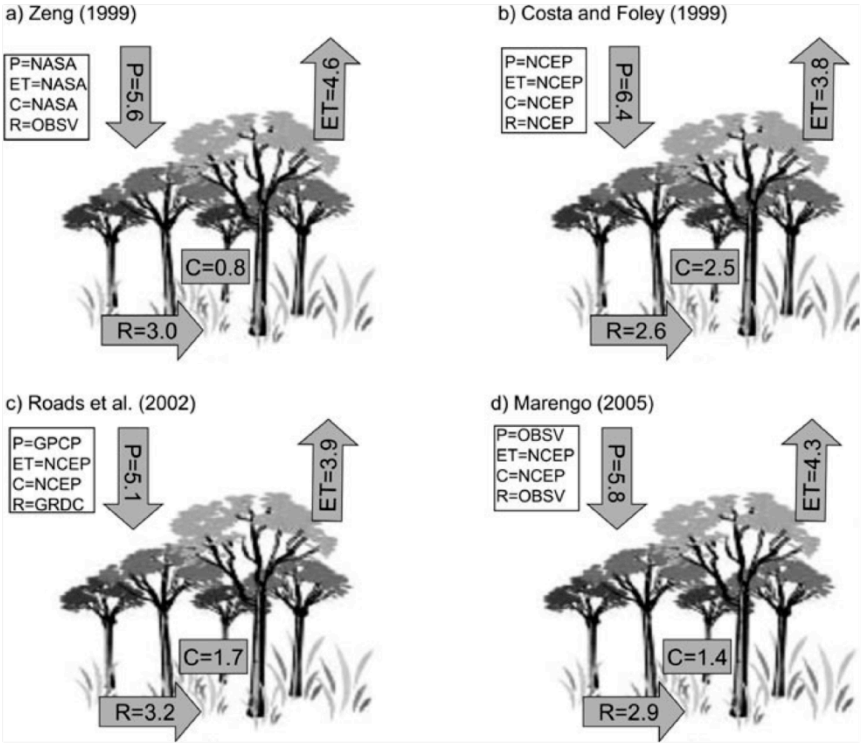

Figure 1- 6:Summary of long-term mean annual water balance components in Amazonia from four studies: (a) Zeng (1999), for the period 1985-93 using estimates of P, ET, and C derived from the NASA-GEOS reanalysis, and R from the Amazon River observations at the Obidos gauging site. (b) Costa and Foley (1999), for the period 1976-96 using estimates of P, ET, R and C from the NCEP reanalysis; (c) Roads et al. (2002), for 1988-99 using estimates of E and C derived from NCEP reanalysis, P from the GPCP gridded observed data sets and R from the GRDC gridded observed data sets; (d) Marengo(2005), for 1970-99 using estimates of E and C derived from the NCEP reanalysis, R from the Amazon River observations at the Obidos gauging site, and P derived from station data. Units are in mm/d.

- **Seasonal cycle of the components of the water balance**

The seasonal cycle of the water balance terms show some differences between the northern and southern sections of the basin ([*Costa and Foley*, 1999; *Marengo*, 2004; 2005; *Zeng*, 1999]). The Amazon River flows exhibit a peak from May to June while basin wide integrated precipitation peak is in between later summer and early fall. This

lag reflects the time needed for surface runoff to travel to the river mouth [*Dai and Trenberth*, 2002; *Marengo*, 2005; *Papa et al*., 2010a]. Recent studies of the Amazon basin hydrological cycle have identified major differences in the water balance characteristics and variability between the northern and southern parts of the basin. The seasonality of the water balance components and the ET/P ratio varies across the basin. In the entire Amazonia, Figure 1-7a shows that there is seasonality in the R and P, where the R peaks between 3–4 months after the peak of P. The largest error bars (determined as percentage of the standard deviation) are shown for rainfall over the entire Amazon basin (Figure 1-7a). Figure 1-7b and c show the differences in the annual cycle of P, C and ET in both sections of the basin. The ET/P ratio, in reality, represents a fraction of continental precipitation. This term shows a larger seasonal cycle in southern Amazonia when compared to northern Amazonia, being the largest ET/P in the dry season while the amplitude of change in ET/P is very low in northern Amazonia. The ET/P ratio is sometimes referred as recycling rate, but in reality is more an indicator of the continental evaporation rate. The ET/P ratio of the dry season is larger than that of the rainy season (Figure 1-7c) and this is especially true in Southern Amazonia, indicating that the role of evaporation (and evapotranspiration) on the water cycle is relatively more important in the dry season than in the rainy season. In general, in present climates, the Amazon basin can be considered as a sink of moisture (P>ET).

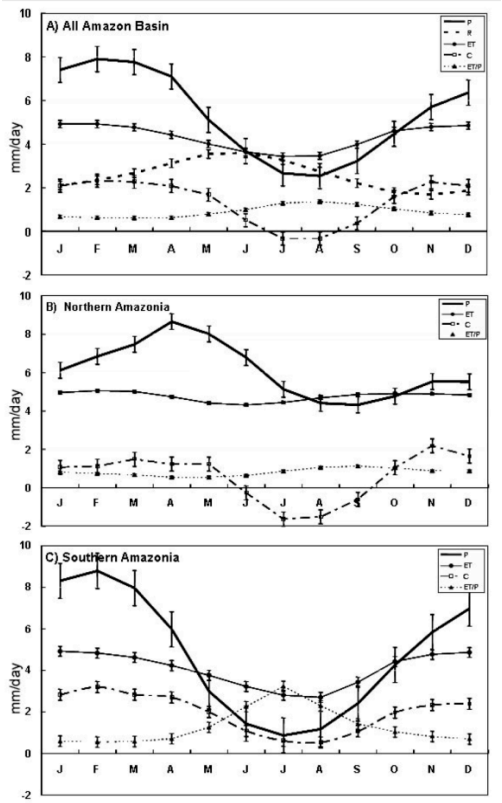

Figure 1- 7: Seasonal variability of the components of the water budget in the Amazon Basin for the period 1970/71–1998/1999. (a) All Amazonia, (b) Northern Amazonia, and (c) Southern Amazonia. P precipitation (from observations), R river runoff (corrected values at the Óbidos gauge site), E evaporation, and C vertically integrated moisture convergence (both derived from the NCEP/NCAR reanalysis). On this figure, +C convergence and -C divergence. No R is available for northern and southern Amazonia. Units are in mm/day. Each vertical bar represents the absolute error from the mean (Marengo, 2005).

1.1.2. Uncertainties in the hydrology variability and water budget

There are large sections of the basin with no data. Therefore, there is a considerable uncertainty on the annual rainfall and its seasonal variability in Amazon. Gridded rainfall and global reanalysis data sets have helped in solving the problems on regional coverage, but they may have added even more uncertainties since there are

differences among the data sets. The choice of rainfall data sets (e.g. CRU, CMAP, GHCN, GPCP, Legates, and others) has an impact in the results of the water budget, and uncertainties in these results may be due to the sensitivity of the rainfall estimates to the rainfall network density, and to numerical interpolation techniques or the use of satellite data to fill gaps in time and space across. This becomes apparent in Table 1-3. The lack of continuous upper-air observations in the basin makes difficult the estimation of moisture transport into and out of the basin, and we have to rely on model data for this such as the reanalysis. Furthermore, the use of uncorrected discharge underestimates the freshwater discharge, and thus adds to the uncertainty in closing the water budget. In addition, there are very few observations of evaporation in some isolated points in the basin. The national hydro meteorological networks are deteriorating, and there are fewer stations in 2000 compared to the 1970's. Although global evaporation estimates is released using remote sensing data and Penman-Monteith or empirical approaches they present evaporation with high difference from each other and few evaluation work has been done for them [*Jimenez et al*., 2010].

Table 1- 2: Water budget 1970-99 for the entire Amazon basin. P is derived from several data sources: Global Historical Climatology Network (GHCN), Xie and Arkin (CMAP), NCEP, Legates-Wilmott (LW), Climate Research Unit (CRU) and from observations derived by Marengo (2004). E and C are derived from the NCEP/NCAR reanalysis, and R is the corrected runoff from historical discharge records of the Amazon River at Obidos. Units are in mm/ d. +C denotes moisture convergence. (Source: Marengo, 2005)

Component	GHCN	CMAP	GPCP	NCEP	LW	CRU	Marengo (2005)
P	8.6	5.6	5.2	6.4	5.9	6.0	5.8
E	4.3	4.3	4.3	4.3	4.3	4.3	4.3
R	2.9	2.9	2.9	2.9	2.9	2.9	2.9
C	1.4	1.4	1.4	1.4	1.4	1.4	1.4
P-E	4.3	1.3	0.9	2.1	1.6	1.6	1.5
P-E-C	+2.9	-0.1	-0.5	+0.7	+0.2	+0.3	+0.1

The components of the hydrological budgets namely; precipitation (P), evaporation (E), runoff (R) and total water storage (S) vary significantly owing to the dynamic geophysical and climatic processes. Water and energy cycles are time-varying 3D quantities. Taking vertical averages in the atmosphere and subsurface, we focus here on 2D horizontal variations. By using time means (monthly), we focus on seasonal to interannual timescales. Consider first the atmospheric water mass conservation equation (see figure 1-8).

$$\frac{\partial W}{\partial t} = E - P - \nabla Q \qquad (1)$$

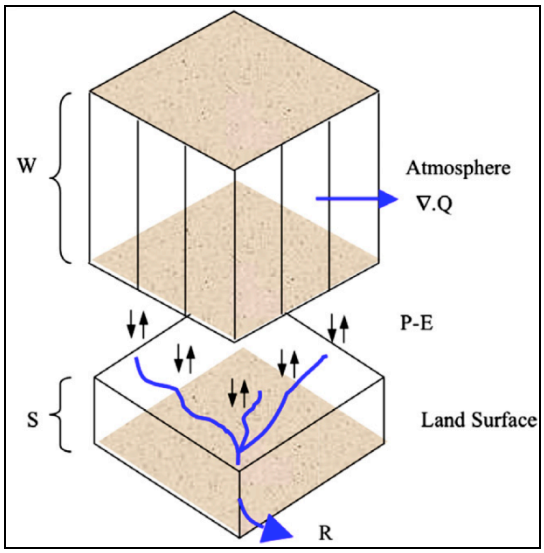

Figure 1- 8:Schematic diagram of land and atmospheric water budget

Where *W is* the vertically (pressure weighted) integrated specific humidity or precipitable water, and ∇.Q is the divergence or net outflow of water vapor across the side of the atmospheric column, and Q is the vertically integrated flux of specific humidity derived from wind and humidity measurements. The next equation (Eq. (2)) is

therefore, employed to compute the divergence in spherical coordinates [*Yirdaw et al*., 2008].

$$\nabla \cdot Q = \frac{1}{R_e \cos\phi}\left(\frac{\partial Q_\lambda}{\partial \lambda} + \frac{\partial (Q_\phi \cos\phi}{\partial \phi}\right) \qquad (2)$$

The vertically integrated vapor fluxes Q_λ and Q_ϕ are estimated according to Equations (3), (4)[*Yirdaw et al*., 2008].

$$Q_\lambda = -\frac{1}{\rho g}\int_{ps}^{pt} qu\,dp \qquad (3)$$

$$Q_\phi = -\frac{1}{\rho g}\int_{ps}^{pt} qv\,dp \qquad (4)$$

Q_λ and Q_ϕ are the east-west and north-south components of vapor flux in (m^2/s), respectively, whilst q the specific humidity (kg/kg), u and v the zonal and meridian components of wind velocity (m/s), p the pressure (kg/m/s^2), g the gravitational constant (9.81 m/s^2) and q is the density of water (1000 kg/m^3). Re is the mean Earth radius taken as $6.3712 \cdot 10^6$ m, λ and ϕ are, respectively, the longitude and latitude in radians. The negative sign arises due to the fact that the hydrostatic assumption was used when converting from elevation to pressure. The limits of integration are the surface pressure (p_s) and the pressure at the top of the atmosphere (p_t).

The water content in the atmosphere, W (m) is computed using Equation (5) as expressed below:

$$W = \frac{1}{\rho g}\int_{ps}^{pt} q^*\,dp \qquad (5)$$

In order to try the balance in the equation 2, we can use different dataset for P,ET and δW/δt from the introduced products in chapter 3. In fact, although water vapor flux might be (reasonably) well determined in reanalysis, the spatial derivative of the flux, flux convergence, may be very poor and this is known to be true especially in the tropics. Therefore, this approach is not accurate enough for water balance.

From a land surface perspective, water balance:

$$\frac{\partial S}{\partial t} = P - ET - \nabla .F \qquad (6)$$

Where S (m) represents the total water content of a land surface column, and ∇.F (m/s) signifies the lateral transport of water (runoff).

Atmospheric water balance has been tried using available reanalysis, observation data [*Syed et al*., 2005]. The monthly $\frac{\partial W}{\partial t}$, in that study, term was taken as the difference between the basin average values on day 15 of each month. The monthly divQ was computed by summing the daily basin-average values. [*Rodell et al*., 2004a] have used alternative methods for summing daily hydrologic fluxes that are also consistent with the timing of GRACE data collection by computing average of two-month observation as follows:

$$S_{2,1} - S_{1,1} = \sum_{1,1}^{2,1} P - \sum_{1,1}^{2,1} ET - \sum_{1,1}^{2,1} R \qquad (7)$$

where S, P, ET, and R are daily values, and the first index represents the GRACE observation period and the second the day number of that period. To be exact, the terms

on the right side of (8) would be integrals of instantaneous values. At continental drainage basin scales, it can safely be assumed that surface drainage divides coincide with groundwater flow divides, so that inputs and outputs of groundwater can be ignored. Rewriting (7) for all pairs of days in the two observation periods and summing all equations yields:

$$[S_{2,1} + \ldots + S_{2,N}] - [S_{1,1} + \ldots + S_{1,N}] = \left[\sum_{1,1}^{2,1} P + \ldots + \sum_{1,N}^{2,N} P\right] - \left[\sum_{1,1}^{2,1} ET + \ldots + \sum_{1,N}^{2,N} ET\right] - \left[\sum_{1,1}^{2,1} R + \ldots + \sum_{1,N}^{2,N} R\right] \quad (8)$$

where N is the number of days per observation period. After dividing both sides by N and simplifying, (9) becomes

$$\Delta\overline{S} = \frac{1}{N}\sum_{n=1}^{N}\sum_{d=D1+n}^{D2+n-1}(P_d - ET_d - R_d) \quad (9)$$

where $\Delta\overline{S}$ is the change in average water storage, n is the day number of the observation period, d is the date, and D is the first date of the observation period denoted by the index 1 or 2. Equivalently,

$$\Delta\overline{S} = \overline{P} - \overline{ET} - \overline{R} \quad (10)$$

where $\overline{P}$, $\overline{ET}$, and $\overline{Q}$ are running-mean flux accumulations. For example, given two consecutive 30-day periods (60 days), ET is the average 30-day evapotranspiration total over all 31 sets of 30 consecutive days within the 60 days. Rewriting the equation (11) for the evaporation as a residual will give:

$$\overline{R} = \overline{P} - \overline{ET} - \Delta\overline{S} \quad (11)$$

The right side of the equation (11) can be estimated from remote sensing data for

precipitation, evaporation and storage terms. The impact of different summation methods on estimated ET is studied and will be discussed in chapter 6. The relative uncertainty in a monthly estimate of R as a quadrature sum of errors in each component can be computed [*Wahr et al*., 2004]:

$$\upsilon_{\overline{R}} = \frac{\sqrt{\upsilon^2_{\overline{P}}\overline{P}^2 + \upsilon^2_{\overline{ET}}\overline{ET}^2 + \upsilon^2_{\overline{\Delta S}}\overline{\Delta S}^2}}{\overline{P} - \overline{ET} - \overline{\Delta S}} \qquad (12)$$

Each term represents the absolute error of a component. This formula is true if all of the variables have Gaussian distribution and are independent of each other. Since P has non-Gaussian distribution and also ET might depend on P on its retrieval, the proposed formula will under-estimate the uncertainties.

We propose to use this method to estimate runoff and then compare it with the observation data. Uncertainties of some of the precipitation, storage data have been done and are available by their authors; but the challenging term is evaporation.

Also, remind the atmospheric balance from equation (1) in terms of precipitable water and moisture convergence and coupled with land water balance:

$$\frac{\partial W}{\partial t} + \nabla . Q = ET - P = -R - \frac{\partial S}{\partial t} \qquad (13)$$

Since relative uncertainties of the monthly precipitable water and divergence terms (using reanalysis data as the only source) are not well characterized at present, this can be done to compute their difference from equation 13 and compare the estimates of this method with reanalysis data.

1.1.3. Past terrestrial water storage studies

The total terrestrial water storage is the sum of the amounts of snow, soil moisture, surface and sub-surface water; changes in storage can now be estimated using the Gravity Recovery and Climate Experiment (GRACE) measurements [*Wahr et al.*, 2004]. Discharge or surface water volume changes have been estimated using altimetry data and height-volume ratios [*D Alsdorf et al.*, 2007; *D E Alsdorf*, 2003; *D E Alsdorf and Lettenmaier*, 2003; *Frappart et al.*, 2008], surface water areas using multi-satellite techniques [*Papa et al.*, 2008b; *Papa et al.*, 2010b; *Prigent et al.*, 2007] and "direct" gauge measurements [*Villar et al.*, 2009,a].

TWS refers to the total amount of water integrated over depth, stored in a catchment (Becker et al 2011). It is comprised of surface waters, soil moisture and underground waters. In some regions, TWS also includes snow. Variation of TWS with time *t* is linked to accumulated precipitation (P), evapotranspiration (ET), surface and subsurface runoff (R) within a given area or basin, through the water balance, written as equation 10.

There are very few studies have dealt with the analysis of the past storage in large basins especially Amazon basin. In one the recent studies Becker et al (2011) investigated the past storage of Amazon basin for more than three decades. They proposed a method that combines GRACE-based TWS spatial patterns with multi-decadal-long in situ river level records, to reconstruct past 2-D TWS over a river basin. The observed timing and regional distribution of the TWSR over the Amazonian Basin during "30 years showed no long-term trend in their study and confirmed the dominant influence of ENSO and

PDO (Becker et al, 2011).

1.2. Problem statement

Understanding, characterizing and predicting the distribution and cycling of terrestrial waters are major goals of hydrology and climate research as well as major requirements for water resource management. However, seasonal and interannual variations of the water budget terms, including precipitation, evapotranspiration, runoff and surface and sub-surface water storage are still not well know, at least at regional to global scale [*Bullock and Acreman*, 2003].

The Amazon basin is of special interest because, with the largest drainage area in the world, covering about 40% of South America, variations of water exchange within its watershed can have a strong regional effects on the global and tropical climate systems: the Amazon in its own right makes the largest contribution (15% -20%) to the total fresh water discharge to the global ocean. Changes in atmospheric circulation and precipitation can translate into changes in the discharge to the ocean and affect the atmospheric moisture transport from the Amazon region to adjacent regions [*Marengo*, 2005; *Villar et al.*, 2009,b]. Moreover, the internal dynamics of this drainage system are complicated by the fact that the watershed extends both north and south of the equator and, as a result, has different wet and dry seasons. In the last few years, the Amazon basin has experienced severe extreme events. For instance, in 2005 a drought that affected the western parts of the basin during the dry season was blamed for lower water levels in the central and eastern parts of the river system, leading to serious effects on human activity

and the biosphere and also to higher sea surface temperature (SST) in the tropical North Atlantic by up to two degrees Celsius [*Marengo et al.*, 2008; *Zeng et al.*, 2008b]. In 2009, the Amazon basin was hit by large and severe flooding with the central and northern regions experiencing their worst flooding in over half a century [*J L Chen et al.*, 2010].

Large-scale water-budget studies for the Amazon basin have been conducted since the late 1970s using different techniques and atmospheric datasets from radiosondes to global reanalysis [*Costa and Foley*, 1997; *Leopoldo et al.*, 1987; *J Roads et al.*, 2002; *Vorosmarty et al.*, 1996]. All these studies have emphasized the importance of remote forcing on the variations of the components of the local water budget. Several studies also investigated the closure of the terrestrial water budget and/or estimated river discharge is the Amazon using in-situ gauge streamflow measurements together with a simple water balance equation method (R=P-ET-ΔS, where R=runoff, P=precipitation, ET=evapotranspiration and ΔS=total water storage changes), or hydrological modeling forced with meteorological observations, numerical simulations or a combination of remote sensing-based water height estimates and height-discharge relations [*Coe et al.*, 2002; *Decharme et al.*, 2008]. Some studies have tried to close the water budget at basin scale or estimate discharge from the water balance equation and have reported large uncertainties in the estimated discharge due to the errors in the individual components of the water budget [*Coe et al.*, 2002; *Getirana*, 2010; *Marengo*, 2005; *Sheffield et al.*, 2009a; *Syed et al.*, 2009; *Syed et al.*, 2005; *Tang et al.*, 2010; *Zeng*, 1999]. Because of the need to calibrate hydrological models to specific locations and their relatively low spatial resolution (global or continental or large basin scales), applying these models to

the Amazon basin with complicated rainfall and evapotranspiration variability is not always accurate [*Getirana*, 2010].

There are different studies on quantifying the water budget components, each trying different methodologies. However they give different estimates that makes the accurate estimate of these components difficult and will be discussed here.

Gauge-based estimates of global and continental freshwater discharge are limited by geographic and political restrictions due to institutional and economic constraints. Existing regional networks are usually located in more affluent countries. Quantifying freshwater discharge into the ocean is further complicated by the fact that existing stream gauges are often located far from the point of inflow into the ocean [*Dai and Trenberth*, 2002]. Also because of technological, economical and institutional limitations, the number of gauging stations and access to river discharge information have been declining since 1980 [*Bjerklie et al.*, 2003]. Even though discharge is an accurate measure of integrated terrestrial runoff, it typically offers little information about the spatial distribution of runoff within a watershed unless the river basins are highly instrumented. Therefore, disaggregation of the river runoff is necessary when spatially distributed runoff information is needed especially in large and complex basins like Amazon [*Fekete et al.*, 2002].

The surface and upper-air observational network in the Amazon region is very sparse and, by itself, cannot provide the comprehensive meteorological information needed to accurately drive numerical models to estimate water-balance. Therefore, imperfect models or products from data assimilation or gridded reanalyses and rainfall

data sets have been used to make these estimates [*Marengo*, 2005]. The National Centers for Environmental Prediction (NCEP), European Centre for Medium Range Weather Forecasts (ECMWF) and National Aeronautics and Space Administration/Data Assimilation Office (NASA/DAO), NASA/Goddard Earth Observation System (GEOS) have developed analysis projects using different global atmospheric models with land-surface physics and data assimilation to characterize features of the terrestrial water budget. However, the level of uncertainty in these estimates of the components of the water budget is not yet well determined [*Marengo*, 2005; *J Roads et al.*, 2002].

Evapotranspiration is estimated from reanalysis models including NCEP-DOE AMIP-II reanalysis (R-2) [*Kanamitsu et al.*, 2002], European Centre for Medium-Range Forecasts (ECMWF), ERA-40 [*Gibson et al.*, 1997], from the empirical Penman-Monteith formulation [*Monteith*, 1965] using different remote sensing data to quantify net surface radiation and surface meteorology inputs [*Mu et al.*, 2007; *Sheffield et al.*, 2010], using model simulations with radiation and meteorological forcing, or employing a water balance residual approach (P-R-ΔS) [*Rodell et al.*, 2004a; *Sheffield et al.*, 2010]. [*Jimenez et al.*, 2010] compared twelve different global evapotranspiration estimates and showed that the largest absolute disagreements occur over tropical rainforest regions. These differences may be due to difference in inputs to the estimates, such as the net radiation, vegetation and meteorological data, or to differences in physics, including whether evaporation from intercepted precipitation or open water on the surface is accounted for.

As discussed up to now, most of the studies in water budget component analysis use one or few component of the water budget. Evaluation of these products in a bigger picture together to derive useful hydro climate output is not very common. Besides, in few available studies high uncertainties are seen, which makes it difficult to rely on them because they mostly have lack of enough hydrological consideration. The travel time for water after reaching the ground until reaches to the mouth of the river is not fully investigated, as many other source of information about the slope, channel shape, the vegetation, and etc are needed to find the "travel time". This issue is more highlighted when the only source of information is remotely sensed measurements. These observations have coarse resolution that detecting the mentioned details is not feasible. Therefore, finding the consistent product that provide reliable water balance along with consideration of lag time between precipitation time and discharge at the end of the basin is critical especially for large basins such as Amazon, Congo, or Mississippi.

In this dissertation, we aim to have a better understanding of the water budget components using satellite observations. The sequence and objectives of this research study are summarized in next chapter.

1.3. Objectives and Sequence

Answering to the question of how far we are from integrating the surface water budget is the goal of this research and answering this question at the end of this dissertation over the two most challenging large sub basins (Amazon and Mississippi) in terms of variability and balance is attempted. The main objective of this research study is

to understand dynamics of the water budget components using different available products. Several analyses will be conducted to evaluate the seasonal variation of water budget components in large basins and sub-basin scale. One of the major novelties of this research study would be conducting and integrating water budget component analysis in sub-basin scale that allows capturing the spatial variability of the components variability in large basins. Runoff is estimated based on the residual of the other components and is evaluated with ground observations. The effect of the lag time between precipitation and runoff will be considered based on a novel approach that uses the water extent or inundation product. Moreover, this research study aims to analyze the interannual variation of water budget components and investigate the dynamics of the water budget components. Besides the past storage of the Amazon basin is constructed based on the water balance analysis in this research study. At the end, the proposed method in Amazon basin is tested in Mississippi basin, which is another large basin to study the capabilities and limitations of remote sensing data. The sequence of this research study will be explained in following sub-sections. After the introduction in this chapter, the data sets used in this research are introduced. Then, chapter 3, 4, and 5 will present the main part of this research. Chapter 6, at the end, will summarize the findings and discuss the potential prospective studies.

1.3.1 WATER BUDGET COMPONENT ANALYSIS WITHIN THE AMAZON BASIN USING SATELLITE DATA (CHAPTER 3)

The components of the Amazon water budget and their spatio-temporal variability are diagnosed using monthly-averaged remote sensing-based data products for the period

September 2002-December 2006. Seasonal variation of each water budget component is studied and differences and similarities are investigated. The large Amazon basin is divided into 14 smaller watersheds, and for each of these SBs, fresh water discharge is estimated from the water balance equation using satellite data products. Several combinations of remote sensing estimates including total water storage changes, precipitation and evapotranspiration are examined. The results are compared to gauge-based measurements and the best spatio-temporal agreement between estimated and observed. There is lag time between precipitation time and runoff due to large scale of the basin. Using the most consistent data combination, we estimate the lag times based on satellite inferred inundation extents.

1.3.2. DYNAMICS OF THE WATER BUDGET AND PAST STORAGE ANALYSIS OF AMAZON BASIN (CHPATER 4)

Based on the most consistent data products in terms of water balance, the dynamic and interannual variation of each water budget components as well as their interaction is studied. An Empirical Orthogonal Function (EOF) approach is tested to find the governing components of the water budget components. The effect of ENSO events on different components is studied. Moreover, based on the developed approach for water balance the past storage for the Amazon basin is constructed for more that 23 years. The possible effects of ENSO events as well as the variation of past storage at wet and dry seasons are explored.

1.3.3. WATER BUDGET ANALYSIS OF LARGE MISSISSIPPI BASIN (CHAPTER 5)

The approach that is proposed in chapter 3 will be examined for Mississippi basin. Similarly, the whole basin will be divided to several SBs based on the location of gages and the topography of the region. Water budget component are analyzed for at sub basin scale using different available product. The runoff will be estimated based on residual of other water budget components. The results are evaluated with ground measurements of runoff. In the next step, the method proposed in chapter 3 for removing the lag time between observed and estimated runoff will be implemented. This study is being done to evaluate the possibility of using proposed method and surface water inundation for other sub basins and also finding the limitation and capabilities of remote sensing data.

CHAPTER 2: DATA SETS

In this chapter, all the data sets used in this dissertation are discussed.

2.1. Topography

The Shuttle Radar Topography Mission (SRTM) Digital Elevation Model (DEM) [*Rabus et al.*, 2003] data are used to delineate the geographic extents of the main basin and its SBs. This information with a resolution of 3 arc sec is used in Arc-GIS to generate watershed boundaries for each runoff gauge and to compute the basin slope and drainage area. Since topography data do not include information from the bottom of the river channel, it is necessary to add river network information to precisely locate the outlet of the SB for each gauge station. The river network data is used from the Environmental Research Observatory (ORE) Geodynamical, hydrological and biogeochemical control of erosion/alteration and material transport in the Amazon basin (HYBAM) as ancillary data to generate the watersheds.

2.2. Precipitation

We used in this study different estimates of precipitation over the Amazon basin.

2.2.1. GPCP

The Global Precipitation Climatology Project (GPCP), established in 1986 by the World Climate Research Program, provides data that quantify the distribution of

precipitation over the whole globe [*Adler et al.*, 2003]. The GPCP version 2.1, which is a combined satellite-gauge (SG) product, provides monthly and pentad, global 2.5° x 2.5° gridded values of precipitation totals from 1979- present [*Huffman et al.*, 2009]. Data from over 6,000 rain gauge stations, and satellite geostationary infrared and passive microwave observations have been merged to estimate monthly rainfall. There are a number of differing assumptions over the ocean and land; for example, GPCP precipitation was corrected for under catch, especially in cold and windy areas.

2.2.2. TMPA

The Tropical Rainfall Measuring Mission (TRMM) Multi-satellite Precipitation Analysis (TMPA) [*Huffman et al.*, 2007] provides a calibration-based sequential scheme for combining precipitation estimates from combined microwave-IR satellites, as well as gauge analyses where feasible, at fine scales (0.25° x 0.25° and 3 hourly). TMPA is is a 3-hourly (also monthly) combined microwave-IR global estimate (with gauge adjustment). The dataset covers the latitude band 50°N–S for the period from 1998 to the delayed present. Early validation results are as follows: the TMPA provides reasonable performance at monthly scales, although it is shown to have precipitation rate–dependent low bias due to lack of sensitivity to low precipitation rates over ocean in one of the input products (based on Advanced Microwave Sounding Unit-B, AMSU-B). At finer scales the TMPA is successful at approximately reproducing the surface observation–based histogram of precipitation, as well as reasonably detecting large daily events. The TMPA, however, has lower skill in correctly specifying moderate and light event amounts on

short time intervals, in common with other fine scale estimators. We used the combined gauge-adjusted product (3B42 version 6), which is scaled to monthly gauge data.

2.2.3. CMORPH

The Climate Prediction Center (CPC) Morphing Technique (CMORPH) uses motion vectors derived from half-hourly 8 km (at the equator) geostationary satellite IR imagery to propagate the precipitation estimates derived from passive microwave data and produces a 3-hourly 0.25-degree product available back to December 2002 [*Joyce et al.*, 2004]. In addition, the shape and intensity of the precipitation features are modified (morphed) during the time between microwave sensor scans by performing a time-weighted linear interpolation. This process yields spatially and temporally complete microwave-derived precipitation analyses, independent of the infrared temperature field. This Half-hourly data has been produced since December 2002 operationally at a grid resolution of 8 km (at equator). CMORPH showed substantial improvements over both simple averaging of the microwave estimates and over techniques that blend microwave and infrared information but that derive estimates of precipitation from infrared data when passive microwave information is unavailable.

2.2.4. PERSIANN

The Precipitation Estimation from Remotely Sensed Information using Artificial Neural Networks (PERSIANN) gives 0.25^{o} by 0.25^{o} 3-hourly global rainfall estimates using infrared satellite imagery and surface information since 2000 [*Hsu et al.*, 1997]. An adaptive training feature enables model parameters to be constantly adjusted whenever

independent sources of precipitation observations from low-orbital satellite sensors are available. The current PERSIANN algorithm has been used to generate multiple years of research quality precipitation data. This data has been used to characterize the variations of water and energy cycle at various spatial and temporal scales.

2.3. Evapotranspiration

Typical approaches for estimating evapotranspiration from remote sensing are based on direct empirical regressions that relate evapotranspiration to surface temperature and vegetation indices (e.g. [*Nemani and Running*, 1989; *Nishida et al.*, 2003] predictive equations that approximate the main evaporative processes (e.g. [*Monteith*, 1965; *Priestlr.Ch and Taylor*, 1972]) or surface energy balance considerations that use radiometric surface temperatures to solve the coupled equations of sensible, latent and available heat energy directly ([*Bastiaanssen et al.*, 1998; *Caparrini et al.*, 2004; *Norman et al.*, 1995; *Su*, 2002]) or through assimilation ([*Caparrini et al.*, 2004]) or off-line modeling) [*Kumar et al*., 2006; *Rodell et al*., 2004b]. A comprehensive overview of methods for estimating surface heat fluxes using satellite radiometric data is given by [*Kalma et al.*, 2008].

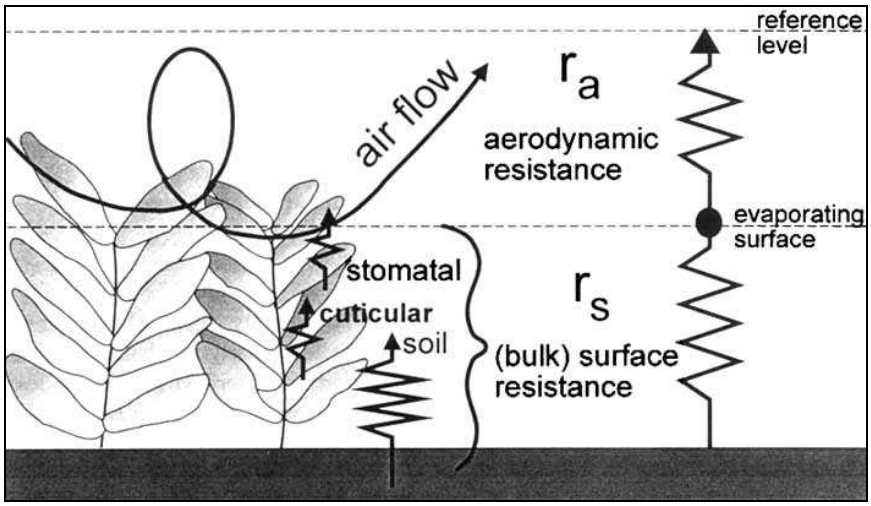

Figure 2- 1:Schematic of evaporation parameters from Penman Equation

We use and evaluate two ET estimates that are based on the Penman-Monteith equation [*Monteith*, 1965] using different remote sensing data as inputs. The goal is to use sub-monthly data, coincident with GRACE estimates. Therefore these two estimates are chosen for this study from among other remote sensing based estimates [*Fisher et al.*, 2008; *Wang et al.*, 2010; *Zhang et al.*, 2010]: the Princeton University and University of Montana products and will be referred as ET-PRI and ET-MON (Mu or Zhang).

[*Sheffield et al.*, 2010] calculated daily estimates of ET-PRI with input radiation and meteorological data from the International Satellite Cloud Climatology Project (ISCCP) and vegetation distribution derived from the Advanced Very High Resolution Radiometer (AVHRR) products for 1984-2006 at 2.5 deg.

The other dataset, ET-MON uses the same algorithm with different input data and gives global 8-day, 0.05-degree, estimates over 2000-2006 [*Mu et al.*, 2007]. The Beta

version ET algorithm is driven with global 1 km MODIS LAI/FPAR (Leaf Area Index/Flux Photosynthetic, Version 5), MODIS land cover (Version 4), 0.05-degree global MODIS surface albedo (Version 4), and Global Modeling and Assimilation Office (GMAO) daily meteorological data. In this study, we have used their global 1 km ET/LE data from 2002 August to 2006.

We also use the monthly evapotranspiration estimates provided by University of Montana, ET-MON-Z, to study inter-annual variations of ET over the Amazon (Chapter 5) [*Zhang et al.*, 2010]. The algorithm quantifies canopy transpiration and soil evaporation using a modified Penman-Monteith approach with biome-specific canopy conductance determined from the normalized difference vegetation index (NDVI) and quantifies open water evaporation using a Priestley-Taylor approach. These algorithms were applied globally using advanced very high-resolution radiometer (AVHRR) Global Inventory Modeling and Mapping Studies (GIMMS) normalized difference vegetation index (NDVI) data, NCEP/NCAR Reanalysis (NNR) daily surface meteorology, and NASA/GEWEX Surface Radiation Budget Release 3.0 solar radiation inputs. This data set gives very similar values to ET-MON with RMS differences of up to 0.4 mm/d (RMS differences with ET-PRI is 1.03 mm/d). Therefore this ET-MON-Z and ET-PRI will be used for the interannual variations over a longer time period (1984-2006) .

2.4. Total water storage (TWS) anomalies from GRACE

The Gravity Recovery and Climate Experiment (GRACE) is a dedicated satellite mission whose objective is to map the global gravity field with a spatial resolution of 400

km to 40,000 km every thirty days. Jointly implemented by NASA and DLR under the NASA Earth System Science Pathfinder Program, GRACE was launched on March 17, 2002, with an intended lifetime of 5 years [*Wahr et al*., 2004Swenson, 2006 #21].

The GRACE mission provides monthly gravity field solutions as sets of Stokes coefficients up to 1 degree at approximately 30-day intervals by measuring the distance between the two satellites since its launch in 2002. These coefficients can be used to estimate TWS changes after correction for atmospheric mass changes. We use these monthly solutions for the period from August 2002 through December 2006, except for June 2003 and January 2004 when GRACE data were unavailable.

Since shorter-wavelength spherical harmonic coefficients of the gravity field have more spatial noise, smoothing is necessary to reduce it [*Seo and Wilson*, 2005]. While a large half-width can reduce the amplitude of the storage change signal, a smaller half-width can significantly decrease the signal-to-noise ratio and may even produce non-geophysical north-south stripes [*Swenson and Wahr*, 2006]. The geoid data are expressed in equivalent water height the assumption that observed gravity variations are caused by surface mass redistribution over land [*Wahr et al.*, 2004].

The GRACE mission consists of two identical satellites in near-circular orbits at 500 km altitude and 89.5° inclination, separated from each other by approximately 220 km along-track, and linked by a highly accurate inter-satellite, K-Band microwave ranging system. The observed gravity signal degrades at higher degrees and orders (shorter length scales), hence there is a tradeoff between signal accuracy and precision in

the delineation of a study region. As the selected minimum averaging radius increases, mass changes from outside the region leak into the estimates (leakage error) (e.g.,[*Swenson et al*., 2003]). Three averaging radii are proposed here to considered: 300 km, 800 km, and 1000 km, each representing the half-wavelength of the Gaussian averaging kernel [*Rodell et al*., 2004a].

We consider two smoothing widths to compare the signal difference in the storage changes at scales of 300 km and 500 km from the Jet Propulsion Laboratory (JPL) and Center for space research (CSR). The comparison of the GRACE estimates and other reanalysis and data assimilation is presented in figure 2-2. As it seen, the GRACE provides larger seasonal amplitude.

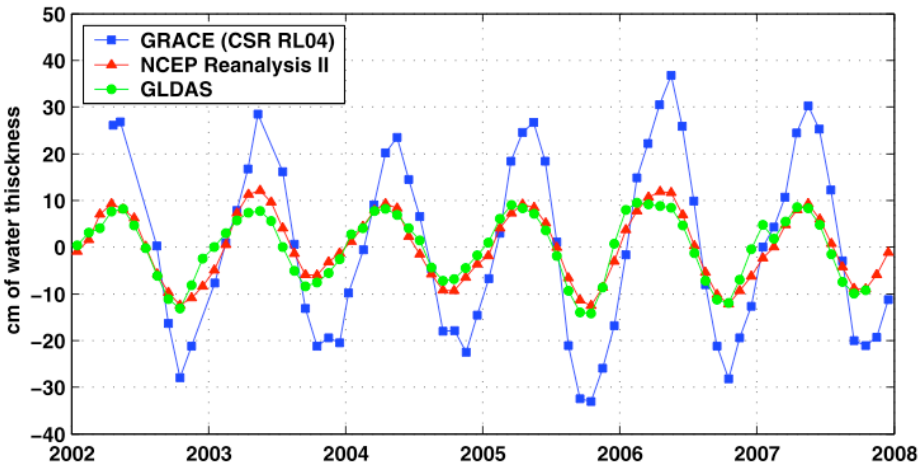

Figure 2- 2:Comparison of land water storages of GRACE and with NCEP and GLDAS model results

2.5. Discharge

Daily water discharge data are obtained from 14 gauge stations from ORE-HYBAM program. Discharge for the downstream SBs (9, 10, 11 and 12) is computed as a residual of the total discharge of the downstream SB and the incoming discharge from upstream SBs. These values are then divided by SB area and lagged one month, as a first estimate, to be consistent with the timing of the other components of the water balance equation following [*Sheffield et al.*, 2009a] in their study for Mississippi basin.

2.6. Multi-satellite derived Inundation datasets

A global dataset of inundated area, covering the period 1993-2008, is derived by a multi-satellite analysis method employing passive microwave land surface emissivities calculated from Special Sensor Microwave Imager (SSM/I) and International Satellite Cloud Climatology Project (ISCCP) observations, (ERS scatterometer measurements and AVHRR visible and near-infrared reflectances [*Papa et al.*, 2010b; *Prigent et al.*, 2007]. The data set reports monthly inundated area fraction for each equal area grid cell (0.25° x 0.25° at the equator) accounting for vegetation effects on the passive microwave signal of open water. The data set has been used to estimate surface water storage variations in large river basins [*Frappart et al.*, 2008; *Frappart et al.*, 2010] or as an indicator of runoff variation similar to the water height at the gauge station [*Papa et al.*, 2008a; *Papa et al.*, 2008b]. We evaluate its ability to indicate the temporal variation of runoff to infer lag times between excess rainfall and integrated runoff at the mouth of each SB and then to the mouth of the whole Amazon.

CHAPTER 3: WATER BUDGET COMPONENT ANALYSIS WITHIN THE AMAZON BASIN USING SATELLITE DATA

In this chapter, the components of the Amazon water budget and their spatio-temporal variability are diagnosed using monthly-averaged remote sensing-based data products for the period September 2002-December 2006. The large Amazon basin is divided into 14 smaller watersheds, and for each of these SBs, fresh water discharge is estimated from the water balance equation using satellite data products. In this Chapter the dynamics of the water budget is examined using satellite date with global coverage. Different data combinations are analyzed and the consistency between P, ET, R and TWSC is investigated. This consistency increases after applying the lagging method on SB scale averaged estimates of R (to the integrated discharge). This lag time is estimated using a simple method which is a function of the flow length and time correlation to the inundation percentage estimates in downstream of the SB. Mean annual precipitation, evapotranspiration and runoff for the whole basin are estimated to be 6.1, 3.2 and 3.0 mm/d respectively but also show large spatial and temporal variations at SB scale. The RMSE using the lagging method decreases from

3.1. Introduction

Understanding, characterizing and predicting the distribution and cycling of terrestrial waters are major goals of hydrology and climate research as well as major

requirements for water resource management. However, seasonal and interannual variations of the water budget terms, including precipitation, evapotranspiration, runoff and surface and sub-surface water storage are still not well know, at least at regional to global scale [*Bullock and Acreman*, 2003].

The spatio-temporal variations of precipitation globally and over the Amazon basin have been analyzed in several studies using remote sensing techniques [*Gu et al.*, 2007; *Huffman et al.*, 2009; *Huffman et al.*, 2007; *Joyce et al.*, 2004], rain-gauge based measurements [*Villar et al.*, 2009,b], a combination of these methods and from climatology. Although the satellite-based estimates are not able to capture the extreme rainfall rates reliably [*AghaKouchak et al.*, 2011a; *AghaKouchak et al.*, 2011b] they can be used to study the seasonal variability of precipitation. [*Villar et al.*, 2009,b] investigated the seasonal and interannual variations of rainfall over different parts of the basin using rain-gauge measurements and reported a clear contrast in the annual phase between northern and southern regions in austral summer (December, January, February, DJF) and austral winter (June-July-Aug, JJA), as well as a systematic decrease of mean rainfall rate since 1983 at -0.32% per decade.

This study aims to investigate seasonal and inter-annual variations of the individual water balance (WB) components and their interactions. For this we investigate the use of different satellite data products over the Amazon, including estimates of precipitation, evapotranspiration, together with water storage changes, to infer the runoff term as a residual from the water balance equation. Results are compared and evaluated with in situ discharge measurements. In order to better understand, the dynamics of each

component and their interactions, the Amazon basin is studied as a whole and also divided into smaller SBs to determine the most consistent combination of data products for quantifying the seasonal and interannual variations of water budget components in all individual SBs. The best data combination is selected based on the best consistency in representing the spatial and temporal variability of estimated runoff compared to observed runoff. The dynamics of the water budget components and their interactions are then investigated at inter-basin and seasonal scales.

Next chapter defines the study area. The spatio-temporal variability over the SBs from each data product is described. Chapter 4 presents estimates of the runoff as a residual from the water balance equation for different precipitation and evapotranspiration data combinations along with an indication of their uncertainties. Chapter 4 explains the choice of the most consistent data combination from the results of Chapter 3 by comparison of the estimated and observed runoff for the SBs. The best precipitation and evapotranspiration data combination is the Global Precipitation Climatology Project (GPCP) precipitation and the evaporation estimates of the University of Montana. The agreement between satellite based and in-situ runoff is significantly improved by using satellite based inundation extent verifications to estimate lag-times between SBs. Finally, the last section of this chapter gives the summary and conclusions.

3.2. The Amazon basin and its SBs

The Amazon is the world's largest drainage system with a total area of 6 x 10^6 km^2 carrying 15-20% of the global fresh water to the ocean [*Richey et al.*, 1986]. Due to its size and its position astride the Equator, the Amazon basin exhibits very complicated rainfall, evapotranspiration and runoff patterns; within its boundaries, the interactions of its many SBs makes it a very interesting dynamic system.

In this study we consider the entire Amazon basin as well as 15 SBs (Figure 3-1, top). We selected these 15 SBs based on a careful analysis of the availability of in-situ stations (at the outlet of each SB) that give their daily discharge data, their location in the basin, data periods, drainage area and mean discharge (Figure 3-1 and Table 3-1). These SBs show drainage areas ranging from 117,000 km^2 (SB 1) to 761,500 km^2 (SB 2, Table 3-1). Following [*Villar et al.*, 2009,a] the geographic extents of the main basin and SBs were estimated using ArcGIS and the Shuttle Radar Topography Mission (SRTM) Digital Elevation Model [*Rabus et al.*, 2003] with a resolution of 3 arc sec and cross-checked with ORE-HYBAM Program generated SBs (Figure 3-1, bottom), (http://www.ore-hybam.org).

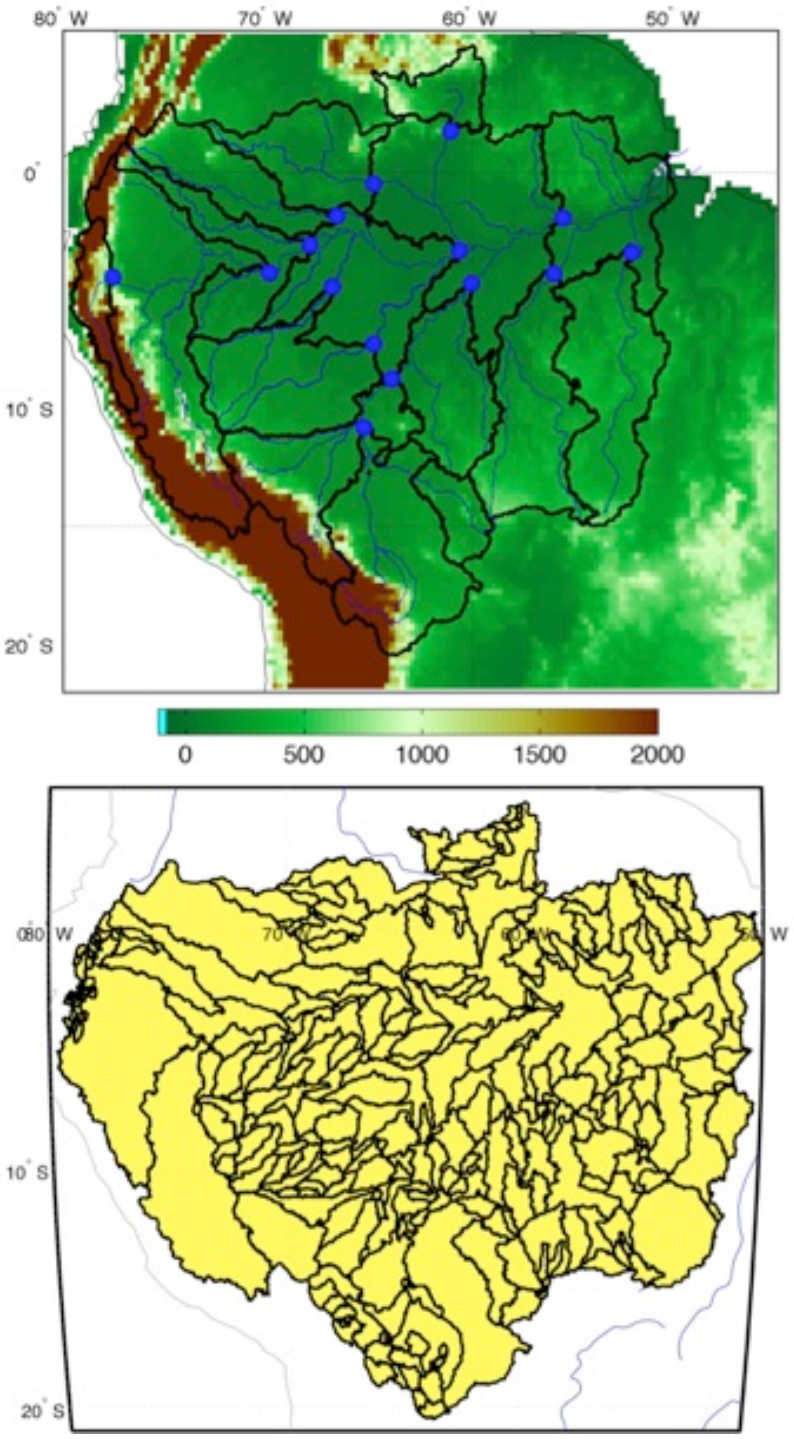

Figure 3- 1:Top:Amazon SBs delineated using topography data and locations of runoff gauge stations, Bottom: Delineated SBs of Amazon from Ore-Hybam program

Table 3- 1.Situation, mean, min and max runoff of SBs (mm/d)

Basin No	Station	River	Lat	Lon	Area (km^2)	Q_{mean}	Q_{max}	Q_{min}
1	Borja	Maranon	-4.43	-77.6	117000	3.65	6.28	1.79
2	Tabatinga	Amazonas	-4.25	-69.93	745300	3.39	5.33	1.24
3	St-Antonio Do Ica	Solimoes	-3.08	-67.93	263000	6.83	11.46	1.93
4	Acanaui	Japura	-1.82	-66.6	251500	4.79	8.31	1.47
5	Serrinha	Negro	-0.48	-64.83	287200	5.06	9.29	1.32
6	Caracarai	Branco	1.83	-61.38	134200	2.14	7.04	0.21
7	Labrea	Purus	-7.25	-64.8	165000	2.07	4.16	0.31
7	Gaviao	Jurua	-4.84	-66.85	258000	1.14	2.74	0.2
8	Guayaramerin	Mamore	-10.8	-65.3	512300	1.68	4.19	0.02
9	Porte Velho	Madeira	-8.74	-63.92	490100	2.59	6.72	-0.17
10	Fazenda VistaAlegre	Madeira	-4.68	-60.03	312900	4.37	7.79	0.2
11	Manacapuru	Sloimoes	-3.31	-60.61	435600	2.88	7.31	-0.87
12	Obidos	Amazon	-1.93	-55.5	706600	2.38	5.57	0.45
13	Itaituba	Tapajos	-4.28	-55.58	441000	1.54	5.12	0.18
14	Altamira	Xingu	-3.38	-52.14	474800	3.02	6.28	1.79
15	-Outletof Amazon	Amazon			415000			

SB 1 is located at the westernmost (upstream) end of the Amazon system and includes part of Andes Mountains with very large rainfall variability. SBs 2 and 3 also include part of the Andes in the northwestern part of the Amazon and contain the upper portions of the Amazonas and Salimoes rivers. SBs 4, 5 and 6 carry water into the Japuru, Negro and Branco rivers in the northern part of the Amazon and make the largest contribution of water to total flow despite their smaller area. SB 7 is composed of two

smaller rivers, the Purus and Jurua, in the midwestern part of the Amazon and both flow into SB 11, the Solimoes River. SB 8, the Mamore River, is in the southern part of the Amazon flowing into SB 9 and eventually 10, the Madeira River. SBs 11, Solimoes, and 12, the Amazon River proper, are in the rainforest part of the Amazon with the largest inundated areas. SB 13, the Tapajos River, and 14, the Xingu River, are in the eastern part of the Amazon and have lower rainfall variability but larger drainage areas.

3.3. Analysis of the different products for each component

3.3.1. Precipitation

Different precipitation products are tested in this study. The map of these products for November and July 2004 are depicted in figure 3-2 and 3-3.

Comparison of the different precipitation products and their mean seasonal variations for 2003-2006 is shown for 9 representative SBs, 2, 3, 5, 7, 8, 10, 11, 12 and 14 in Figure 3-4. Annual mean precipitation reported by these products for the entire Amazon ranges from 5.5 mm/d (TMPA) to 6.52 mm/d (PERSIANN). Spatial patterns of different satellite precipitation data sets are significantly different as previously highlighted [*AghaKouchak et al.*, 2011a]. This could have a considerable impact on the estimated runoff in this study in different SBs.

The primary and calibration sensors of GPCP and TMPA are similar and as a result they show good agreement over space and time except for the SB 1, probably because the TMPA results are adjusted to the older gauge measurements of the older GPCP data (Version 1). Generally, these two gauge adjusted products give smaller

estimates in wet seasons compared to CMORPH and PERSIANN, which have precipitation greater than 3.3 mm/d, (not-shaded areas in Figure 3-4). However, these differences are reversed in SBs 1, 3, and 6 during dry or less rainy seasons (not shown). Another difference in seasonal cycle of the precipitation products is the start of the wet season; PERSIANN and CMORPH start in SB 5,11 and 12 from August while climatology records and GPCP and TMPA estimates start the wet season with one or two months delay.

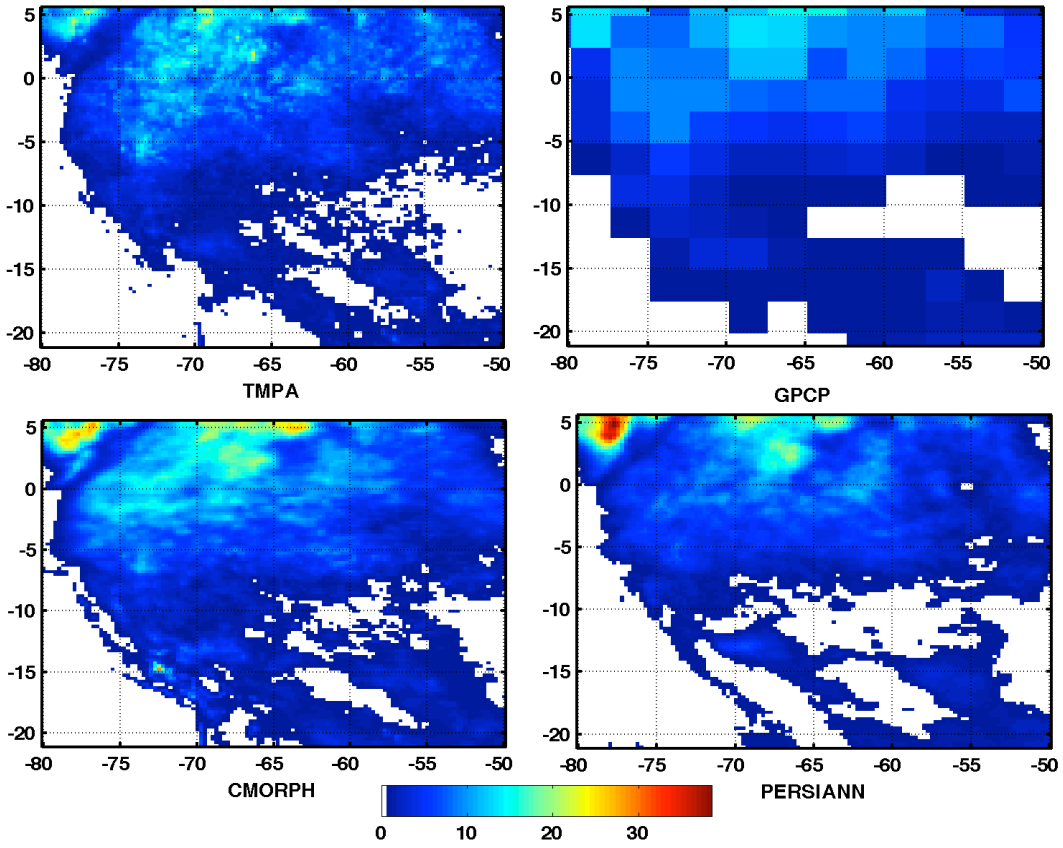

Figure 3- 2:Monthly precipitation estimates in July 2004

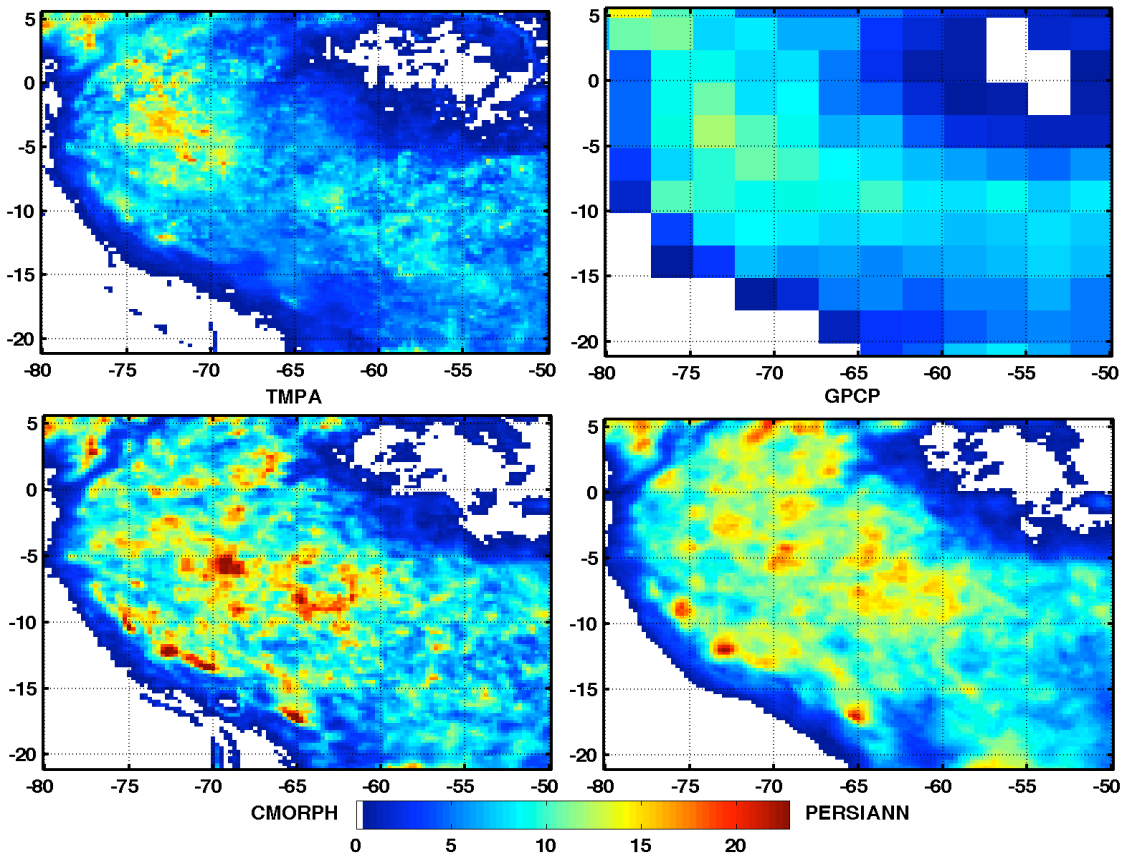

Figure 3- 3:Monthly precipitation estimates in Nov 2004

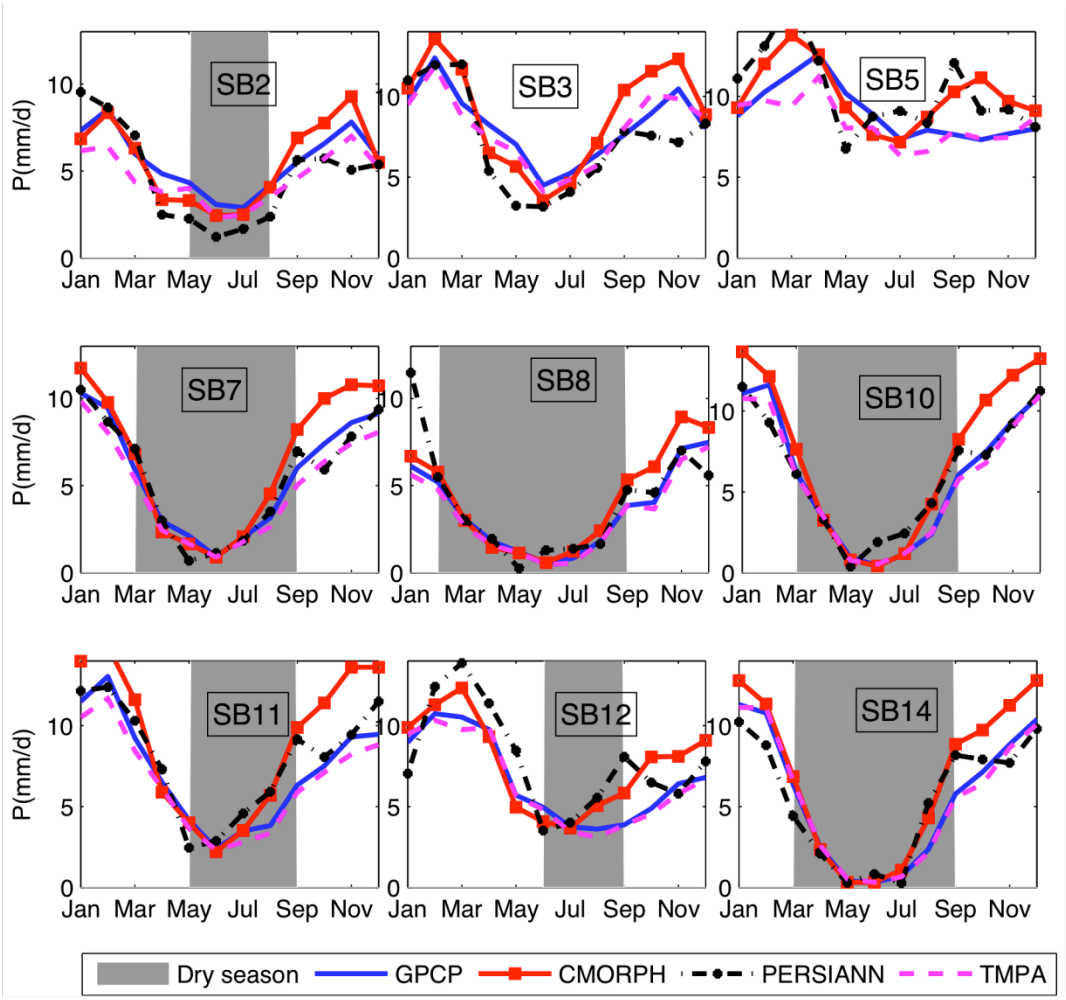

Figure 3- 4: Seasonal variability of precipitation from different datasets for different SBs with dry seasons (P of GPCP <3.2 mm/d) shown with shaded areas. For more information on SBs see Table 3-1.

3.3.2. Evapotranspiration

The maps of different ET product from university of Princeton and University of Montana have been shown in figure 3-5 for July and November 2004. Comparison of the three datasets (ET-MON, ET-Mon-Z, ET-PRI) is shown in Figure 3-6 for different SBs with their dry season shown by the shaded area. Both University of Montana products

agree better with each other over different SBs than ET-PRI. The differences between ET-MON and ET-PRI vary among the SBs: 1 mm/d maximum mean difference (bias) between the two data sets is seen in the northern SB 6 and the 0.15 mm/d minimum difference is seen in southern SB 8. [*Getirana*, 2010] used hydrological modeling and water balance for the Negro river (SB 5) for 1997-2006 to estimate annual mean, wet and dry season mean ET of 3.2, 3.5 and 2.6 mm/d respectively. The same values for ET-MON are 3.23, 4.1 and 2.42 mm/d and for ET-PRI they are 4.32, 5.2 and 3.33 mm/d. Note that neither dataset accounts for evaporation from inundated areas even though SBs 11 and 12 have extensive and variable inundated areas [*Papa et al.*, 2008b; *Papa et al.*, 2010b].

Open water bodies and flooded areas in the Amazon can be important contributors to ET. Evapotranspiration estimates from Princeton University, with a map grid of 2.5 degrees, are less sensitive to the inundated areas near the river. On the other hand, the ET estimates from University of Montana, ET-MON, have finer resolution (1 km), but do not account for evaporation from flooded areas. ET-Mon-Z estimates for open water bodies are based on land cover classification maps and, therefore, do not include the effects of seasonal flooding [*Papa et al.*, 2010b]. In fact, this dataset shows a decrease in ET in the season with increased flooding. Also, there does not seem to be a significant increase in ET in SB 8, which contains the reservoir of the Samuel Dam. Therefore, all three ET estimates need to carefully account for the evaporation from open water areas.

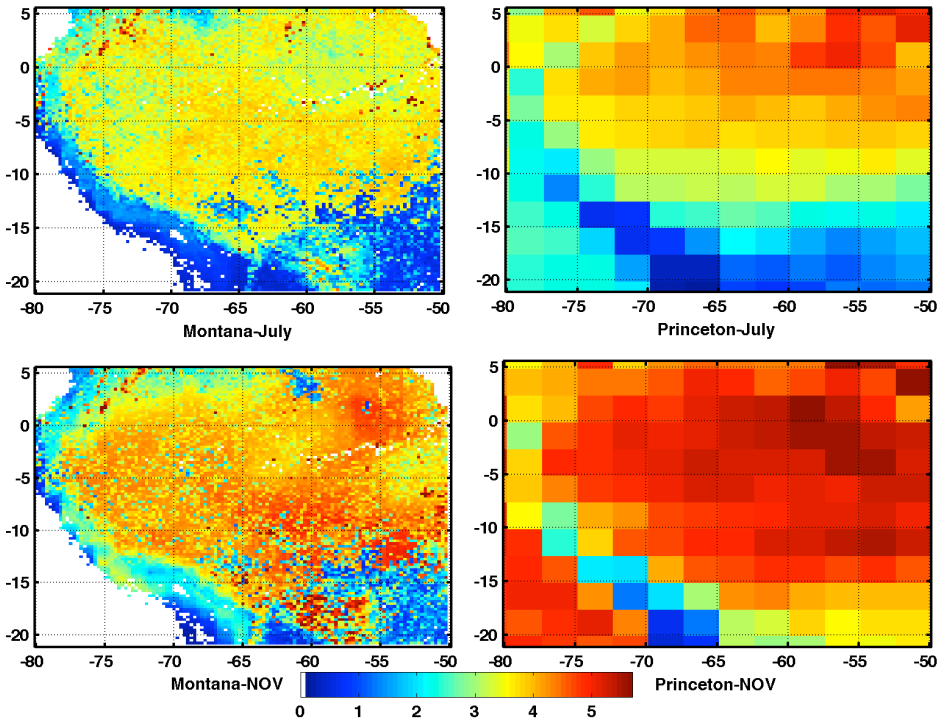

Figure 3- 5: Evaporation estimates from MON and PRU for July and Nov of 2004(mm/day)

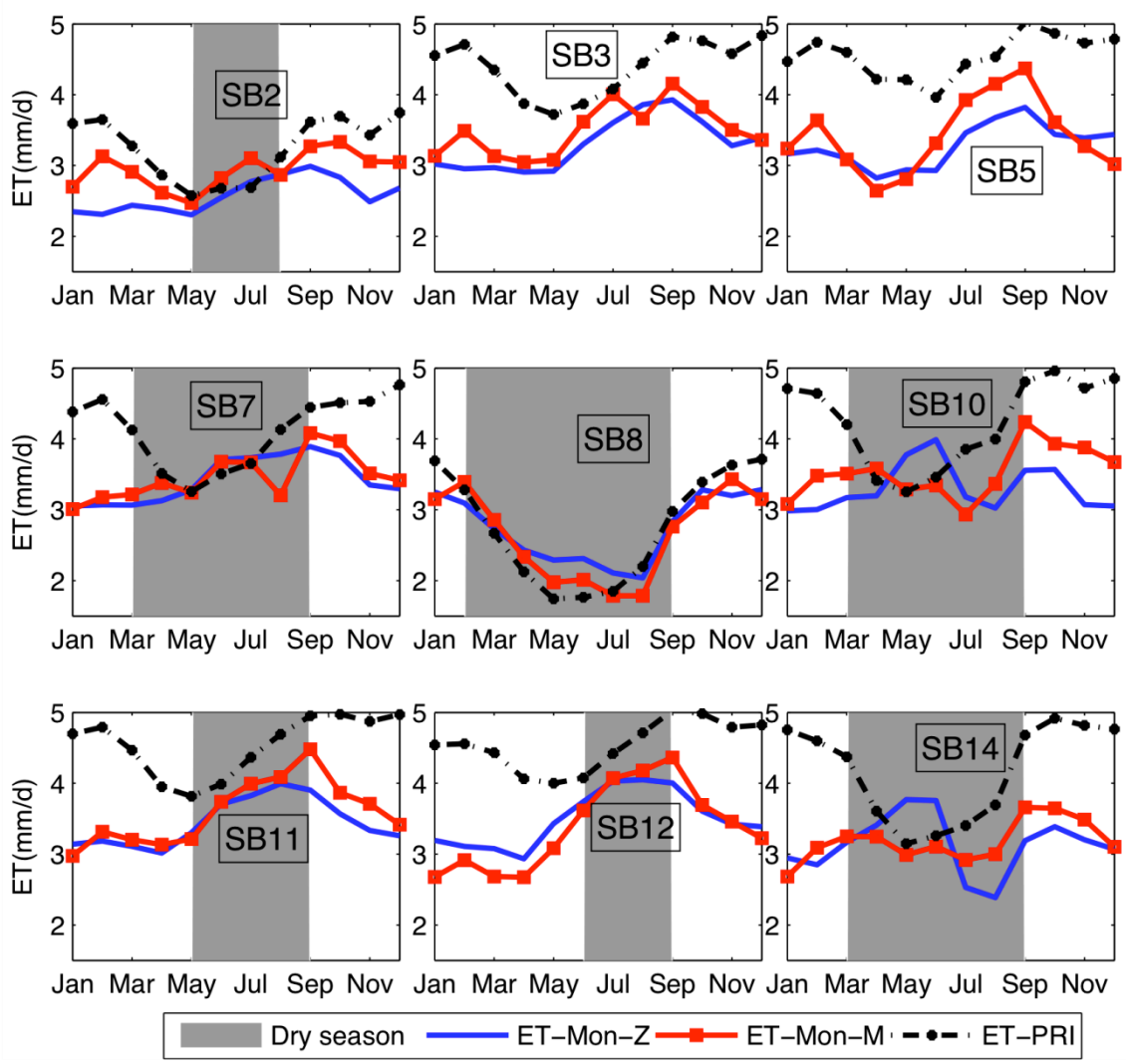

Figure 3- 6: Seasonal variability of evaporation from different datasets for different SBs with dry seasons (P<3 mm/d) shown with shaded areas. For more information on SBs see Table 3-1.

Generally ET exhibits small seasonal variation and decreases over the dry season due to water stress. However, ET increases during less rainy months in SBs 5, 11, 12, and 15 which have no dry season. This will be discussed more in section 5 investigating the dynamics of the water.

Thus for the study of the seasonal dynamics we use ET-MON and for the inter-annual variation we use ET-MON-Z and ET-PRI because of their long time coverage. Although these ET estimates show different seasonal patterns over the Amazon, they agree in interannual variation exhibiting correlation coefficient of 0.98 between ET-MON and ET-Zhang and 0.91 between ET-MON and ET-PRI.

3.3.3. Total water storage (TWS) anomalies from GRACE

We consider two smoothing widths to compare the signal difference in the storage changes at scales of 300 km and 500 km from the Jet Propulsion Laboratory (JPL) and Center for space research (CSR). Figure 3-7 shows monthly variation of the TWS obtained with these two smoothing radii for different SBs. The 500 km radius smoothes the storage changes but appears to lose some of the information as [*Swenson and Wahr*, 2006] concluded especially in downstream SBs 11 and 12. Also, the seasonal variations of the water storage changes are in better agreement with the known dry and wet seasons of the SBs except in SB 12, where the minimum occurs in the beginning of the dry season (shaded areas in Figure 3-7). This happens because of the coincidence of the dry season, and hence decreased runoff, from the upstream SBs discharging into this SB (5 and 11).

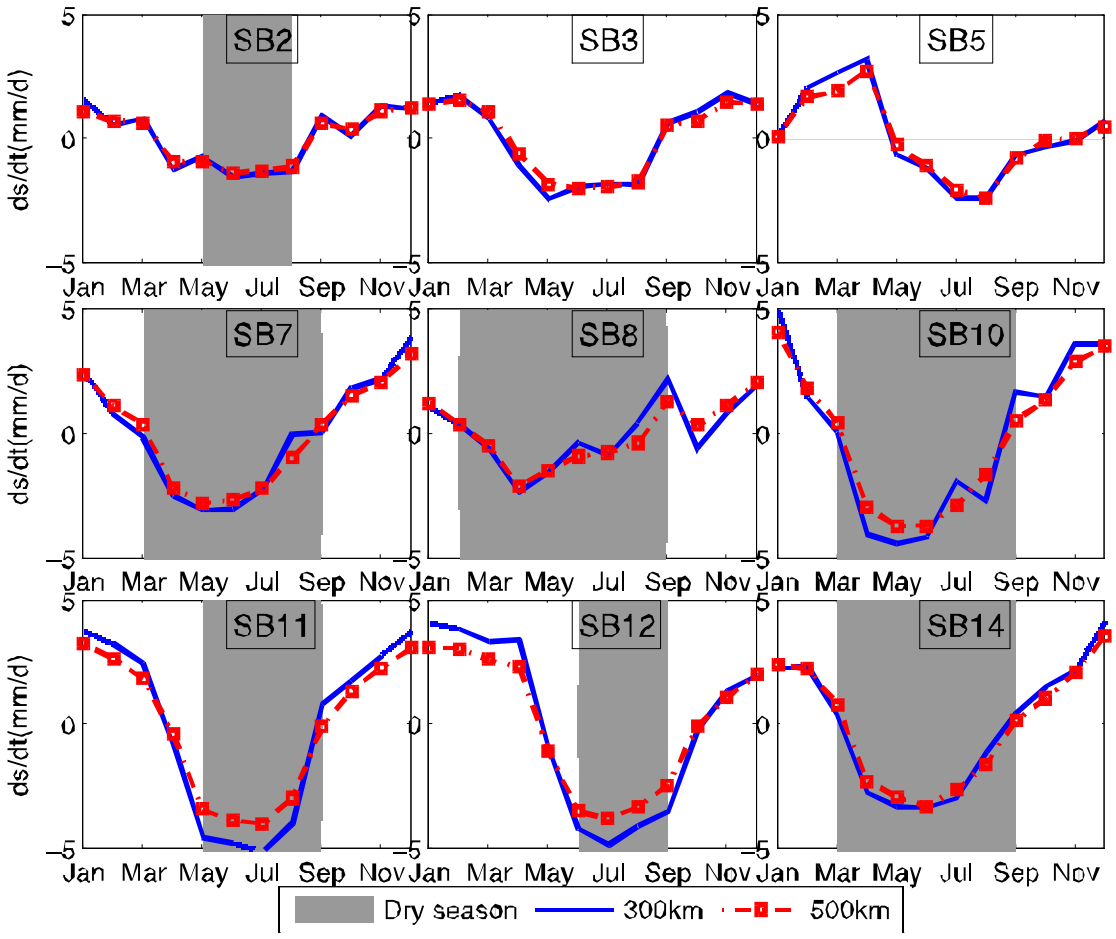

Figure 3- 7: Seasonal variability of the water storage changes in different SBs. For more information on SBs see Table 3-1.

While the analysis of the GRACE measurements can characterize terrestrial freshwater changes across a range of temporal (monthly and longer) and spatial scales (area>150,000 km^2, the lower limit of GRACE water storage detectability) [*Rodell and Famiglietti*, 1999], it can't resolve important features of the distribution of terrestrial surface waters at higher spatio-temporal frequencies. In smaller SBs it is expected that GRACE substantially underestimates the seasonal cycle of terrestrial water storage because of attenuation by the spatial smoothing [*J Chen et al.*, 2007]. This was also seen

in a study for the smaller Sacramento-Klamath basins with total area of 110,000 km^2 [*Tang et al.*, 2010]. In the Amazon most of the SBs have total areas $>2x10^5$ (km^2), except SB 1 which has an area of 117,000 km^2.

3.3.4. Discharge

Precipitation, evapotranspiration and water storage changes are averaged over each SB area. Because the observed runoff data are the total discharge at the mouth of each SB, net runoff from in-SB sources was computed as downstream minus upstream runoff. Therefore, the net runoff from SB 2 is that measured at Station 2 minus runoff from SB 1 and the net runoff from SB 3 is the total runoff from SB 3 minus that from SB 2. SB 9 obtains runoff from SB 8 and then discharges into SB 10. SB 11 collects water from SBs 3, 4 and 7 while SB 12 discharges most of its water from SBs 5, 6, 10, and 11. As seen in the Table 3-1 the minimum streamflow occurs in the easternmost SB 13 with a mean of 1.84 mm/d and the maximum occurs in the western SB 3 with a mean of 6.83 mm/d. We aim to investigate daily variability of the water budget components, but the coarse time resolution of GRACE data limits our initial study to monthly mean data that are used to investigate seasonal variations. Once the best precipitation and evapotranspiration combination is selected, their daily information can be used to study the water dynamics in more detail.

The seasonal variation of the observed runoff is plotted in Figure 3-8 for different SBs along with the estimated runoff estimated runoff from water balance (the comparison of two will be discussed in chapter 4). Monthly variation of the observed runoff depends

more on P, which has larger seasonal amplitude, than ET for most of the SBs. However in the downstream SBs 11 and 12, net runoff has smaller seasonality because P-ET and TWS have opposite phase indicative of opposite seasonal phases for upstream SBs. SB 11 has maximum runoff in its local dry season because of abundance of stored water from upstream SBs.

3.3.5. Multi-satellite derived Inundation datasets

Figure 3-9 shows a map of the maximum annual inundation percentage difference of each map cell. Maximum inundated areas appear in the downstream SBs 11,12 and 15 and the southern upstream SB 8. Large inundation fractions in the latter SB are due to the storage of the water in the river upstream of the Samuel dam located at the mouth of this SB.

As expected from several previous studies cited above in different environments, the temporal variation of inundation exhibits a close correlation with runoff variations as illustrated here for nine representative SBs in Figure 3-9 (right). These time series will be used in Chapter 4 to compute the delay time for the water in upstream SBs to reach to the downstream SB instead of simply lagging one month for the whole Amazon. As seen in this figure, the correlation coefficient between the time series of accumulated discharge at the outlet of each SB and its inundated fraction varies from 0.69 to 0.92, which indicates the ability of this data to detect the seasonal variation of surface water discharge.

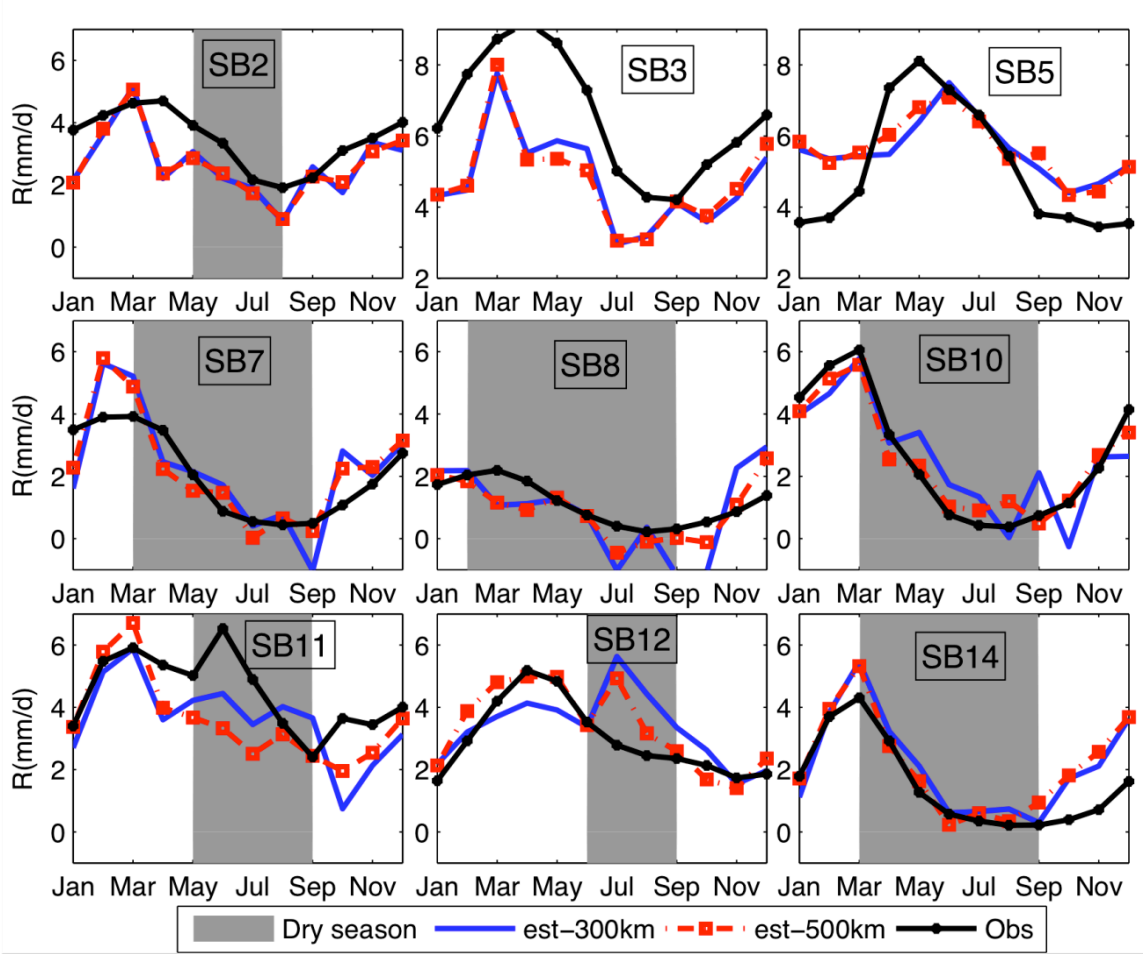

Figure 3- 8: Monthly variation of observed runoff (solid line) and estimated using two smoothing radii for TWSC of GRACE (dashed lines) in different SBs. For more information on SBs see Table 3-1.

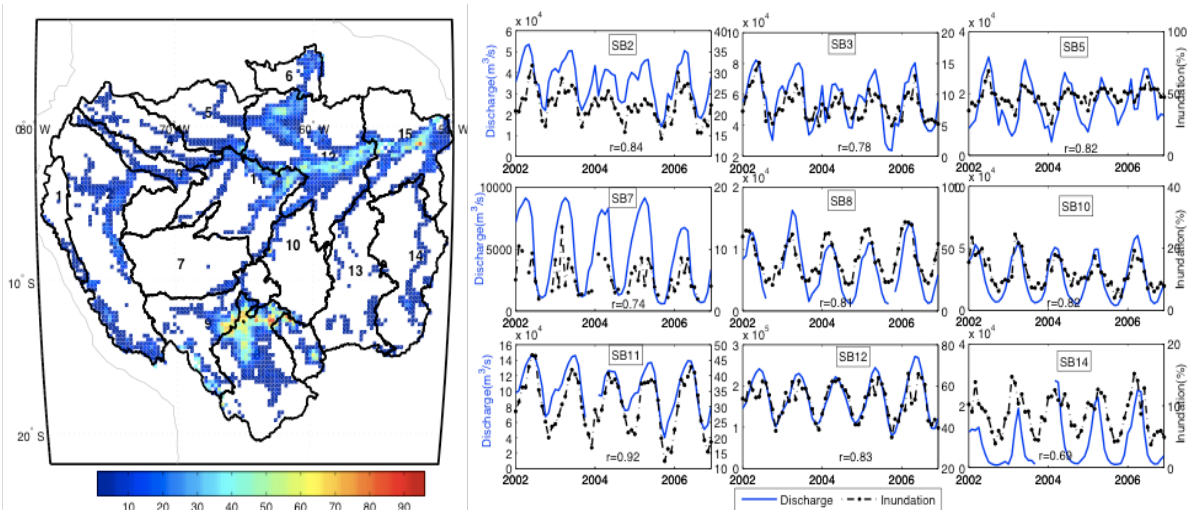

Figure 3- 9: a) Annual range of gridded inundation fraction (max-min) for 2003-2006, b) Time series of inundation percentage and gauge runoff in different SBs. Correlation coefficient for each SB is shown in each plot by r.

Comparing all the components shows that, generally, P is greater than ET over the whole Amazon basin, as previously deduced; but that ET exceeds P in the dry season in SBs 5, 8, 9, 10, 11 and 12. In SB 1, P is less than R, which probably indicates errors in the precipitation estimates as discussed previously. The water balance approach helps evaluate different combination of datasets for the water budget components and to understand their dynamics in Amazon basin as will be discussed in the next chapter.

3.4. Analysis method: Estimates of runoff and uncertainties

The terrestrial water balance for a drainage area can be written as

$$P-ET-\Delta S=R \qquad (13)$$

Where ΔS is the changes in terrestrial water storage (TWS) from GRACE as the difference between one monthly observation and the previous observation, P is the total

precipitation (mm) for the observation month, ET is the evapotranspiration (mm) for that month, and R is the net discharge from the basin. In conventional hydrological models, the net runoff from Eq. 13 is estimated based on the storage in soil and groundwater, but not surface water, and then is routed in the second stage using river characteristics for the surface storage term. But GRACE data represent total water storage including the surface water. Therefore, using GRACE-based estimates of ΔS in Eq. 13 to determine runoff requires estimation of the travel time of the water from to the mouth of a basin.

A better estimate of the discharge of the whole, very large Amazon basin is obtained by dividing it into smaller SBs that have smaller lag times and comparing the estimates to the observed discharge time series (hydrograph). The surface inundation dataset is then used in each SB to compute the lag time between estimated runoff and the time series of the inundation percentage at the location of the gauge by a simple lag correlation. Then the lagged discharge is compared to the gauge observations for each SB. The computed lag–time for the smaller upstream SBs, 1-4, is zero months, while for the SBs 5-8 and 11-14, it is one month. The lag-time for SBs 9 and 10 is also less than a month. Therefore accumulated delay time for the water from SBs 3 and 4 to reach mouth of the SB 12 is three months. The summed and lagged estimated total runoff would be explained more in Chapter 4.

The relative uncertainty in a monthly estimates of R, $\upsilon_{\bar{R}}$, can be estimated as the root mean square of the errors of each component divided by the value of R, assuming that the errors of the separate components are independent (Equation 12).

Given $\upsilon_{\overline{R}}$, the relative error for $\overline{R}$, the 95% confidence limits on $\overline{R}$ are $\pm \upsilon_{\overline{R}} R$. [*Wahr et al.*, 2004] estimated the GRACE uncertainties to about 1.0-1.5 cm for the Amazon basin. Therefore, the absolute error of the water storage changes between two observation months would be at least $\sqrt{2}$ times the of the one observation error.

The assumption of independent errors of each component needs a more careful investigation because derived ET estimates might depend on P estimates. In this step, only uncertainties of GPCP are available, and therefore will be used to compute the resultant uncertainties of the estimated runoff from equation (12) for this combination for all 14 SBs. Also note that the given equation (2) can only be used for the data with Gaussian distribution. Although P does not have Gaussian distribution, this formula can be used as a rough estimate about the uncertainty expecting even larger values dues to sever events.

The spatio-temporal variability of the absolute error for GPCP data is presented by [*Huffman et al.*, 2009]. The average error over the whole Amazon basin is 0.94 mm/d that ranges from 0.49 mm/d in SB 1 to 1.19 mm/d in SB 5. Note that the uncertainties for this product increases for the larger precipitation values. The uncertainties of other precipitation products are not available over South America at this time.

Mean Absolute Error (MAE) of ET reported by [*Mu et al.*, 2007] is 0.33 mm/d in their improved version based on the evaluation at eddy flux towers. [*Jimenez et al.*, 2010] compared ET estimates of satellite based, re-analysis and other empirical methods globally and reported the largest absolute differences in monthly mean latent heat flux

values over tropical regions; the maximum difference in Amazon SB is 24 W/m^2 (0.85 mm/d). Therefore, the assumption of ET uncertainty needs more evaluation. Note that the accuracy of the discharge measurements is not given from ORE-Hybam. However, analysis of the potential errors in river discharge measurements suggests that 5–10 % is a reasonable estimation of the error in observed mean discharge [*Coe et al.*, 2002], which translates into 0.15-0.3 mm/day.

3.5. Results

3.5.1. Estimates of runoff and choice of the most consistent data combination

There are four P and three ET data sets available for this study, which produce different estimates of R (ΔS is taken only from GRACE). Table 3-2 shows the relative error, Bias and RMSE of the estimated and observed runoff from different combinations of data over the whole Amazon. These error values are computed with different lag times: two months lag gives the maximum correlation (Min error) for most of the cases. Both TMPA and GPCP combined with ET-MON have smaller relative error compared to the observed value of 15 and 23 %. Therefore ET-MON produces slightly smaller total error with two pairs of P than ET-PRI. In the other hand, PERSIANN based estimates produces larger error with both ET combinations.

Table 3- 2:Relative, Bias, and RMS error of estimated runoff from different data combination for the whole Amazon basin

Data combination	Relative(%)	Bias (mm/d)	RMSE (mm/d)
TMPA-PRI	48	-1.40	0.7
PERSIANN-PRI	60	-0.49	2.1
GPCP-PRI	31	-0.89	0.7
CMORPH-PRI	41	-1.18	1.2
TMPA-MON	23	-0.65	0.6
PERSIANN-MON	63	0.27	2.2
GPCP-MON	15	-0.43	0.60
CMORPH-MON	30	-0.40	1.1

The estimated absolute error is 1 to 1.45 mm/d for the other three P pairs for the whole Amazon. To show more detail, the Bias and RMSE are computed at SB scale and shown in Table 3-3 for three P products. Since the annual variation of the TWS is small, we computed annual P-ET-R to obtain the bias and then removed it to compute the RMSE. This comparison shows where in the large Amazon basin, the estimated runoff works better and vice versa for each combination. Also these results are demonstrated in Figure 3-10 for three SBs and the Whole Amazon and show GPCP-based combination gives larger correlation coefficient and smallest RMSE than the other combinations. The GPCP combination gives smaller RMSE in most of the SBs. In northern SBs 2-5 and SBs 11-12, RMSE shows large variation among three P combinations. Although the relative error shown in table 3-2 is small (15% for GPCP, ET-MON combination) for the whole

Amazon, it is greater in smaller SBs especially in SBs 1,6,8 and 14 it increases as high as 128%.

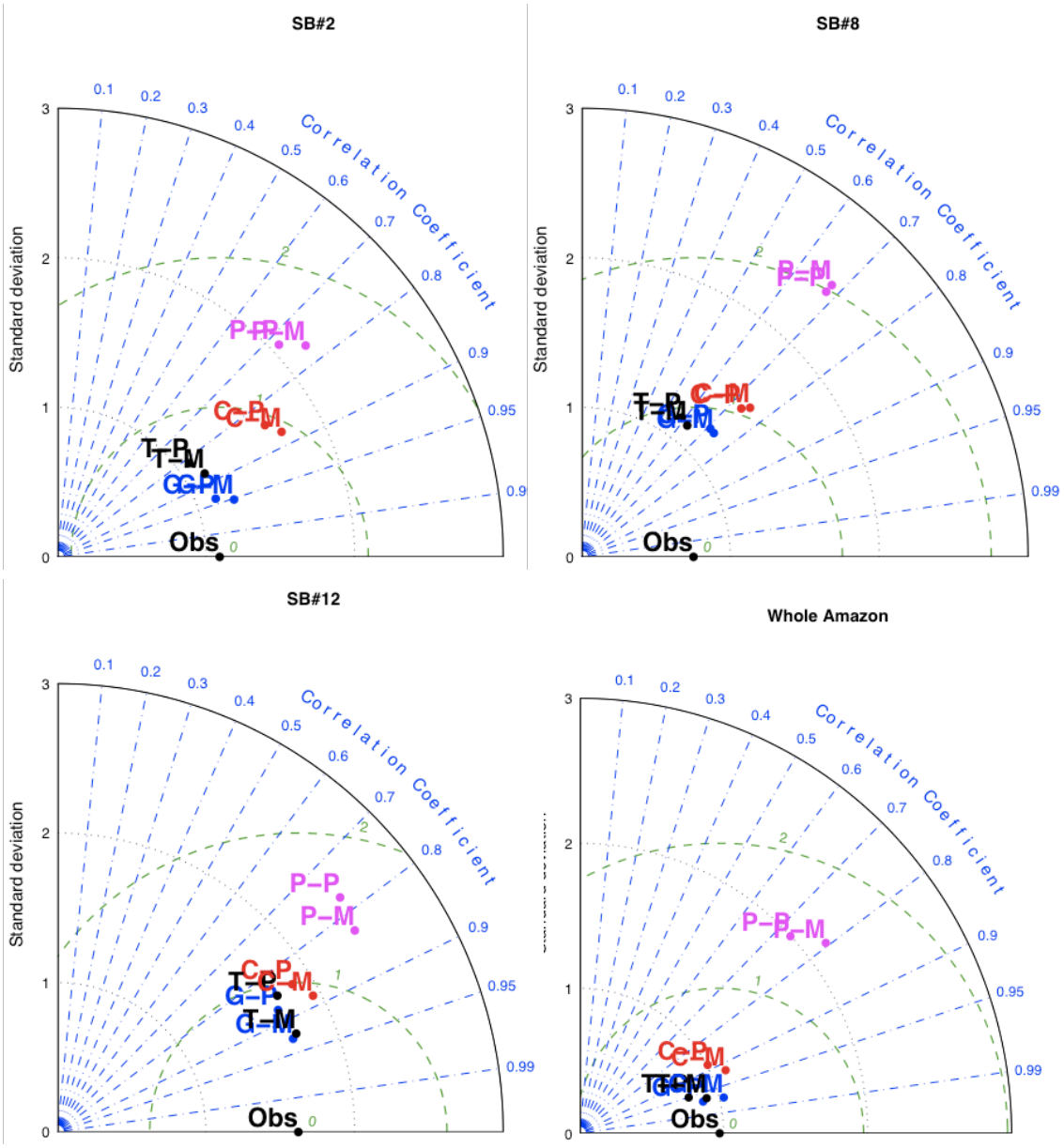

Figure 3- 10. Taylor Diagram of the estimated runoff in different SBs of Amazon.

Table 3- 3:Bias and RMSE of the estimated runoff from different P, and ET data in different SBs of Amazon (mm/d). Bias is computed as a difference of annual P-ET-R.

SBs	GPCP, ET-MON		GPCP, ET-PRI		CMORPH, ET-MON		CMORPH, ET-PRI		TMPA, ET-MON		TMPA, ET-PRI	
	Bias	RMSE	Bias	RMSE	Bias	RMSE	Bias	RMSE	Bias	RMSE	Bias	RMSE
1	-3.2	1.1	-4.0	1.1	-3.6	1.4	-4.4	1.4	-4.4	1.3	-5.2	1.3
2	-1.1	0.6	-1.3	0.8	-0.8	1.5	-1.0	1.5	-2.1	0.9	-2.3	1.1
3	-2.1	1.3	-2.9	1.5	-0.8	2.6	-1.6	2.6	-2.4	1.5	-3.2	1.7
4	0.0	1.1	-0.8	1.1	1.2	2.1	0.4	2.1	-0.4	1.8	-1.1	1.8
5	0.2	1.2	-0.9	1.2	1.9	2.2	0.8	2.3	-0.4	1.8	-1.5	1.7
6	0.9	0.9	-0.3	0.9	0.2	1.3	-1.0	1.2	-0.3	1.1	-1.4	1.0
7	-0.1	0.7	-0.7	1.0	1.2	1.7	0.6	1.8	-0.7	0.9	-1.3	1.0
8	-0.4	0.8	-0.5	0.8	0.4	1.2	0.3	1.2	-0.7	0.8	-0.7	0.8
9	-0.1	0.8	-0.3	0.8	0.6	1.1	0.4	1.2	-0.7	0.8	-0.9	1.0
10	-0.5	1.1	-1.1	1.2	1.3	1.2	0.8	1.5	-0.7	1.3	-1.3	1.4
11	-1.2	1.4	-2.2	1.4	1.2	2.5	0.2	2.5	-1.7	1.5	-2.6	1.5
12	0.3	1.4	-0.8	1.5	1.4	1.9	0.3	2.0	0.2	1.3	-1.0	1.5
13	-0.3	0.6	-1.1	0.7	1.4	1.0	0.5	1.0	-0.2	0.6	-1.0	0.7
14	0.7	0.8	-0.2	0.9	2.3	1.4	1.4	1.3	0.5	0.8	-0.4	0.9

A dam controls the flow in SB 8 and therefore its storage changes differ from the natural rivers. This shows that one should be careful about using the smoother data because of loss of information that is a different effect than the attenuation effect investigated previously [*J Chen et al.*, 2007]. While estimated runoff is in good agreement in amplitude and seasonal phase with observed runoff for all the SBs, except SB 3 (Table 3-3), there is a phase lag and amplitude difference between the observed and estimated runoff for the entire Amazon basin, even for the combination with the best average agreement. This phase lag can arise because the satellite estimated runoff is averaged

over the SB whereas the observed runoff represents integration at the mouth of the whole basin. Performing the same comparison in the smaller SBs supports this hypothesis: the results show much better agreement in phase and amplitude in all cases (table 3-3). Mean absolute errors for each SB from both P-ET combinations are shown in Table 3-4 along with the estimated uncertainties. Comparison of the uncertainties and MAE (mean absolute error) in Table 3-4 shows that the errors are not always within the uncertainties for all of the SBs; but are very close to these values except for the large differences in SB 1 and 3. This could be due to major limitation of satellite data sets over mountainous regions, highlighted in [*Sorooshian et al.*, 2010] but also is seen in other in-situ based studies below.

Table 3- 4:Mean absolute error of the estimated runoff from two different P and ET combinations and estimated uncertainty of the GPCP and ET-MON data for different SBs

SB	Estimated	Mean absolute	Mean absolute
	GPCP, ET-MON	GPCP, ET-MON	CMORPH, ET-PRI
1	0.78	3.03	4.12
2	1.11	1.00	2.14
3	1.26	2.14	3.98
4	1.31	1.38	2.79
5	1.34	1.27	2.89
6	1.07	1.37	2.27
7	1.16	1.33	2.36
8	0.95	0.90	1.13
9	1.03	0.86	1.24
10	1.12	1.28	2.20
11	1.23	1.74	2.83
12	1.17	1.63	2.25
13	1.15	1.03	1.57
14	1.12	1.69	2.18
Total	1.03	1.37	1.75

[*Coe et al.*, 2002] used the IBIS ecosystem model, together with the HYDRA surface hydrology model, to simulate the Amazon Basin flooded area and discharge from historical climate records from 1939–1998. Evaluation of their results against diverse observations indicates that estimates of precipitation are likely greatly underestimated outside of the Brazilian portion of the Amazon Basin. As a result, flooded area and discharge and are consistently underestimated for watersheds with significant input from non-Brazilian portions of the basin [*Coe et al.*, 2002]. [*Costa and Foley*, 1997] found a similar negative bias in their simulated discharge of the Andes SBs and concluded that estimations of the runoff for Andes SBs were unusually low compared to those inside Brazil and suggested that this large negative bias is likely associated with errors in the precipitation data set outside Brazil rather than with the calculation of evapotranspiration. Also some other studies of rainfall variability in the Amazon basin using a large number of rainfall gauges showed that rainfall decreases at higher altitudes in the Andes [*Villar et al.*, 2009,b]. GPCP V2.1 and TRMM3B42 data are adjusted to monthly gauge data (but different versions), but this adjustment does not increase significantly the microwave-based estimates in SB 1. Although, GPCP version 2.1 has larger rainfall estimates in the Andes than the previous version [*Huffman et al.*, 2009], there is still a large difference between incoming and outgoing components of the water balance. Even CMORPH and PERSIANN data, which rely solely on satellite measurements and over-estimate rainfall in other parts of the Amazon, give smaller estimates than GPCP in the Andes.

To evaluate the evapotranspiration data, we note that the net radiation used to produce the ET-PRI is generally larger over rainforest areas than that used to produce

other remote sensing-based ET datasets [*Jimenez et al.*, 2010]. Since radiation is the most important term in the Penman-Monteith formula, this difference can explain the larger ET values obtained for the Amazon. As seen in Table 3-3, after removing bias from the estimates, RMSE values are generally smaller in ET-MON based combinations except in SBs 4, 5, 6, 8 and 11 where it is the same for both ET estimates. ET-MON is chosen for further study of the dynamics since there is no objective basis for removing the bias from ET-PRI.

3.5.2. Estimated runoff using lagging method

As mentioned in the comparison of the estimated and observed seasonal variations of runoff, there are magnitude differences and a phase lag between the two estimates for the whole Amazon basin (at the downstream station) but not in the smaller SBs. Therefore, the method used in the smaller SBs to shift the observed runoff is applied at this stage to estimate the total runoff at the mouth of whole Amazon similar to an element-to-element routing method. The estimated runoff downstream is the sum of the runoff from each upstream SB with a lag time computed from the lag correlation analysis between inundation data and estimated runoff. These correlation computations are used to determine the accumulated flow into SBs 10 and 3, then into SB 11 and finally into SB 12. The lag times from each source are computed as the flow length divided by the velocity of the flow. As a first estimate of the average velocity, we use 1.5 miles/hr according to Smithsonian National Zoological Park. Then the time series of the lagged estimated runoff for different SBs is compared to the time series of inundation to adjust the velocity. Table 3-5 shows the lag time based on the assumed velocity range from the

mouth of each upstream SB to the mouth of the SB 12 (Obidos station) and the best-correlated lag-time with the inundation data set. The total lag-time indicates the average travel time needed from the mouth of the SB to mouth of the whole Amazon plus the intra-SB travel time. This intra-SB time varies for different SBs depending on the shape and size of the SB. SBs with one-month intra-SB lag time are marked with (*). The total travel time for the flow from SBs 1 and 2 to downstream is three months.

Table 3- 5:Distance and travel time from mouth of each SB to the Obidos station along with the total lag time from the upstream of each SB to its mouth. The total lag time in SBs with (*) has one-month inter-SB travel time.

SB	Distance (km mouth-to-mouth)	Travel time range (v=0.45-0.9 m/s) days	Total lag-time (months)
1	3300	43- 86	3
2	2200	29 – 58	3*
3	1800	24 – 48	2
4	1650	22 – 44	1
5	1350	17 – 35	1
6	1400	18 – 36	1
7	1800	23 – 47	2
8	1850	24 – 48	1
9	1450	18 – 38	1
10	780	10 – 20	0
11	750	10 – 20	1
12	0	0	0
13	0	0	1*
14	0	0	1*

The correlation coefficient between lagged estimated runoff and observed increases from 0.72 to 0.88 using the GPCP and ET-MON combination and from 0.68 to 0.90 using the TMPA and ET-MON combination. Similarly, the RMSE decreases from 0.98 to 0.61 for

GPCP and from 0.95 to 0.84 for TMPA. The estimated runoff from this method, for the whole Amazon is compared in Figure 3-11 to the observed runoff and the previous (unadjusted) values. This figure shows that the lagged runoff at the mouth of the whole Amazon agrees much better in phase and magnitude with the observed data which supports our explanation and does not require including underground discharge to resolve the differences as described by [Syed et al., 2005].

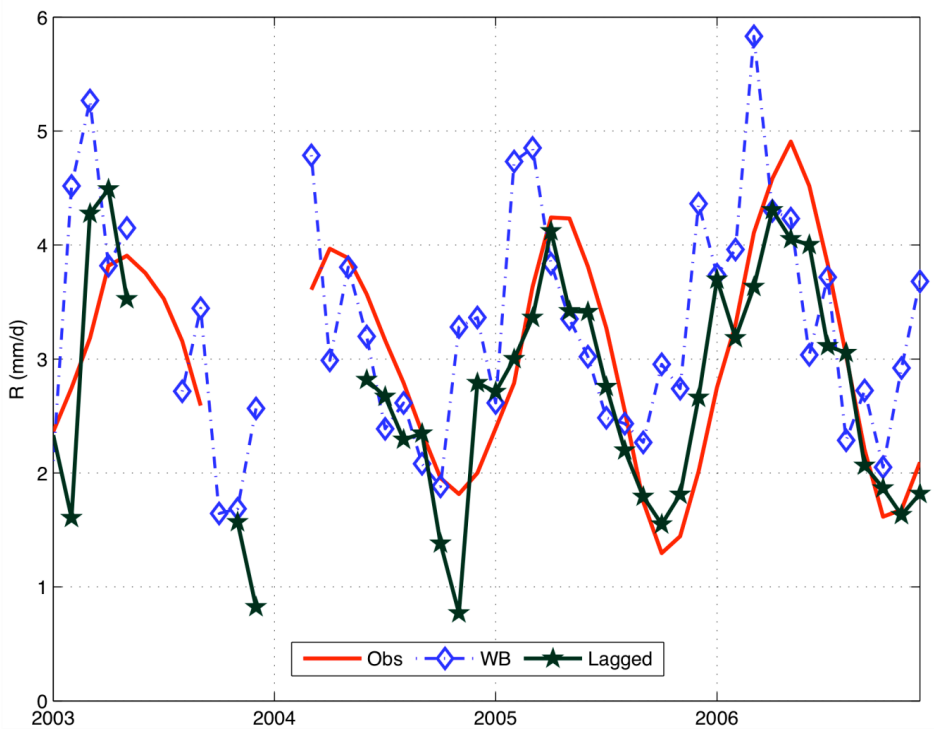

Figure 3- 11: Comparison of observed total runoff with estimated runoff from WB and after lagging method using GPCP combination for 2003-2006. total error decreased from 1.1 mm/d to 0.65 mm/d (21%).

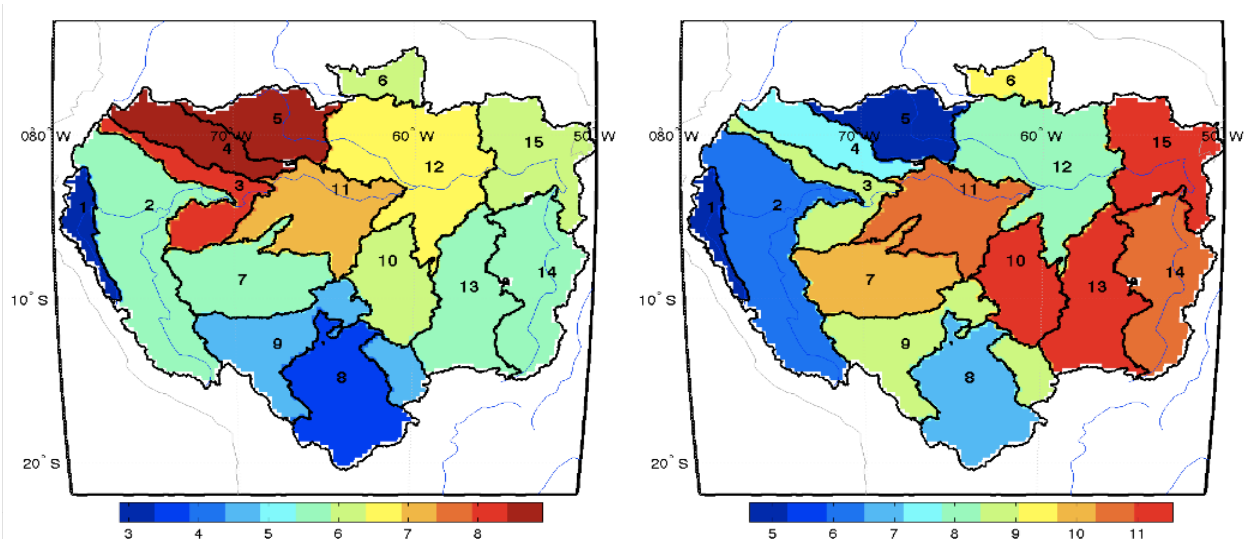

Figure 3- 12: Annual precipitation (left) and its seasonal range (max-min) (right) (mm/d) in different SBs using GPCP for different SBs for 2003-2006. For more information on SBs see Table 3-1.

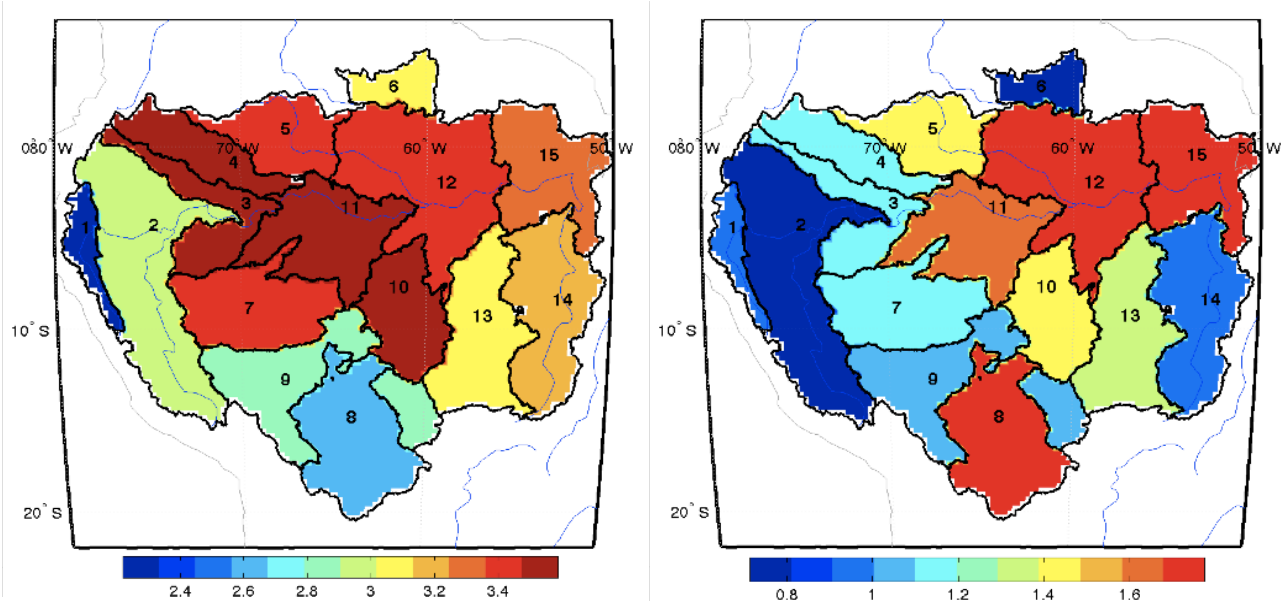

Figure 3- 13: Mean annual evapotranspiration (left) and its seasonal range (max-min) (right) (mm/d) for different SBs (numbers) using ET-MON for 2003-2006. For more information on SBs see Table 3-1.

Using GPCP data for precipitation, ET-MON for evapotranspiration, GRACE with smoothing radius of 500km for total water storage changes and the observed discharge data, the imbalance, relative error in the basin is decreased compared with previous studies from 50% [*Marengo*, 2005] to 21% over the whole basin. Generally, estimated runoff using the GPCP-MON combination is higher than observed in the northern parts of the Amazon basin but significantly lower in the western parts, mostly because of uncertainties in the precipitation data. Dividing the basin into five parts with similar climate and SB response, the imbalance in the western part of Amazon is +1.55 mm/d (SB 1, 2, 3), +0.62 mm/d in the northern part (SBs 4, 5, 6), +0.17 mm/d in the southern Amazon (8, 9, 10, 13, 14) and +0.07 mm/d in the central Amazon (SB 11, 12). The average precipitation, evaporation, and runoff over the 15 SBs of Amazon, after removing bias from P in SBs 1 and 3, are thus 6.10, 3.20 and 3.0 mm/d, respectively.

3.6. Summary and conclusions

This study focuses on the spatial and seasonal variability of the water budget components of the Amazon using different combination of remote sensing data products and observed gauge measurements. New information about TWS changes from GRACE and satellite based ET estimates are used to evaluate terrestrial water balance for more than four years at intra-basin and whole basin scales. Different datasets for precipitation and evaporation are examined and the most consistent data combination is selected for the study of dynamics using a land water balance approach and spatio-temporal consistency. The best data set for precipitation is GPCP in combination with ET data from University of Montana. The average annual rainfall for the entire basin from GPCP,

after removing its bias in SBs 1 and 3, is 6.1 mm/d, evaporation from ET-MON is 3.2 and runoff from in-situ data is 3.0 mm/d. This method based on water balance give smaller RMSE than previous atmospheric moisture convergence method [Syed et al., 2005] (0.61 and 1.28 mm/d respectively) over the Amazon basin and has a potential to be used to estimate discharge at different sub-parts of a large tropical basin.

The estimated runoff time series have better agreement at SB scale than the total runoff for the whole Amazon. Therefore the estimated runoff from the balance method for each SB is integrated downstream using an element-to-element routing method. An inundation data set is used to compute delay times instead of specifying flow velocities. This delay time is computed based on the maximum lag-correlation between upstream and downstream SBs. The estimated lagged runoff resolves the dynamics of the surface runoff better and can be used to estimate the runoff in different parts of the large Amazon. The monthly mean error for the whole Amazon basin decreases from 1.1 to 0.61 mm/d for the GPCP and ET-MON combination using the lagging method. This lagging method based on the TWS from GRACE and time series of inundation fractions is simple since it does not need assumptions about the channel Manning roughness and slope of the river and therefore, can be used in distributed routing models to get the hydrograph (time series) of the runoff at different locations for any large-scale watershed.

There are diverse uncertainties among different remote sensing retrieved data that affect water balance in the basin. The estimated uncertainty for GPCP is 0.8 mm/d over the entire basin [*Huffman et al.*, 2009], but larger biases occur in the smaller SBs 1 and 3 located in Andes and northwest part of the Amazon, exhibiting underestimates of 3.2 and

2.3 mm/d, respectively, based on water balance. Comparison of two different ET estimates shows that there is 1 mm/d difference between them over the Amazon. Improvements in remote sensing products especially time resolution, may come from the future GPM for precipitation, soil moisture from SMOS and SMAP, and runoff from the SWOT mission and may help reduce the uncertainties in the water budget and increase the knowledge of dynamics at finer time scales over the tropics. Also, other procedures for analyzing GRACE data might help to reduce noise and attenuation effects of smoothing of the data sets.

CHAPTER 4: DYNAMICS OF THE WATER BUDGET AND PAST STORAGE ANALYSIS OF AMAZON BASIN

Using the most consistent data combination from chapter 3, the seasonal dynamics of the water budget within the Amazon system are examined. The analysis is conducted in sub basin scale to capture different seasonality of the sub basins. The results reveal not only variations of the basin forcing but also the complex response of the inter-connected SB water budgets. Inter-annual and inter-sub basin variation of the water components are investigated and show large anomalies in north-western and eastern downstream SBs; aggregate behavior of the whole Amazon is more complex than can be represented by a simple integral of the forcing over the whole river system. The seasonal dynamics of the water budget within the Amazon system are also examined.

Total Water Storage changes (TWSC) is estimated from water balance equation using remote sensing based data as P and ET and in-situ runoff measurements for different SBs of the Amazon basin. The estimated values are compared to the anomalies of GRACE data set using EOF analysis. The results for the 2002-2006 period show significant agreement between both estimates and hence the estimated values since 1984 are used to reconstruct TWSC for the past (1984-2006). First five modes of the estimated TWS represent 82% of the variability of the data and are used to reconstruct the past TWS changes considering the other 18% as noise. Also, trend analysis of the

inter-annual changes are tried for the annual mean and climatologically wet and dry seasons in different SBs of the Amazon as a complex system. There is not a significant trend in TWSC of the annual TWSC for most of the parts; but significantly increasing and decreasing trends for wet and dry seasons of some SBs. This is consistent with trends of the inundated areas since 1993.

4.1. Introduction

Terrestrial water storage (TWS) as an important component of water budget plays a key role in the residence time of the fresh water in the continents. It can provide a feedback procedure to the climate variability as total of snow, soil moisture and surface water storage [*Koster et al.*, 2004; *Zeng et al.*, 2008a]. Seasonal and interannual variation of the TWS is of interest because it can point to the climate predictions.

Since this component is the total of soil moisture, ground water, snow and surface water storage variation, its quantification is difficult because of limited measurements in soil moisture and snow storage terms. The traditional method of estimating TWS is use of moisture convergence method (MCR) [*Marengo*, 2006; *Rasmusso.Em*, 1968; *J Roads et al.*, 2002; *Seneviratne et al.*, 2004]. This method considers both atmospheric and land surface water balance and hence precipitation and evapotranspiration vanish from the equation (Eq. 4-3).

Land: $d(TWS)/dt=P-ET-R$ (4-1)

Atmosphere: $dW/dt = ET- P - divQ$ (4-2)

$d(TWS)/dt = -divQ - dW/dt - R$ (4-3)

W is the vertically integrated water content of the atmosphere, or precipitable water, and dW/dt is the rate of change of precipitable water over time. The volume of water in the atmosphere is assumed to remain constant over time, so that dW/dt is expected to be close to zero over periods longer than approximately one month. Q is the vertically integrated moisture flux vector, and divQ is the vertically integrated moisture

flux divergence. Appling this method using the recent reanalysis data, seems to produce reasonable estimates over several river basins [*J O Roads et al.*, 1994; *Zeng*, 1999]. However in remote regions like Amazon with lack of radiosonde data, it fails to produce robust estimates [*Marengo*, 2005; *Zeng et al.*, 2008a].

Other studies have tried to quantify soil moisture using in-situ, remote sensing techniques, and data assimilation [*Dirmeyer et al.*, 1999; *Engman and Chauhan*, 1995; *Rodell et al.*, 2004b]. Although these studies give a better estimate of the soil water storage, they have either limited coverage, uncertainties because of vegetation influence in the moisture signal, or are dependent on the model use. The latter methods might be successful in providing soil moisture and TWS variation in large basin scale, they are too short to demonstrate the decadal TWS variability.

For a long time, the simple PER method has not been used in the studies because of lack of global observation based ET estimates and high uncertainties of the ET in the outputs of land surface models [*Marengo*, 2005; *Syed et al.*, 2005]. Later it is used to estimate TWS changes using observation based P and R and estimates of a land surface model for ET and therefore more observational constrain compare to the moisture convergence method [*Zeng et al.*, 2008a]. The results of the study for the large Amazon basin shows its ability in depicting long-term water storage changes, in a way significantly more robust than the moisture convergence method [*Zeng et al.*, 2008a].

Since 2002, there have been large-scale observational data - Gravity Recovery and Climate Experiment (GRACE) was lunched in 2002. Becker et al. [*Becker et al.*, 2011] reconstruct the past terrestrial water storage in the Amazon using the EOF analysis

and correlation of the in-situ river runoff data with GRACE leading modes for the 1980-2008 period. They concluded that there is no trend in long-term variability of the estimated TWS.

In this chapter, first we analyze the inter annual variation of Amazon sub basins, and then we propose to use PER method using remote sensing based P, ET and in-situ river runoff data for the Amazon (1984-2006). In order to detect the spatial variation of the TWS we divide Amazon to 12 smaller basins and compute the average values for each basin to be consistent with the runoff values. We also use multi-satellite based estimates of the inundation fraction (1993-2006) to compare to the inter-annual variation of the estimated values.

4.2. Spatio-temporal variation of the water budget components using the most consistent data combination

Based on the analysis of different products in water balance study in chapter 3, the spatio-temporal variation of the water budget components using the most consistent data combination is studied. Figure 4-1 shows the mean and seasonal variation of the precipitation estimates from GPCP data. While the northwestern SBs receive the largest rainfall amounts, they exhibit smaller seasonal variations such that they never have a dry season with rainfall less than 3.5 mm/d. The eastern SBs, 10, 13, 14, and 15 have larger seasonal variations of 10-12 mm/d despite generally smaller annual mean amounts. Generally the western SBs have the wet season prior to the eastern SBs. Note also that precipitation in SB 6 has the opposite seasonal variation than the other SBs

because of its latitudes.

The mean ET map from ET-MON in Figure 4-2 (left) shows values from about 3 to 3.6 mm/d over the Amazon, smaller in SBs 6, 8 and 9 with partly flooded Savannah vegetation and SB 2 located in the Andes. Seasonal variability of ET, as a difference of extreme values (Figure 4-2, right), varies among the SBs, exhibiting maximum variation in SBs (5, 8, 12, 15). Maximum ET accruing in the dry season in these particular forested SBs (11, 12, 15) from all three ET estimates is consistent with the analysis by [*Alan K Betts and Silva Dias*, 2010; *da Rocha et al.*, 2004; *da Rocha et al.*, 2009], which they explain by larger radiation in this season and more water storage (drainage from upstream SBs). However, SB 8 has larger ET in the wet season because of the water stress in a longer dry season (figure 3). The vegetation type of this SB is savannah, which makes it different than SB 11 and 12.

The annual mean and variance of the total water storage (TWS) are shown in Figure 4-3 from the JPL 500 km smoothing radius version. The annual mean is negligible for the most of the SBs (±0.07 mm/d) with a positive sign in the western SBs and a negative sign in the eastern ones. Seasonal variation of TWS (Figure 4-3 right), as a difference of maximum and minimum, shows SBs with larger storage variation due to accumulation of water from upstream SBs. In this figure, SB 15 which is outlet of the whole Amazon, shows smaller seasonal variation that the upstream SBs although its intra-basin P and ET have large variations. This is because this SB and SB12 receive contributions from upstream SBs with different wet and dry seasons and therefore are flooded during their local dry season.

Annual mean and seasonal variation of discharge are shown in Figure 4-4 based on In-situ data. Northwestern SBs shows larger contributions in net runoff than southern SBs; but the larger areas of the latter ones produce large discharge to the outlet of Amazon. The distribution of annual net runoff among the SBs follows the precipitation distribution: the largest discharge is observed in northwest SBs (3 to 5) with the largest annual mean precipitation. In particular SB 3 exhibits an annual mean discharge of 12 mm/d, and receives the largest annual mean precipitation. This correspondence is not seen in the seasonal variation range of runoff. Since this component is response of the variations of other components of the water budget, its seasonal variation follows the combination of the other three (Figures 4-1, 4-2, 4-3 and 4-4 right).

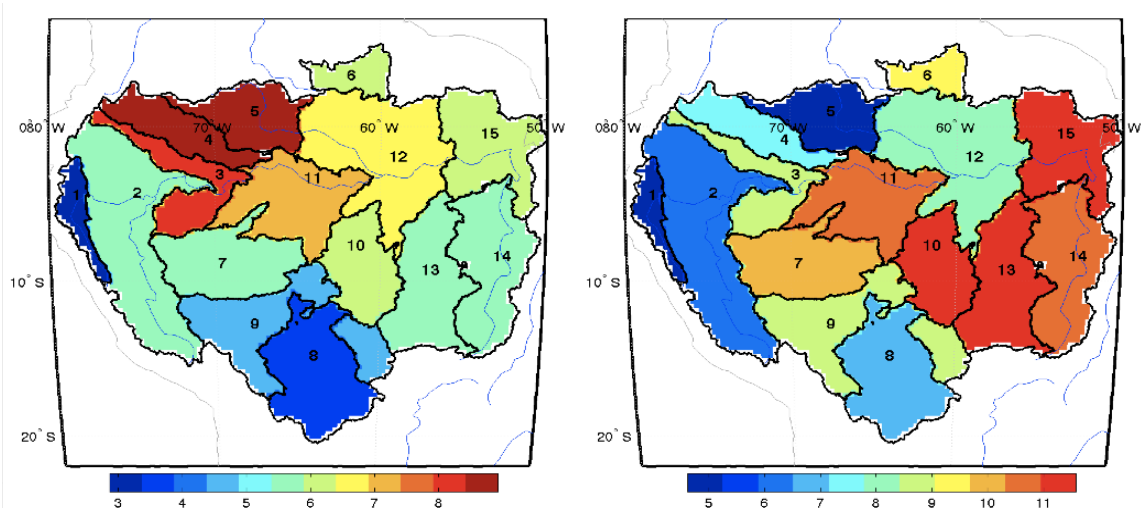

Figure 4- 1: Annual precipitation (left) and its seasonal range (max-min) (right) (mm/d) in different SBs using GPCP for different SBs for 2003-2006. For more information on SBs see Table 3-1.

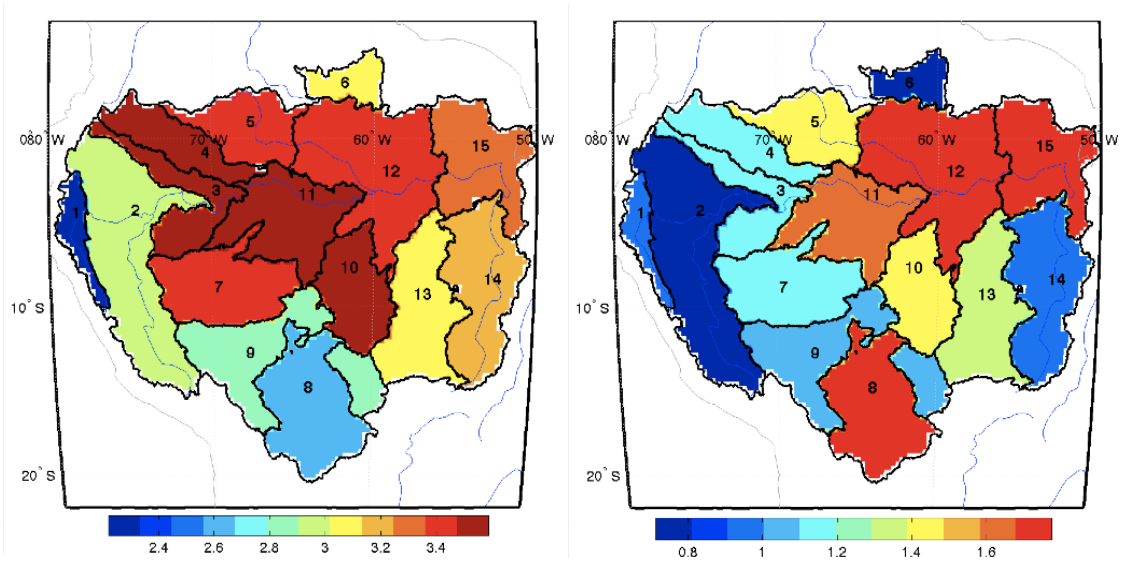

Figure 4- 2: Mean annual evapotranspiration (left) and its seasonal range (max-min) (right) (mm/d) for different SBs (numbers) using ET-MON for 2003-2006. For more information on SBs see Table 3-1.

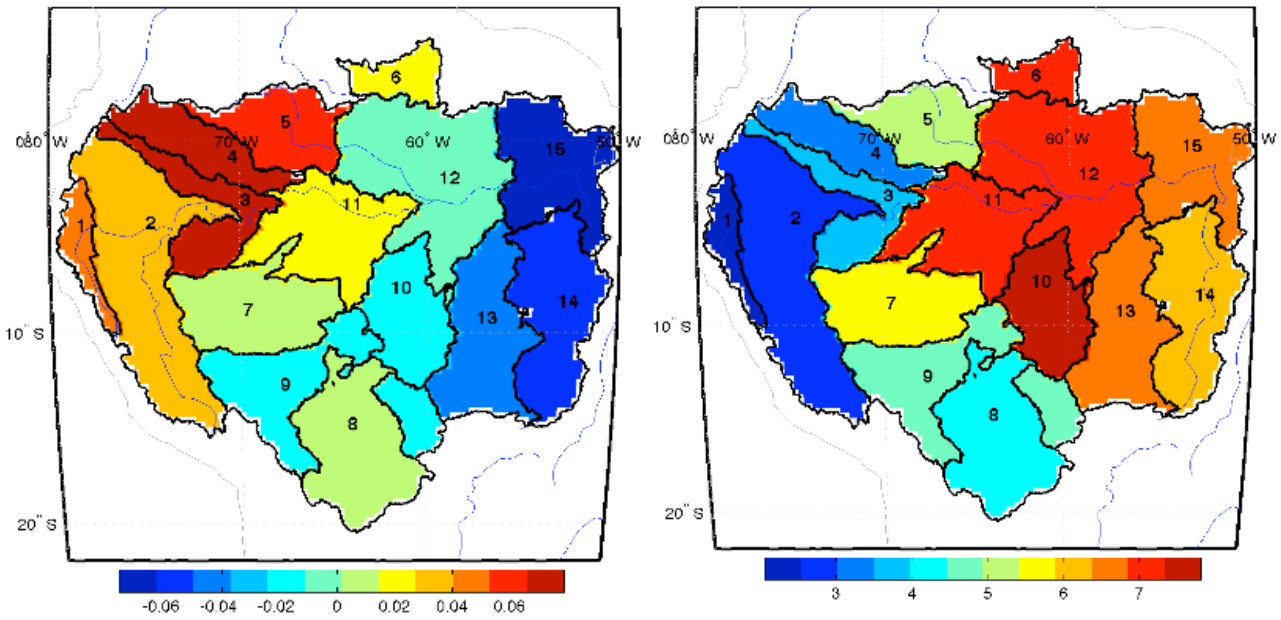

Error! Bookmark not defined.

Figure 4- 3: Mean and annual water storage changes (left) and its seasonal range (max-min) (right) (mm/d) using GRACE 500km smoothing radius for 2003-2006. For more information on SBs see Table 3-1.

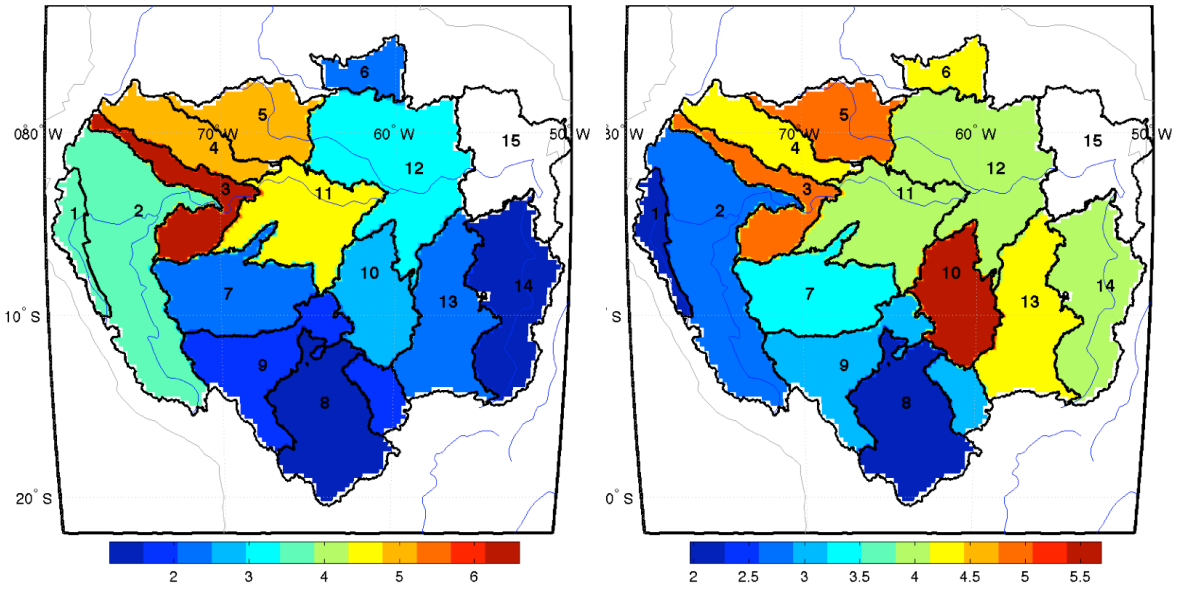

Figure 4- 4: Mean (left) and seasonal range (max-min) (right) of runoff (mm/d) for different SBs using in-situ data for 2003-2006. For more information on SBs see Table 3-1.

4.3. Dynamics of the water budget

After choosing the most consistent data set for precipitation and evapotranspiration in chapter 3, along with inundation data and observed runoff and storage changes, we investigate the dynamics of the water balance in the Amazon SBs. Since the whole Amazon has a very large drainage area within which wet and dry seasons, vegetation and topography all vary, study of the dynamics provides more detail on the interaction of the atmosphere and land and might provide a clearer indication of the controlling processes.

The water budget components are linked temporally so that generally when rainfall increases in the wet season, ET, R and TWS change as a response. Usually this response is an increase but there are some contradictory cases that will be discussed here. For instance, TWS in SB 12 is a minimum during the dry season and decreased runoff in upstream SBs while its local dry season occurs two months later (Figure 3-7). ET in SBs 5, 11, 12, and 15 with short dry seasons increases with decreasing P in the dry season because of increased net radiation (Figure 3-6). This increase of ET in the dry season in the eastern tropical forests is reported in extended measurements during LBA by [*da Rocha et al.*, 2004; *Goulden et al.*, 2004] and contradicts earlier studies showing little seasonal variation of ET. Conversely, reanalysis ET data from ERA-40, exhibits larger seasonal variations of ET because of insufficient moisture storage in the model root-zone [*Alan K Betts and Silva Dias*, 2010].

To investigate inter-annual variation of the water budget components, normalized and de-seasonalized anomalies of each component are computed for the entire Amazon basin and displayed in Figure 4-5 for the 1984-2006 period. Note that since TWS from GRACE is available after 2002, it is not included in this analysis and therefore observed runoff is used. Generally there are opposite sign anomalies of P and ET while runoff anomalies follow P with a lag. Although the total anomalies are not sensitive to El Niño-Southern Oscillation (ENSO) indices (correlation coefficients less that 0.5), in extreme events they exhibit larger variation. The two ET estimates have a better agreement in interannual variability except during La-Nina of 1999 when ET-PRI increases with the increased P while ET-Zhang decreases.

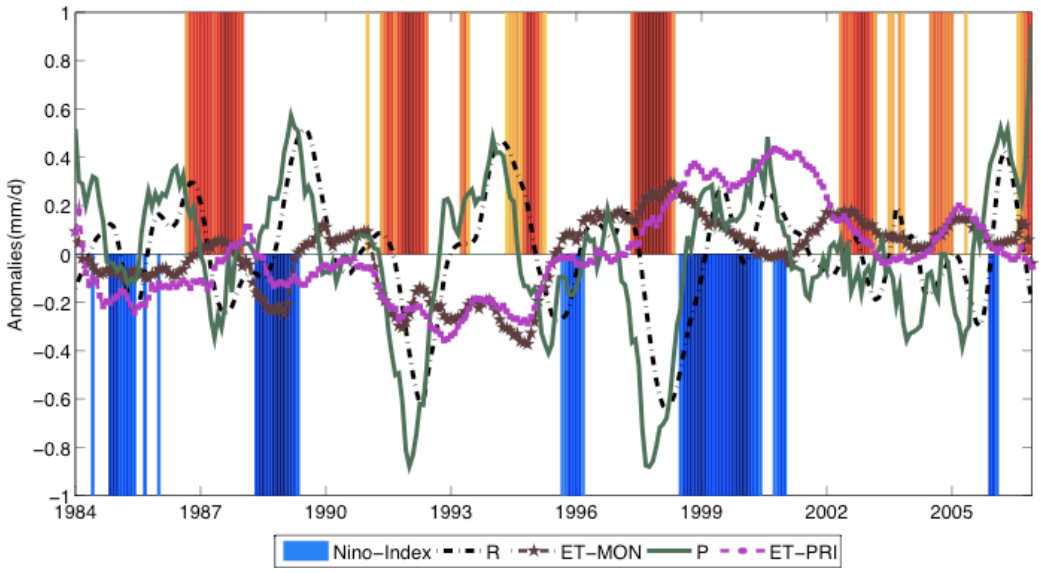

Figure 4- 5: Normalized de-seasonalized anomalies of water budget components for the entire Amazon basin. P based on GPCP, ET from ET-PRI and ET-Mon-Z, R is in-situ measurements. Indexed Large ENSO events with positive and negative signs are shaded.

Figure 4-6 shows the standard deviation of de-seasonalized anomalies of the three components (P,ET and R) based on GPCP, ET-Zhang and in-situ runoff gauges. Northern and downstream eastern SBS exhibit large interannual variability. These anomalies are as large as 0.82 mm/d for P, 0.22 for ET and 0.80 mm/d for R. Since these SBs also show large annual mean values, these results are expected. This might also suggest that in order to investigate long-term and significant variability of the water in Amazon, one should focus on the regions with large P and R variation.

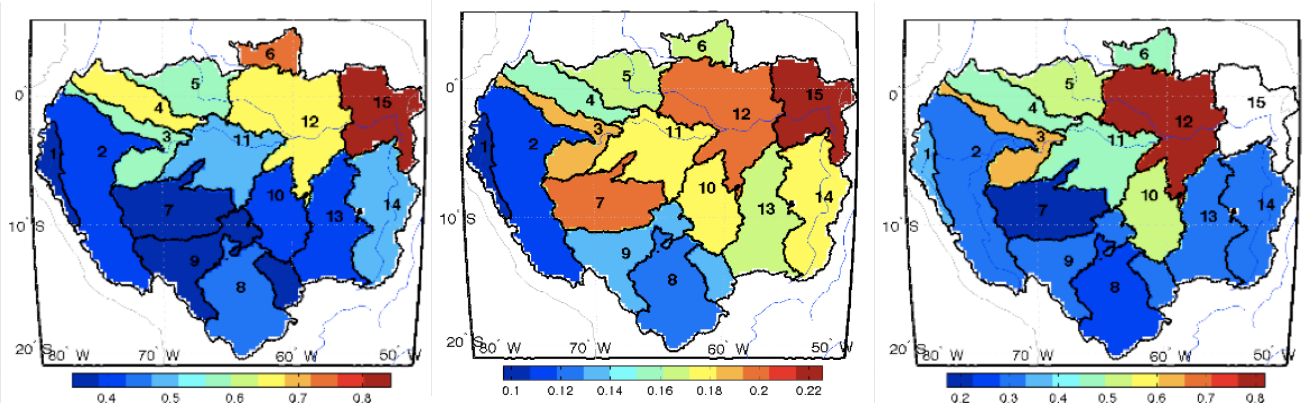

Figure 4- 6: Interannual standard deviation (mm/d) of P based on GPCP (left), ET based on ET-Zhang (middle), and R based on gauges (right) from 1984 to 2006 after filtering high frequencies using 12 months running mean.

In order to analyze the impact of ENSO events on the water budget components of Amazon SBs, they are divided into their local wet and dry seasons because of the seasonal impact of these events. Out of 15 SBs of the Amazon, only four exhibit significant correlation ENSO. Precipitation in SBs 5, 6, 12 and 15 show significant correlations of 0.65 to 0.8 with the Pacific Nino index (Nino 3.4) for the Dec-Feb

months. Runoff follows P with a lag time in SBs 5,6, and 11 and also is cross-correlated in SB 12 to ENSO (-0.65) during its dry season. ET does not show any significant correlation with the ENSO for the entire Amazon.

4.3. Past storage analysis

TWS is computed for each SB from surface water balance and then compared to the observed GRACE data in 2002-2006. Also inundation fraction data is also analyzed and plotted against TWS to investigate their agreement for the same time period. Then the estimates of TWS for the 1984-2006 will be used to investigate the interannual variation of the storage. To analyze this in detail, interannual variation of the estimated TWS will be tried in annual, wet, and dry seasons.

The datasets have different resolutions. Precipitation and ET are over gridded areas while runoff is measured at specific points using gauges along the Amazon river and its tributaries. To distribute the runoff over the total area, the Amazon basin is divided into 14 subbasins (Figure 3-1). The net runoff over each subbasin is the runoff at the mouth of the basin minus incoming flow into the subbasin.

$$R_{net} = R_{total} - R_{incoming} \quad (4\text{-}4)$$

Inundation data is available since 1993 and will be compared to the estimated TWS as another independent data. Although it does not cover the entire period, its long estimates (14 years) can be used to test the robustness of the time series of estimated TWS.

4.3.1. Comparison of TWS from WB, GRACE and inundation areas

TWS changes is estimated from water balance method and compared to the GRACE estimates in different SBs (Figure 4-7). Also inundated areas are averaged for each SB and then the differences between normalized inundation areas of two months are computed. These estimates are zero for two small SBs 1 and 6 where flooding areas don't vary in the data sets. Therefore, d(inundation) is not shown for the two mentioned SBs. Correlation coefficients between the estimated TWSC, normalized inundation fraction, and GRACE data is computed and shown by r_1 and r_2, respectively, in Figure 4-7. As it is seen in Figure 4-7, generally there is a strong agreement between all three estimates for most of the SBs. Water balance method under-estimates, mostly because of P, the storage changes in the mountainous regions (SBs 1 and 3) as it is also reported in a dynamics study [*Azarderakhsh et al.*, 2011]. The correlation coefficient between estimated and GRACE TWSC for most of the SBs is higher than 0.67, which indicates the ability of the water balance to detect the seasonal variations well. Also this Figure shows that the inundation data cannot be used to represent the variation of the storage in SB 13 and 14 that might be because of lower variation of the surface water areas in these basins.

Consequently, the estimated TWSC from WB will be used to estimate the variation of storage in longer period. Since d(inun) has area units, and not consistent with TWS, its time series will be used to validate the estimated variations (correlation coefficients).

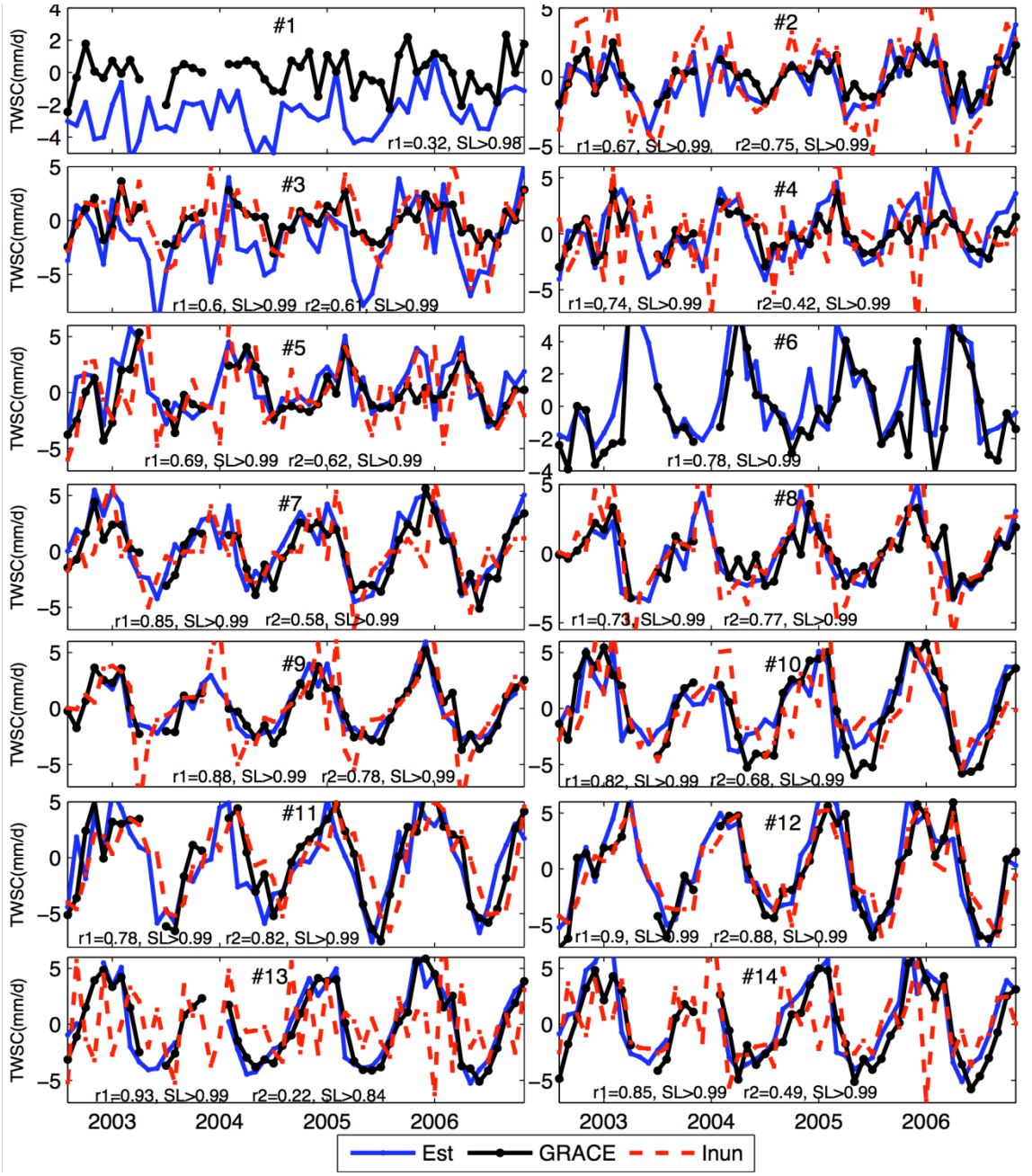

Figure 4- 7: Comparison of the estimated TWS from WB method, normalized d(inundation) and GRACE for over 2002-2006 period is different SBs (shown with numbers). r1,r2 are correlation coefficients between GRACE and WB and d(inun) respectively and SL is the significance level.

4.3.2. EOF analysis of the estimated TWS

We used EOF analysis to show the spatio-temporal variation of the TWSC for the 23 years period. We compared the EOF modes in 2002-2006 from WB to GRACE to see if they both give the same spatio temporal variation. Since estimated values from WB for the SBs 1 and 3 gives large errors, we remove these SBs and therefore they are not shown in the results. Figure 4-8 shows the first three leading modes of the estimated TWSC and their time variation. The interannual variation of the TWC associated with ENSO events occurs in seasonal cycle and therefore cause decrease or shift in seasonal cycle. There fore, filtering 12 months running average or removing annual cycle will also reduce the ENSO related signals. For this reason, the EOF analysis is applied on the absolute values without taking the seasonal cycle and seasonal cycle is expected to appear in the first mode as figure 4-8 also shows. The first three leading modes of WB represent 96% of the variation in the data set and are very close to those from GRACE.

Then we applied EOF analysis on the longer record to investigate the anomalies in longer period and also to see if the theory of stationarity of TWSC over Amazon is correct [*Becker et al.*, 2011].

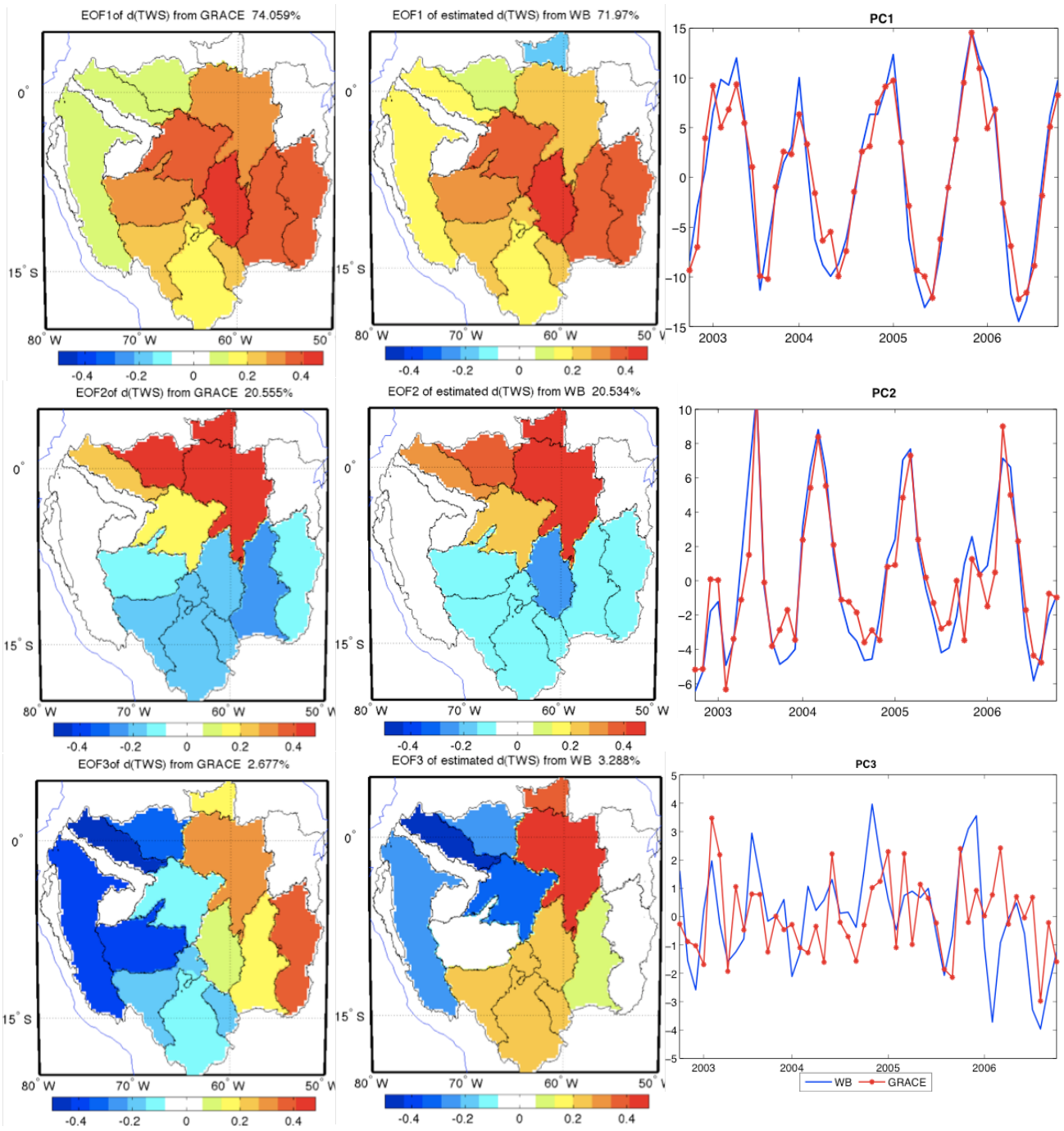

Figure 4- 8:Leading modes of TWSC from GRACE and WB for 2002-2006 period.

The mean and seasonal variation of the estimated past TWSC are computed and shown in figure 4-3. As seen in this figure mean annual TWSC is very small and ignorable while seasonal variation of it varies in different SBs from 2.5 to 7.5 mm/d. To investigate the interannual variation, de-seasonalized anomalies for each SB is computed and then shown in figure 4-5. In most of the SBs, large anomalies are associated with ENSO events. These anomalies are larger in downstream SBs 11 and 12 and smaller in the northern SBs. The anomalies are larger during ENSO events; but there is no clear relationship between different ENSO events and storage.

Comparison of the d(Inun) anomalies for the 1993-2006 with the estimated anomalies for different SBs is also shown in the figure and shows well agreement between the two.

Earlier studies have studied interannual variation of the P and R using observation based data sets over different regions [*Villar et al.*, 2009,b; *Villar et al.*, 2009,a] and reported trends in wet and dry seasons of the regions. Therefore, we divide the estimated TWSC to local wet and dry seasons and then investigate the significant trends (>99%) in each. Figure 4-9 shows that the mean TWSC shows decreasing trend over 23 years. This trend is positive in wet season of SBs 5 and 12 while is negative during their dry seasons. Also southern SB 7 and 8 shows significant decreasing trend in storage changes especially during the dry season. Since the surface and under ground storage capacity of train does not vary significantly over time any change in TWSC changes would be a

function of residual of P, E, and R. In other words, anomalies in P, E, and R will impose anomalies in storage.

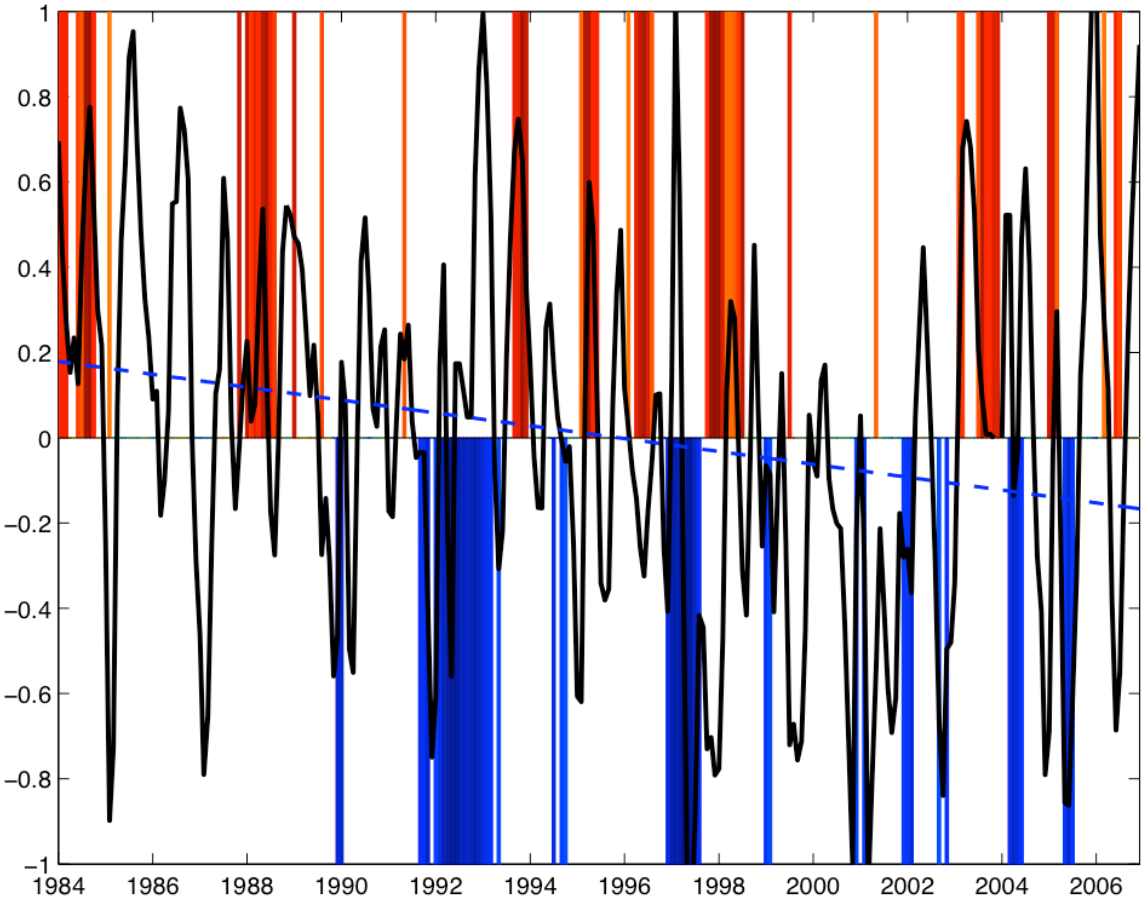

Figure 4- 9: Trend of TWS variation for wet and dry season and annual average (1984-2006). El-Nino years are highlighted in the background.

4.4. Conclusion

Study of intra-basin dynamics, based on the consistent data set, shows that the water budget components, except ET, exhibit large seasonal variations within the Amazon basin. The northwest SBs have the largest rainfall amounts, approximately 8.5 mm/d, while the southern SBs average 5 mm/d. Storage change is also very dynamic and is

larger during the extreme changes of the intra-SB precipitation. For the two downstream SBs the seasonal variation is stronger during the dry and wet seasons of their upstream SBs with larger discharge contribution.

Interannual variation of the de-seasonalized anomalies of P, ET, R for a longer period of 23 years are investigated for the whole basin. During this period, there are large anomalies in all of these three components especially during ENSO events. The spatial pattern of the interannual variation of the components follows the mean annual values so that these anomalies are smaller in southern SBs and larger in northern and downstream SBs.

Seasonality is not significant in evaporation except for southern SB 8 with Savannah vegetation and in Negro and Amazon rivers as large as 0.6 mm/d as a result of decreased cloudy days and larger net radiation. This is seen in all three remote sensing based ET data sets while earlier reanalysis based ET estimates did not show this pattern. Also the effect of smoothing the GRACE data can introduce more uncertainties to the data.

Average P over the whole Amazon basin based on the water balance and consistent data combination, after removing bias in SBs 1 and 3, for the 2003-2006 period, is 6.10 mm/d. This value for ET is 3.2 mm/d. Also the average discharge over the whole area of Amazon at its mouth would be 3 mm/d. Compare to the previous studies on Amazon, The estimated P from this study is larger than estimated values from other studies. However, R is very close to the estimated values by Marengo. TWSC over the

whole Amazon has strong seasonal variation as high as 2.37 mm/d. This value is much more is downstream SBs and smaller in upstream ones.

Moreover, the past total water storage was constructed for more than 23 years. First, based on the most consistent products and ground measurements, the total water storage was estimated for the period of time that GRACE observations are available. The Results were compared and promising consistency was found. Then, using the same method the past total water storage (TWS) was estimated. The relationship between this past storage and surface water inundation was consistent. A trend analysis was conducted using this record. The record was not long enough to draw a firm conclusion. The results based on 23 years reveals that the dry seasons are getting drier and wet season are changing to wetter seasons, and the whole seasons has slightly decrease in storage.

CHAPTER 5: WATER BUDGET ANALYSIS OF LARGE MISSISSIPPI BASIN

In this chapter, we are trying to present our studies of water budget analysis over large Mississippi basin. This is based on what we learned at chapter 3 and 4 to investigate the potentials and limitations of using remotely sensed data in hydrologic and hydro climate studies. First, the basin is introduced and its characteristics are highlighted. The whole basin based on topography maps and the locations of gage stations are divided to several sub basins. We apply different combinations of different products of water budget components to estimate the runoff over the whole basin. The mean annual runoff for the whole basin based on ground observations is about 0.35 mm/day. This amount of runoff compared to Amazon basin, 3 mm/d, is very small, and has even smaller seasonal variation of 0.16 mm/d (0.95 mm/d in whole Amazon basin). Therefore, the uncertainties of the remote sensing based estimates might be as large as the runoff and might seem unreliable. Therefore, I examine the ability of different remote sensing based estimates using Taylor Diagrams, which analyzes the standard deviation of the errors, RMSE and correlation coefficient. The results confirm the results of the Amazon basin, which indicates that P is the driving factor in water balance and the remote sensing-only products have largest uncertainty in the water budget. Also, lagging method at this basin is applied to compare to the Amazon basin and test it in this mid-latitude basin. Since surface runoff has smaller annual and seasonal variability in most the far SBs and larger

variability in eastern and southern SBs which have smaller delay time, the lag time is smaller and therefore does not change the seasonal variability of the integrated runoff from the average over the whole basin. This will be discussed more in this chapter.

5.1. Introduction

The Mississippi River is the largest river system in North America. Flowing entirely in the United States, this river rises in western Minnesota and wanders to the south for 2,320 miles (3,730 km)[5] to the Mississippi River Delta at the Gulf of Mexico. The Mississippi basin drains all or parts of 31 U.S. states between the Rocky and Appalachian Mountains and even reaches into southern Canada. The Mississippi ranks fourth longest and tenth largest among the world's rivers. The Mississippi River drainage basin is the world's second largest, draining 4.76 million square kilometers (1.83 million square miles), including tributaries from thirty-two U.S. states and two Canadian provinces. The Mississippi River watershed encompasses 40 percent of the contiguous United States. Major tributaries include the Missouri, Ohio, Arkansas–Red–White, and Tennessee Rivers.

Several studies have dealt with water budget analysis of Mississippi river basin. Syed et al (2005) proposed a method for estimating monthly river basin outflows based on the use of new GRACE satellite estimates of terrestrial water storage changes in a coupled land-atmosphere water balance. Their method was tested on the Amazon and Mississippi river basins, and could ultimately be applied to the major drainage regions and river basins of the globe. Estimated total basin discharge in the Mississippi river

showed good temporal covariance; but had greater annual amplitude than observed streamflow (Fig 1-3.a). Results for both basins highlight important differences between estimated total basin discharge and observed streamflow, at least part of which can be attributed to groundwater storage changes (RMSE of 0.7 mm/d). Atmospheric moisture data and methods of GRACE data processing also contributed to the differences over Mississippi basin [Syed et al, 2005].

In another similar study by [*Sheffield et al.*, 2009a], the total runoff for Mississippi is estimated using satellite data for P, ET and TWSC (Figure 1-4). As described in Chapter 1, the estimated runoff from this method, even after removing seasonal bias from precipitation data, does not agree with the observed runoff and over estimates the flow (RMSE of CMORPH and TMPA based estimates are equal to 1.6 and 1.7 mm/d respectively). The authors tried to remove the seasonal bias from the estimates and then computed the smaller RMSE values to be 1.3 and 1.4 mm/d respectively.

Figure 5- 1: Mississippi river basin and its major tributaries (Courtesy of USGS)

5.2. Seasonal Cycle of Water budget components from different data sets over Mississippi basin

Mississippi basin has 5 major sub basins. However, in this study we divide the whole basin to 12 sub basins based on Hydro 1k topography data and the locations of the gage stations as shown in Figure 5-2.

Monthly discharge data sets are collected from US Geological Survey, Water Resources Data. Similar to Amazon basin, Net runoff from each SB is computed as difference between the outgoing and in-coming flows and then compared to the SB-

averaged estimated residual of the other components. The location of the gages and their drainage areas are shown in Table 5-1.

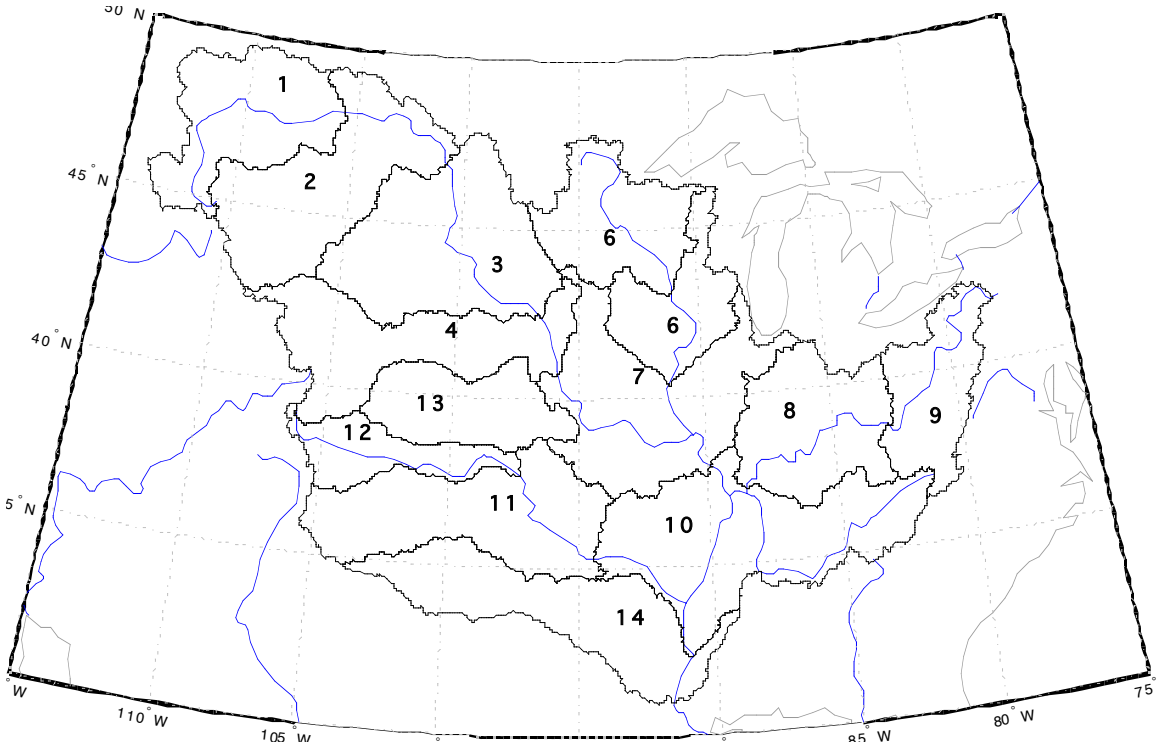

Figure 5- 2: The location of 12 Mississippi sub basin based on topography maps and the locations of the gages

Seasonal variation of P from different P estimates is shown in Figure 5-3. The detail information about the data sets is in Chapter 2. CMORPH and PERSIANN exhibit larger annual and seasonal P values in most of the SBs of Mississippi than GPCP and TMPA. The differences between mentioned estimates from different P data sets are similar in SBs of Mississippi than Amazon where CMORPH and PERSIANN give smaller estimates in western SBs than GPCP and TMPA. Since both ET data give same seasonal cycle and very smaller difference (bias is less than 0.4 mm/d), the differences in estimated runoff as residual of will depend on P differences. Also this Figure shows that

SBs located in Upper Mississippi and Ohio contribute large annual P values for the whole basin than western SBs.

Table 5- 1. Location and drainage area of gage stations of SBs of Mississippi basin

SB	Sation	Latitude (deg)	Longitude (deg)	Drainage area (km2)
1	Missouri River near Wolf Point MT	48.07	-105.53	213039
2	Missouri River at Bismarck, ND	46.81	-100.82	482567
3	Missouri River at Sioux City, IA	42.49	-96.41	814462
4	Missouri River at Nebraska City, NE	40.68	-95.85	1061441
5	Mississippi River at McGregor, IA	43.03	-91.17	174749
6	Mississippi River at Keokuk, IA	40.39	-91.37	308077
7	Mississippi River at Chester, IL	37.90	-89.84	1834481
8	Ohio River at Smithland Dam, Smithland, KY	37.16	-88.43	372799
9	Ohio River at Greenup Dam near Greenup, KY	38.65	-82.86	160511
10	Mississippi River AT VICKSBURG, MS	32.32	-90.91	2962974
11	Arkansas River at Ft. Smith, Ar.	35.39	-94.43	388273
12	Arkansas River AT WICHITA, KS	37.64	-97.34	104824
13	Arkansas River AT DESOTO, KS	38.98	-94.96	154701

Comparison of the two ET estimates, ET-MON and ET-PRI, for different SBs of Mississippi is shown in Figure 5-4. The differences between two estimates are smaller than Amazon basin and they have larger agreement in seasonal variation of ET. Mean annual ET varies from 0.86 mm/d in SB 2 to 1.82 mm/d in SB 10 while its seasonal variation varies from 0.81 mm/d in SB 11 to 1.3 mm/d in SB 8.

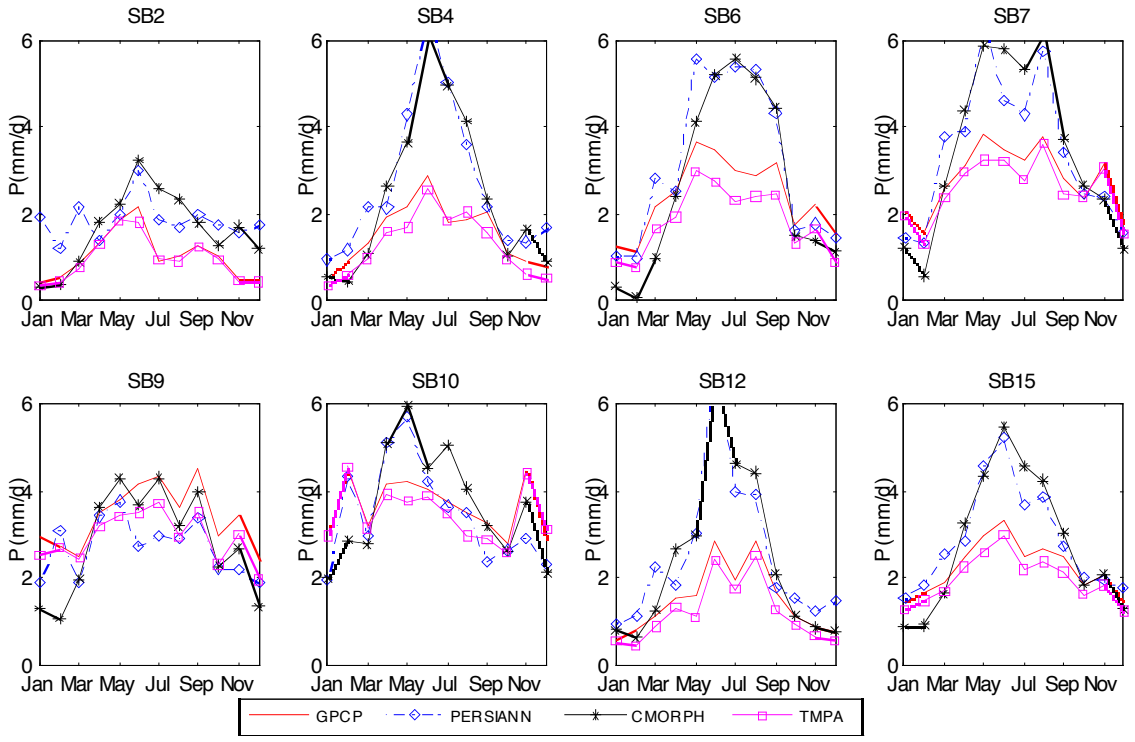

Figure 5- 3: Seasonal variation of P for 2003-2006 from different data (mm/d) over SBs of Mississippi.

Figure 5-5 shown the seasonal variation of the TWSC in different SBs using GRACE 500 km smoothing radius from different centers. As seen, in this figure, upstream western SBs, unlike the seasonal variation of P and R, have seasonal variation as large as downstream SBs (up to 1.5 mm/d). The maximum seasonal variation occurs in SB 10 of 0.83 mm/d, which is larger than the values at downstream SB 14 (0.75). TWSC in Amazon basin was larger in downstream SB because of accumulation of water and large natural capacity of the streams and floodplains at these parts. This also might be because of the changes by human constructed storage structures (Dams).

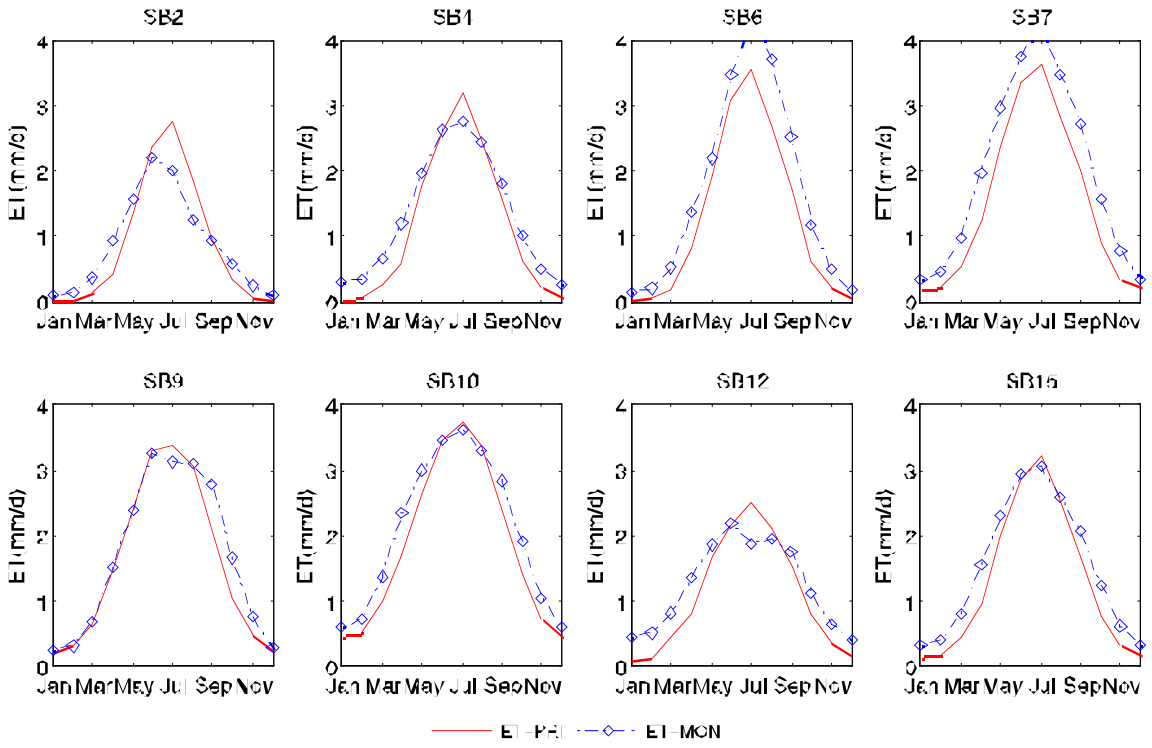

Figure 5- 4: Seasonal variation of ET for 2003-2006 from two estimates (mm/d).

Seasonal variation of runoff using in-situ and also estimates from WB based on two different combinations is shown in Figure 5-6. As seen in this figure, Runoff is western SBs is very small, 0.08 mm/d, and has even smaller seasonal variation values (up to 0.05 mm/d). While the total runoff (SB 15), measured at Vicksburg station, exhibits very small seasonal changes of 0.11 mm/d, it increases as large as 0.6 mm/d in SB 9, which is also one of the main contributors to the total discharge in Mississippi basin. GPCP-MON based estimates give closer values to the observed in all SBs than CMORPH based estimates. The error and uncertainty analysis of the estimates will be discussed in next section.

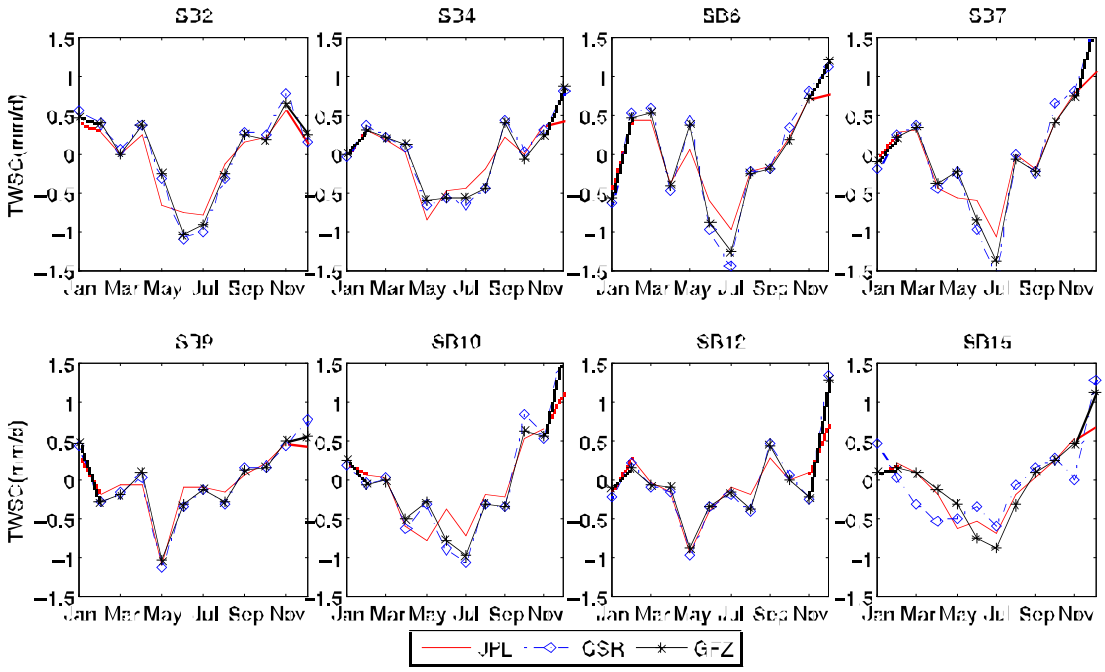

Figure 5- 5: Seasonal variation of the TWSC for 2003-2006 from GRACE estimates.

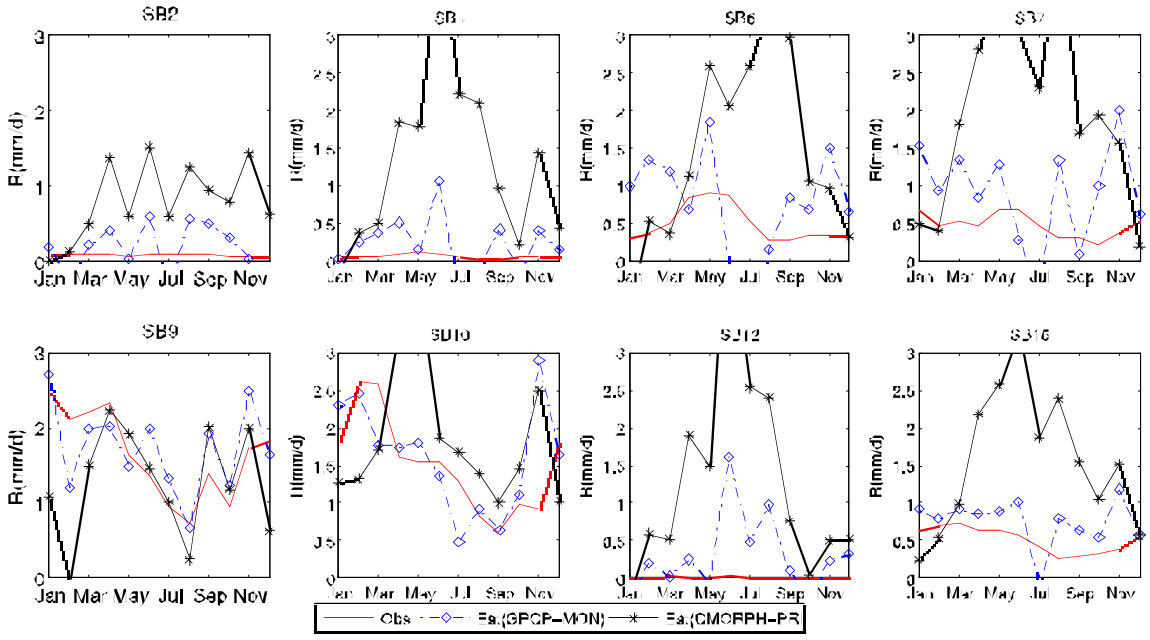

Figure 5- 6: Seasonal variation of runoff for 2003-2006 from in-situ data and two different estimates from WB in different SBs of Mississippi.

Similar to Amazon basin Inundation data are used to investigate the seasonality of the surface water extent and shown in Figure 5-7. This Figure shows the maximum changes in inundation percentages in Mississippi. The seasonal variation of surface water in western SBs 1,2, and 3 is zero; or might not be detectable by the surface water extent data; while it increases as large as 90% in north and eastern parts. To look at this in more detail, the time series are compared and the correlation coefficient between the in-situ runoff and inundation data is computed. Figure 5-8 shows the time series in four dynamic SBs. As seen the correlation between the estimated values from GPCP and ET-MON combination is smaller than the inundation percentage in all of the SBs, which exhibit larger seasonal inundation. Therefore, this data set will be used to estimate the lag time from upstream SBs to the downstream ones.

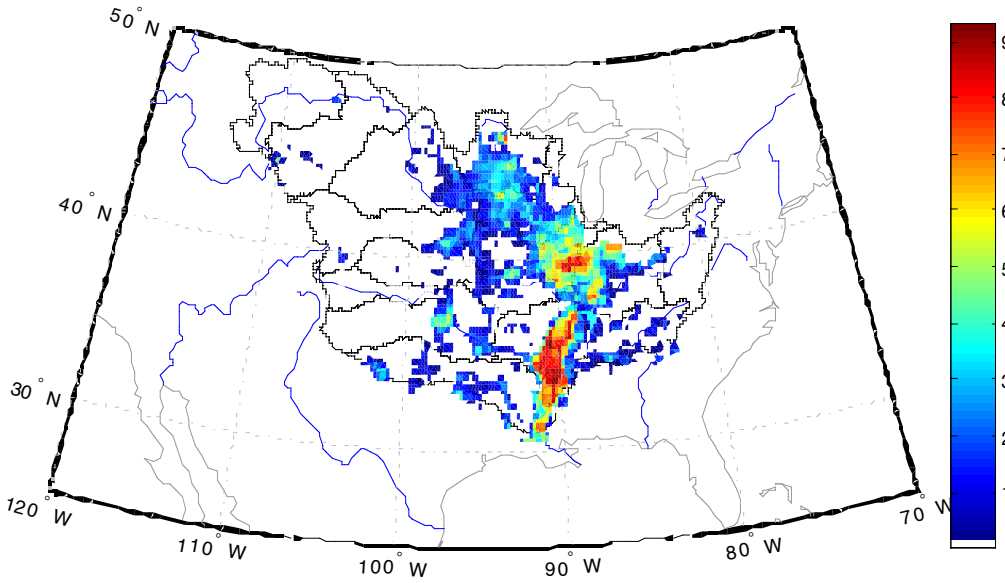

Figure 5- 7: Seasonal variation of the inundation percentage estimates (max-min) in Mississippi.

To evaluate the validity of the estimated runoff values in individual SBs, Taylor diagram is drawn and shows three important factors in evaluation of the model (Figure 5-9). This figure shows that for the whole Mississippi basin (SB 15) all of the data combinations give close correlation coefficient of 0.8 while they exhibit different STD and RMSE values. The correlation coefficient in western SBs is smaller (0.15 to 0.4) for all of the P and ET pairs. These SBs have very small seasonal runoff variation (Obs in the plot); while estimated values have larger STD values. All of the pairs have smaller RMSE and closer STD to the observed values in eastern and north SBs. Therefore, the error is not distributed equally in the whole basin and therefore averaging the values for the large Mississippi basin will produce more uncertainty in seasonal variation of the runoff.

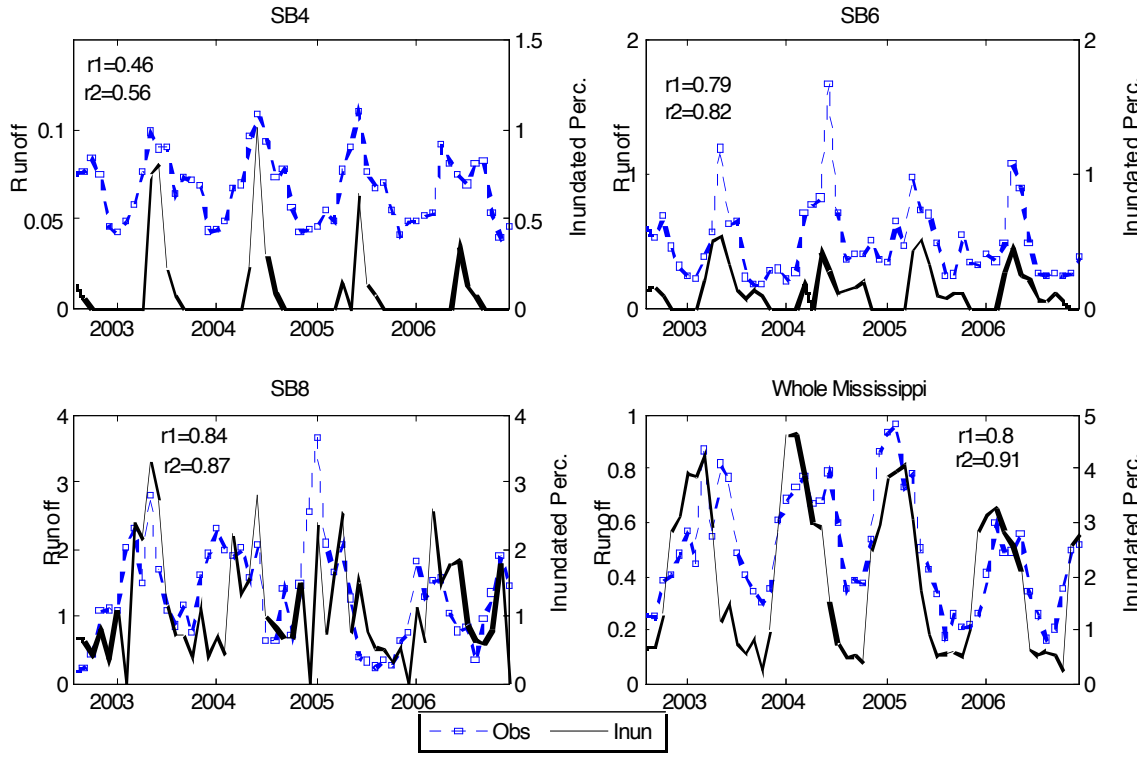

Figure 5- 8. Time series of cumulated runoff and inundation percentage in 4 SBs of Mississippi.

Correlation coefficients between the observed runoff and estimated runoff (r1) and inundation (r2) for each SB are shown in each plot.

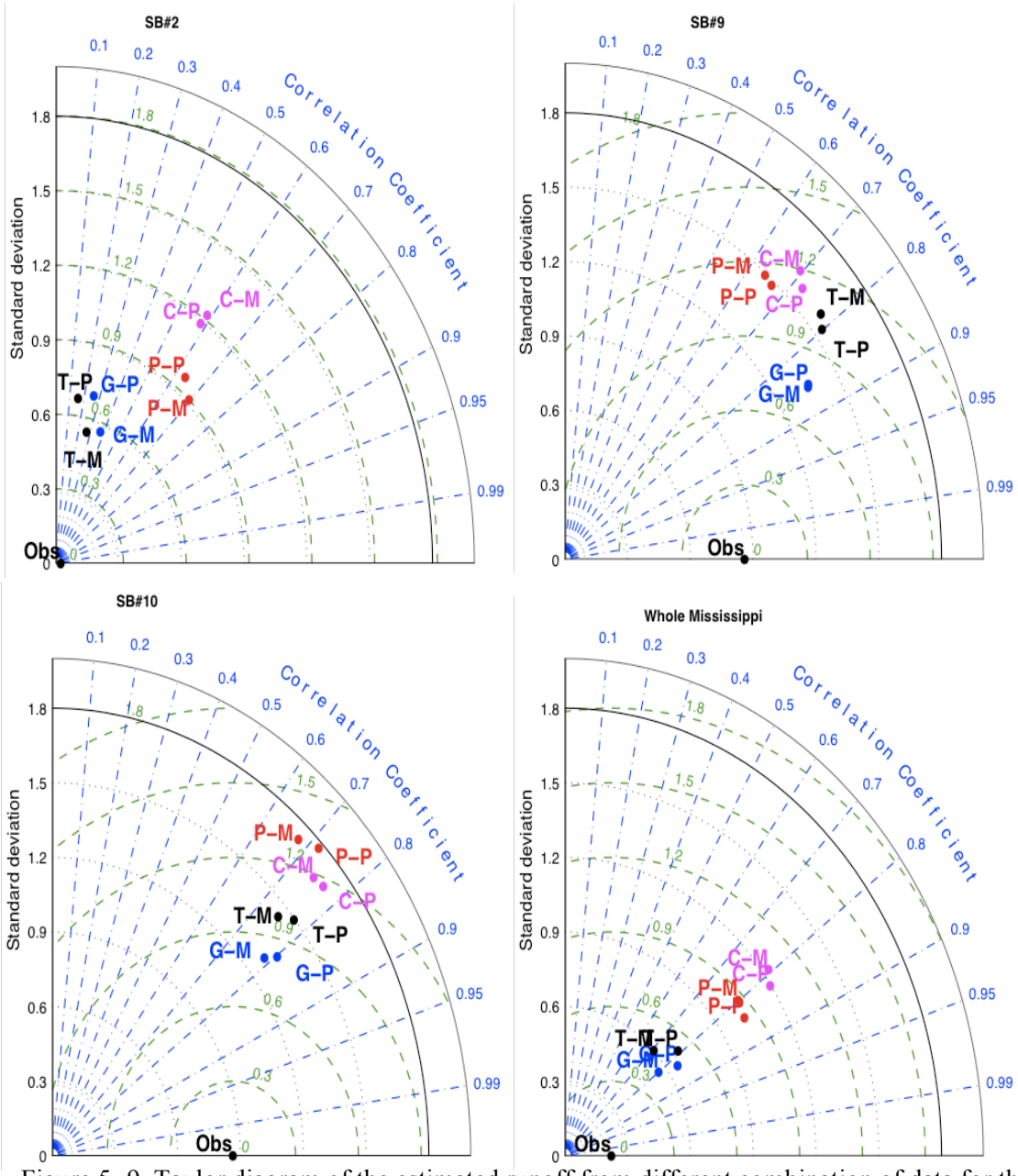

Figure 5- 9. Taylor diagram of the estimated runoff from different combination of data for the whole Mississippi and three SBs

After applying the lagging method in Mississippi basin, the RMSE and correlation coefficients are compared to the former values. Figure 5-10, shows the time series of the total runoff from Mississippi before and after applying lagging compare to the observed values. As seen in this figure, RMSE decreases for GPCP-MON pair from 0.48 mm/d to 0.37 mm/d. Also the correlation coefficient for this pair increases from 0.81 to 0.90. In other words, these results support the idea that averaging over space, diminishes the signal and results in larger seasonal variation than what river streams and flood plains do in smoothing the discharge time series. Therefore, to better analyze the seasonal variability of the water budget components, we should look at smaller scale variability and apply the lagging method for the larger scale.

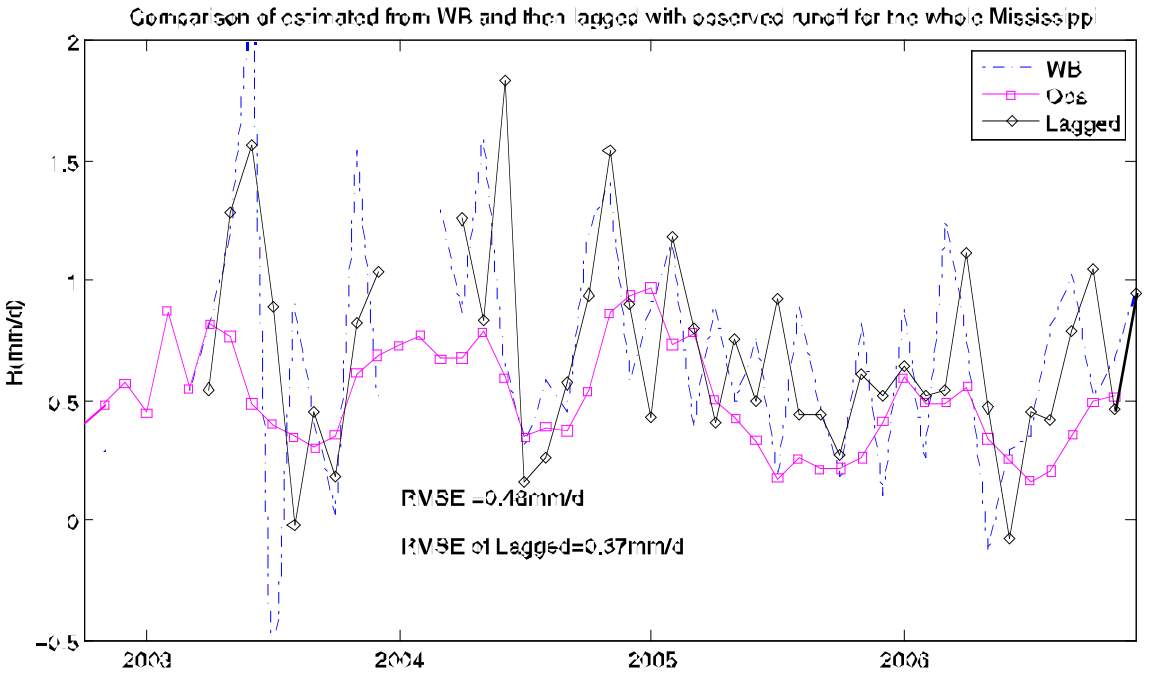

Figure 5- 10: Comparison of WB estimated total runoff and then lagged to the observed at the Vicksburg station.

These results of this study are in better agreement with runoff compared to the previous studies that used GRACE observations. The RMSE error computed based on the lagging method is 0.37 mm/d for the whole Mississippi basin, while this error for the previous studies at the same scale is 0.7 mm/d for [*Syed et al.*, 2005] and 1.3 mm/d [*Sheffield et al.*, 2009a]. Moreover, their results show that simple WB method and data sets couldn't be used to study seasonal variation of the water budget components because of large seasonal amplitude of the estimated values of R.

To evaluate the estimates of this method, we compared P from GPCP and its estimated uncertainties to the estimated P from water balance assuming 15% error in ET, R and TWSC fro GRACE (Figure 5-11). The estimated uncertainty of ET might be smaller than the assumed values, because of the calibration of the estimates to the available flux-nets at this basin. However, Runoff data does not have equal uncertainties. Especially in SBs 11 to 13 and 1-3, the quality of the data is explained by Fair in USGS website. Therefore, these uncertainty bars computed and shown in Figure 5-11 might be even larger. As seen in this figure, most of the estimates of P from GPCP are within the estimated values from WB in Mississippi basin. However, GPCP results in smaller seasonal amplitude than the estimated P in SBs 6, 8, 9, and 10. Therefore, it under-estimates peak values and over-estimates, minimum P rates.

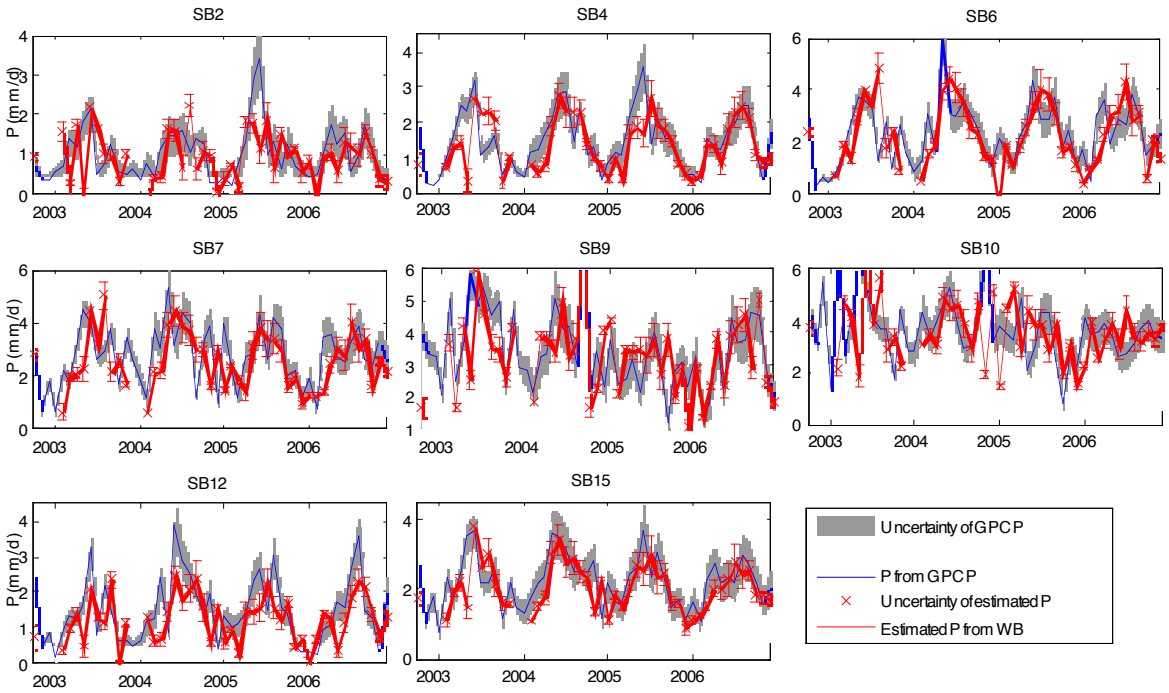

Figure 5- 11: Comparison of estimated uncertainties of P from GPCP and WB for SBs of Mississippi basin.

Figure 5-12 shows the variability of hydrological cycle in different SBs of Mississippi based on the best GPCP for P and ET-MON, TWSC from JPL-500 km smoothing radius and in-situ gage runoff data. As seen in this Figure, in some of the SBs, the magnitude of ET is more than 50% of P and in some SBs it is as large as P. Therefore, residual R does not follow seasonal variation of P, which is the driving force in estimated R over Amazon basin. The Amazon basin exhibits much smaller ET and larger TWSC variability than Mississippi basin and therefore the dynamics of water is totally different in this basin. However, the results show that this method can be used in other large scale drainage systems.

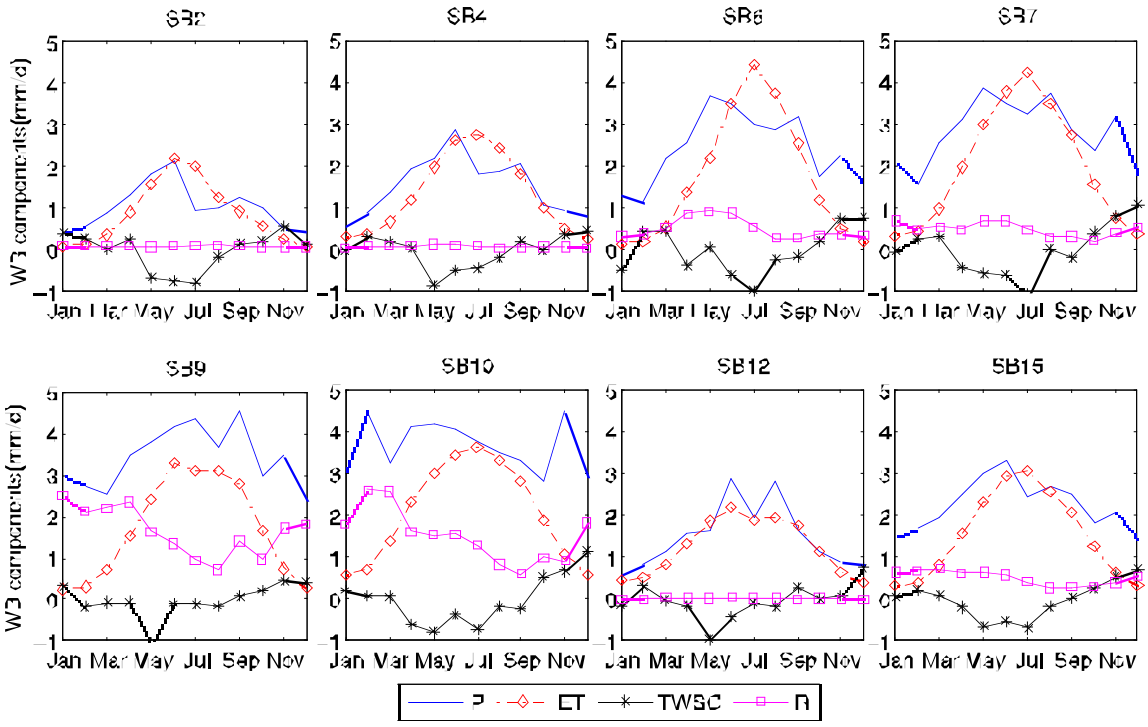

Figure 5-12. Seasonal variation of water budget components over different SBs of Mississippi

5.3. Summary and Conclusion

The water balance study is conducted for Mississippi basin that covers about half of the continuous U.S. The whole Mississippi basin is divided to 12 SBs based on topography maps and the location of gages. The water balance proposed in chapter 3 is applied on the whole Mississippi using different precipitation data sets, GRACE, and ET of university of Montana and Princeton University. The results for all combinations show larger seasonal amplitude compared to observed runoff when averaged over the whole

Mississippi basin especially in satellite only products. The differences have different characteristics in smaller scale SBs. GPCP based runoff estimated have smaller error and larger correlation coefficient than other P data. However, it results in smaller seasonal amplitude in Northern and eastern SBs where P has larger seasonal variability.

The results in large basin scale show that the variability in estimated runoff often exceeds the observed runoff (mean observed=0.54 mm/d, mean estimated from GPCP, ET-MON=0.74 mm/d, RMSE=0.57 mm/d). These differences are larger in other CMORPH and PERSIANN based estimates. [Syed, 2005 #6] obtained similar results using atmospheric moisture convergence method for the whole Mississippi basin (RMSE=0.77 mm/d). The mentioned study reports over-estimation of the peak discharge and negative low flows and interprets that as difference between the total discharge and surface water measured by gauges. Although comparison of the estimated runoff values to in-situ from this study shows that it over-estimates both in wet and dry seasons in large Mississippi basin and therefore these differences might not related to the ground water discharge but simply to the uncertainties in other components of WB.

Focusing on smaller SBs shows that these differences vary over the basin so that it depends on P rates. As monthly estimates of P increases in eastern SBs, the estimates result in negative low flows and positive peak flow. In other words, GPCP over-estimates during the dry season and under-estimates in wet season in SBs with large annual precipitation (3.5 mm/d). However, in western SBs 1 to 4, which have smaller annual P (1.25 mm/d), it over-estimates during the year. Therefore, the total discharge estimated from this method, which is averaged over the basin, will result in smoothed estimates.

This result helps to understand the characteristics of the errors, which is mainly P than other components in Mississippi basin. Also the comparison of different P estimates in Mississippi shows that, GPCP gives closer estimates to the observed runoff; but exhibits smaller seasonal variation than CMORPH and PERSIANN.

We also applied our proposed method for consideration of lag time using remotely sensed-based inundation product. Comparison of the inundation data to the observed The results after applying this method are more consistent with observed runoff. The lag time in Mississippi basin is much smaller than Amazon due to regulation of flow by dams and smaller seasonal amplitude in Runoff and storage. In other words, western SBs, which are far from the mouth of Amazon basin and have higher lag time, have larger runoff contribution to the whole. Therefore, applying the lagging results in better total runoff estimates in Amazon than Mississippi in which western SBs contribute almost zero runoff. We also constructed the precipitation for Mississippi basin based on the total of other water budget components. The results are consistent with the uncertainty of the GPCP data in all of the SBs indicating that these data sets can be used to study seasonal variability of the water budget components over Mississippi. Also, because this basin is mainly regulated, its storage variability is small, seasonal variation of up to 2 mm/d and runoff imposes variation in this component after evapotranspiration. In other words, in Amazon basin, runoff, which is not controlled here, is a function of the storage changes and therefore its variation is smaller than other components in Amazon.

CHAPTER 6: CONCLUSION AND PROSPECTIVE WORKS

This dissertation aims to explore the dynamics of water budget components in large basins using satellite data. The potential of using satellite data was investigated by incorporating different products for different water budget components. The gauge measurements are limited spatially and their temporal coverage depends on several factors. However, remote sensing observations don't have these limitations and their spatial and temporal coverage are incomparably greater, but these observations might not provide accurate measurements as direct measurements provide. Therefore, these limitations and potential of using remote sensing data have to be investigated before any applications. In introduction, some previous studies in using satellite data were presented. These studies had uncertainties about 50%. In this research, we tried to use different products to find the consistent products that are consistent with other components of the hydrological cycle. With this research, we are able to reduce this uncertainty to about 25% by using similar simple water balance method but careful analysis over Amazon. Since Amazon is a complex system, its dynamics of water budget components are not linear. Therefore it is divided to smaller sections and then the dynamics of the components between each other and spatially was studied. The other achievement of this research dissertation is looking at sub basin scale and taking into account the spatial variability of the basin. Also, the interaction of the water budget components was studied according the sub basins and the effect of different seasons in different part of the basin was explored. The possibility of constructing past water storage was examined and using

more than 23 years data, and significant trends were found in dry and wet seasons over Negro river and downstream of the Amazon river. Moreover, the proposed method was tested on another large basin (i.e. Mississippi) and promising results were found. The results and conclusions of this study are summarized in the following section.

6.1 Summary of results

6.1.1. WATER BUDGET COMPONENT ANALYSIS WITHIN THE AMAZON BASIN USING SATELLITE DATA

In chapter 3 of this dissertation, the study of diagnosing water budget components in Amazon basin was presented. This chapter focused on the spatial and seasonal variability of the water budget components of the Amazon using different combination of remote sensing data products and observed gauge measurements. GRACE and satellite based ET estimates were used to evaluate terrestrial water balance for more than four years at intra-basin and whole basin scales. We studied different datasets for precipitation and evaporation. The consistent products were selected based on better water balance results. One of the advantages of this research study is that the whole basin in this case Amazon was divided to 14 sub basins. Then, the most consistent data combination was selected for the study of dynamics using a land water balance approach and spatio-temporal consistency. The best data set for precipitation is GPCP in combination with ET data from University of Montana. The average annual rainfall for the entire basin from GPCP is 6.33 mm/d, evaporation from ET-MON is 3.28 and runoff from in-situ data is 3.06 mm/d. This method based on water balance give smaller RMSE than previous

atmospheric moisture convergence method [Syed et al., 2005] (0.61 and 1.28 mm/d respectively) over the Amazon basin and has a potential to be used to estimate discharge at different sub-parts of a large tropical basin.

The estimated runoff time series had better agreement at SB scale than the total runoff for the whole Amazon. Therefore the estimated runoff from the balance method for each SB is integrated downstream using an element-to-element routing method. An inundation data set is used to compute delay times instead of specifying flow velocities. This lag time is computed based on the maximum lag-correlation between upstream and downstream SBs. The estimated lagged runoff resolves the dynamics of the surface runoff better and can be used to estimate the runoff in different parts of the large Amazon. The monthly mean error for the whole Amazon basin decreases from 1.1 to 0.61 mm/d for the GPCP and ET-MON combination using the lagging method. This lagging method based on the TWS from GRACE and time series of inundation fractions is simple since it does not need assumptions about the channel Manning roughness and slope of the river and therefore, can be used in distributed routing models to get the hydrograph (time series) of the runoff at different locations for any large-scale watershed. In total, this study reduced the errors in water balance from %50 to less than %25.

There are diverse uncertainties among different remote sensing retrieved data that affect water balance in the basin. An error analysis was conducted to account for uncertainties in this study.

6.1.2. DYNAMICS OF THE WATER BUDGET IN AMAZON BASIN

In chapter 3, we used our conclusion in chapter 4 for the most consistent products to study the interannual and dynamics of the water budget in whole Amazon and sub basins. Study of intra-basin dynamics, based on the consistent data set, shows that the water budget components, except ET, exhibit large seasonal variations within the Amazon basin. The northwest SBs have the largest rainfall amounts, approximately 8.5 mm/d, while the southern SBs average 5 mm/d. Storage change is also very dynamic and is larger during the extreme changes of the intra-SB precipitation. For the two downstream SBs the seasonal variation is stronger during the dry and wet seasons of their upstream SBs with larger discharge contribution.

Interannual variation of the de-seasonalized anomalies of P, ET, R for a longer period of 23 years are investigated for the whole basin. During this period, there are large anomalies in all of these three components especially during ENSO events. The spatial pattern of the interannual variation of the components follows the mean annual values so that these anomalies are smaller in southern SBs and larger in northern and downstream SBs.

Seasonality is not significant in evaporation except for southern SB 8 with Savannah vegetation and in Negro and Amazon rivers as large as 0.6 mm/d as a result of decreased cloudy days and larger net radiation. This is seen in all three remote sensing based ET data sets while earlier reanalysis based ET estimates did not show this pattern. Also the effect of smoothing the GRACE data can introduce more uncertainties to the data.

Moreover, the past total water storage was constructed for more than 23 years. First, based on the most consistent products and ground measurements, the total water storage was estimated for the period of time that GRACE observations are available. The Results were compared and promising consistency was found. Then, using the same method the past total water storage (TWS) was estimated. The relationship between this past storage and surface water inundation was consistent. A trend analysis was conducted using this record. The record was not long enough to draw a firm conclusion. The results based on 23 years reveals that the dry seasons are getting drier and wet season are changing to wetter seasons, however, and the whole seasons has slightly decrease in storage.

6.1.3. WATER BUDGET ANALYSIS OF LARGE MISSISSIPPI BASIN

To examine the proposed method in chapter 4 for another large basin, we studied the water balance of Mississippi basin that covers about half of the continuous U.S. With the same procedure, the whole Mississippi basin was divided to 12 SBs based on topography maps and the location of gages. The water balance proposed in chapter 5 was applied on the whole Mississippi using different precipitation data set, GRACE, and ET of university of Montana. Preliminary results without any adjustment in delay time showed that all combinations have significant larger seasonal amplitude compared to observed runoff. Gauge adjusted estimates of GPCP and TMPA results in smaller total error and RMSE (RMSE from these two is about 0.7 mm/d compared to CMORPH and PERSIANN of 2.3 mm/d). After this step, the proposed method for accounting for the lag time using remotely sensed-based inundation product was done. The results after

applying this method are more consistent with observed runoff (RMSE decreased from 0.5 to 0.31 mm/d). Since the runoff at this basin does not have significant seasonal variation in most of the SBs of Mississippi (due to lose of the surface water by large ET at these areas), the lagged discharge from different SBs will be different than averaged over the whole. Therefore, once again, the proposed method works in another mid-latitude basin not because of larger seasonal variation of P, and as a result runoff, from different SBs and larger water path, but also because of the larger seasonal variation of ET and smaller variability of TWSC in eastern parts. The results of estimated runoff in SB scale are consistent with observed values similar to the Amazon basin. Mississippi observes much smaller annual P than Amazon and therefore, gives even smaller runoff values. However, the proposed simple water balance method using satellite data and applying lagging method, gives consistent results with relative error of 36% (15% in Amazon). The total error in the estimated values from this study in Mississippi is 0.22 mm/d compare to the 0.45 mm/d in Amazon.

6.2. Prospective works and remaining issues

As it was mentioned in previous sections, the remote sensing data sets still have significant uncertainties compared to ground measurements because of their different measurements and spatial resolution. However because of their spatial and temporal sampling advantage, we are able to study dynamics of the water in very large basin. Improvements in remote sensing products especially time resolution, may come from the future GPM for precipitation, soil moisture from SMOS and SMAP, and runoff from the SWOT mission and may help reduce the uncertainties in the water budget and increase

the knowledge of dynamics at finer time scales over the tropics. Also, other procedures for analyzing GRACE data might help to reduce noises and attenuation effects of smoothing of the data sets.

The results presented in chapter 5 are preliminary as our main focus in this research study is Amazon basin. We plan to extend our water budget analysis for Mississippi basin more carefully to investigate the inconsistency that was found in this study. Also, the variation of water components, spatially and temporally, will be tried to find the features of this large basin and its relationship with other hydro climate studies.

The relationship between large basins and their interaction could be possible with extending the present study. For instance, Congo basin which we already have some of its preliminary results (was not presented in this dissertation) is another large and important tropical basin. Discovering the dynamics and the interactions between Amazon and Congo in continental scale would be interesting.

Some improvements in the algorithm of present water budget components can reduce the uncertainties of the water balance. For instance, inclusion of open waters in estimation ET might reduce the uncertainties of this component.

6.3. Conclusions

In this research study, there were some important lessons in research studies using satellite data sets. First, evaluating different products could help us to have a better picture of these data sets. Examining different components of the water budget with just using satellite observations was interesting that could reveal the consistency of the

product in an application, which was water balance study. It was shown that although remote sensing data may not provide accurate estimates of water budget components, they still have an excellent spatial and temporal coverage that could be used for variety of applications. Some errors, uncertainties, and limitation of these satellite measurements were discussed. Using other source information to improve our study was part of novelty of this research. The inundation product as representative of amount of surface water was incorporated to mitigate the discrepancies in water balance study due to delay time. The results could improve the analysis. Moreover, looking in sub-basin scale improved the water balance studies and the sub basins that couldn't satisfy the water balance was found. The different wet and dry season of the whole Amazon basin at different sub basin was interesting that explained some dynamics of water in the whole basin. Using the proposed consistent products, the past total storage was estimated for more than 20 years. This showed the capabilities of remote sensing data for applications that need longer record of data such as trend analysis.

Comparing the characteristics of the errors in different SBs of both basins shows that P is the most uncertain component of the water budget. Inundation data set used in this study for evaluation of the estimated values can be used in future studies to calibrate the estimates in order to reduce the uncertainties in estimated runoff.

BIBLIOGRAPHY

Adler, R. F., et al. (2003), The version-2 global precipitation climatology project (GPCP) monthly precipitation analysis (1979-present), *J. Hydrometeorol.*, *4*(6), 1147-1167.

AghaKouchak, A., N. Nasrollahi, J. J. Li, B. Imam, and S. Sorooshian (2011a), Geometrical Characterization of Precipitation Patterns, *J. Hydrometeorol.*, *12*(2), 274-285.

AghaKouchak, A., A. Behrangi, S. Sorooshian, K. Hsu, and E. Amitai (2011b), Evaluation of satellite-retrieved extreme precipitation rates across the central United States, *J. Geophys. Res.-Atmos.*, *116*.

Alsdorf, D., P. Bates, J. Melack, M. Wilson, and T. Dunne (2007), Spatial and temporal complexity of the Amazon flood measured from space, *Geophys. Res. Lett.*, *34*(8).

Alsdorf, D. E. (2003), Water storage of the central Amazon floodplain measured with GIS and remote sensing imagery, *Annals of the Association of American Geographers*, *93*(1), 55-66.

Alsdorf, D. E., and D. P. Lettenmaier (2003), Tracking fresh water from space, *Science*, *301*(5639), 1491-+.

Azarderakhsh, M., W. B. Rossow, F. Papa, and R. Khanbilvardi (2011), Diagnosing water variations within the Amazon basin using satellite data, *J. Geophys. Res.*, *Under review*.

Bastiaanssen, W. G. M., M. Menenti, R. A. Feddes, and A. A. M. Holtslag (1998), A remote sensing surface energy balance algorithm for land (SEBAL) - 1. Formulation, *J. Hydrol.*, *213*(1-4), 198-212.

Becker, M., B. Meyssignac, L. Xavier, R. Alkama, and B. Decharme (2011), Past terrestrial water storage (1980–2008)

in the Amazon Basin reconstructed from

GRACE and in situ river gauging data, *Hydrol. Earth Syst. Sci.*, *15*(2).

Betts, A. K. (2007), Coupling of water vapor convergence, clouds, precipitation, and land-surface processes, *J. Geophys. Res.-Atmos.*, *112*(D10).

Betts, A. K., and M. A. o. F. Silva Dias (2010), Progress in understanding land-surface-atmosphere coupling from LBA research, *Journal of Advances in Modeling Earth Systems*, *2*(Art. #6), 20 pp.

Bjerklie, D. M., S. L. Dingman, C. J. Vorosmarty, C. H. Bolster, and R. G. Congalton (2003), Evaluating the potential for measuring river discharge from space, *Journal of Hydrology*, *278*(1-4), 17-38.

Brubaker, K. L., D. Entekhabi, and P. S. Eagleson (1993), ESTIMATION OF CONTINENTAL PRECIPITATION RECYCLING, *Journal of Climate*, *6*(6), 1077-1089.

Bruno, R. D., H. R. da Rocha, H. C. de Freitas, M. L. Goulden, and S. D. Miller (2006), Soil moisture dynamics in an eastern Amazonian tropical forest, *Hydrological Processes*, *20*(12), 2477-2489.

Bullock, A., and M. Acreman (2003), The role of wetlands in the hydrological cycle, *Hydrology and Earth System Sciences*, *7*(3), 358-389.

Caparrini, F., F. Castelli, and D. Entekhabi (2004), Estimation of surface turbulent fluxes through assimilation of radiometric surface temperature sequences, *Journal of Hydrometeorology*, *5*(1), 145-159.

Chen, J., C. Wilson, J. Famiglietti, and M. Rodell (2007), Attenuation effect on seasonal basin-scale water storage changes from GRACE time-variable gravity, *J. Geodesy*, *81*(4), 237-245.

Chen, J. L., C. R. Wilson, and B. D. Tapley (2010), The 2009 exceptional Amazon flood and interannual terrestrial water storage change observed by GRACE, *Water Resour. Res.*, *46*.

Chen, T. C., J. H. Yoon, K. J. St Croix, and E. S. Takle (2001), Suppressing impacts of the Amazonian deforestation by the global circulation change, *Bulletin of the American Meteorological Society*, *82*(10), 2209-2216.

Coe, M. T., M. H. Costa, A. Botta, and C. Birkett (2002), Long-term simulations of discharge and floods in the Amazon Basin, *J. Geophys. Res.-Atmos.*, *107*(D20).

Costa, M. H., and J. A. Foley (1997), Water balance of the Amazon Basin: Dependence on vegetation cover and canopy conductance, *J. Geophys. Res.-Atmos.*, *102*(D20), 23973-23989.

Costa, M. H., and J. A. Foley (1999), Trends in the hydrologic cycle of the Amazon basin, *J. Geophys. Res.-Atmos.*, *104*(D12), 14189-14198.

da Rocha, H. R., M. L. Goulden, S. D. Miller, M. C. Menton, L. Pinto, H. C. de Freitas, and A. Figueira (2004), Seasonality of water and heat fluxes over a tropical forest in eastern Amazonia, *Ecol. Appl.*, *14*(4), S22-S32.

da Rocha, H. R., et al. (2009), Patterns of water and heat flux across a biome gradient from tropical forest to savanna in Brazil, *J. Geophys. Res.-Biogeo.*, *114*.

Dai, A., and K. E. Trenberth (2002), Estimates of freshwater discharge from continents: Latitudinal and seasonal variations, *J. Hydrometeorol.*, *3*(6), 660-687.

Decharme, B., H. Douville, C. Prigent, F. Papa, and F. Aires (2008), A new river flooding scheme for global climate applications: Off-line evaluation over South America, *J. Geophys. Res.-Atmos.*, *113*(D11).

Dirmeyer, P. A., A. J. Dolman, and N. Sato (1999), The pilot phase of the Global Soil Wetness Project, *Bulletin of the American Meteorological Society*, *80*(5), 851-878.

Eltahir, E. A. B., and R. L. Bras (1994), PRECIPITATION RECYCLING IN THE AMAZON BASIN, *Quarterly Journal of the Royal Meteorological Society*, *120*(518), 861-880.

Engman, E. T., and N. Chauhan (1995), Status of Microwave Soil-Moisture Measurements with Remote-Sensing, *Remote Sensing of Environment*, *51*(1), 189-198.

Fekete, B. M., C. J. Voro smarty, and W. Grabs (1999), Global, Composite Runoff Fields Based on Observed River Discharge and Simulated Water Balances, *Tech Report, Global Runoff Data Centre, Germany*.

Fekete, B. M., C. J. Vorosmarty, and W. Grabs (2002), High-resolution fields of global runoff combining observed river discharge and simulated water balances, *Global Biogeochemical Cycles*, *16*(3).

Fisher, J. B., K. P. Tu, and D. D. Baldocchi (2008), Global estimates of the land-atmosphere water flux based on monthly AVHRR and ISLSCP-II data, validated at 16 FLUXNET sites, *Remote Sensing of Environment*, *112*(3), 901-919.

Frappart, F., F. Papa, J. S. Famiglietti, C. Prigent, W. B. Rossow, and F. Seyler (2008), Interannual variations of river water storage from a multiple satellite approach: A case study for the Rio Negro River basin, *J. Geophys. Res.-Atmos.*, *113*(D21).

Frappart, F., F. Papa, A. Guntner, S. Werth, G. Ramillien, C. Prigent, W. B. Rossow, and M. P. Bonnet (2010), Interannual variations of the terrestrial water storage in the Lower Ob' Basin from a multisatellite approach, *Hydrol. Earth Syst. Sci.*, *14*(12), 2443-2453.

Getirana, A. C. V., Bonnet, M.-P., Rotunno Filho, O. C., Collischonn, W., Guyot, J.-L., Seyler, F. , Mansur, W. J. (2010), Hydrological modelling and water balance of the Negro river basin: evaluation based on in situ and spatial altimerty data,, *Hydrol. Process.*, *n/a. doi: 10.1002/hyp.7747*.

Gibson, J. K., P. Kållberg, S. Uppala, A. Nomura, A. Hernandez, and E. Serrano (1997), ERA Description. ECMWF Re-Analysis Final Report Series,

, 1, 71pp.

Goulden, M. L., S. D. Miller, H. R. da Rocha, M. C. Menton, H. C. de Freitas, A. Figueira, and C. A. D. de Sousa (2004), Diel and seasonal patterns of tropical forest CO2 exchange, *Ecol. Appl.*, *14*(4), S42-S54.

Gu, G. J., R. F. Adler, G. J. Huffman, and S. Curtis (2007), Tropical rainfall variability on interannual-to-interdecadal and longer time scales derived from the GPCP monthly product, *J. Climate*, *20*(15), 4033-4046.

Hsu, K., X. Gao, S. Sorooshian, and H. V. Gupta (1997), Precipitation estimation from remotely sensed information using artificial neural networks, *J. Appl. Meteorol.*, *36*, 1176-1190.

Huffman, G. J., R. F. Adler, D. T. Bolvin, and G. J. Gu (2009), Improving the global precipitation record: GPCP Version 2.1, *Geophys. Res. Lett.*, *36*.

Huffman, G. J., R. F. Adler, D. T. Bolvin, G. J. Gu, E. J. Nelkin, K. P. Bowman, Y. Hong, E. F. Stocker, and D. B. Wolff (2007), The TRMM multisatellite precipitation analysis (TMPA): Quasi-global, multiyear, combined-sensor precipitation estimates at fine scales, *J. Hydrometeorol.*, *8*(1), 38-55.

Jimenez, C., et al. (2010), Global inter-comparison of 12 land surface heat flux estimates, *J. Geophys. Res.*, *submitted*.

Joyce, R. J., J. E. Janowiak, P. A. Arkin, and P. P. Xie (2004), CMORPH: A method that produces global precipitation estimates from passive microwave and infrared data at high spatial and temporal resolution, *J. Hydrometeorol.*, *5*(3), 487-503.

Kalma, J. D., T. R. McVicar, and M. F. McCabe (2008), Estimating Land Surface Evaporation: A Review of Methods Using Remotely Sensed Surface Temperature Data, *Surveys in Geophysics*, *29*(4-5), 421-469.

Kanamitsu, M., W. Ebisuzaki, J. Woollen, S. K. Yang, J. J. Hnilo, M. Fiorino, and G. L. Potter (2002), NCEP-DOE AMIP-II reanalysis (R-2), *Bulletin of the American Meteorological Society*, *83*(11), 1631-1643.

Koster, R. D., et al. (2004), Regions of strong coupling between soil moisture and precipitation, *Science*, *305*(5687), 1138-1140.

Kumar, S. V., et al. (2006), Land information system: An interoperable framework for high resolution land surface modeling, *Environmental Modelling & Software*, *21*(10), 1402-1415.

Labraga, J. C., O. Frumento, and M. Lopez (2000), The atmospheric water vapor cycle in South America and the tropospheric circulation, *J. Climate*, *13*(11), 1899-1915.

Leopoldo, P. R., W. Franken, E. Salati, and M. N. Ribeiro (1987), TOWARDS A WATER-BALANCE IN THE CENTRAL AMAZONIAN REGION, *Experientia*, *43*(3), 222-233.

Marengo, J. A. (2004), Interdecadal variability and trends of rainfall across the Amazon basin, *Theoretical and Applied Climatology*, *78*(1-3), 79-96.

Marengo, J. A. (2005), Characteristics and spatio-temporal variability of the Amazon River Basin Water Budget, *Climate Dynamics*, *24*(1), 11-22.

Marengo, J. A. (2006), ON THE HYDROLOGICAL CYCLE OF THE AMAZON BASIN:

A HISTORICAL REVIEW AND CURRENT STATE-OF-THE-ART, *Revista Brasileira de Meteorologia*, *21*(3), 1-19.

Marengo, J. A., C. A. Nobre, J. Tomasella, M. D. Oyama, G. S. De Oliveira, R. De Oliveira, H. Camargo, L. M. Alves, and I. F. Brown (2008), The drought of Amazonia in 2005, *J. Climate*, *21*(3), 495-516.

Matsuyama, H. (1992), THE WATER-BUDGET IN THE AMAZON RIVER BASIN DURING THE FGGE PERIOD, *Journal of the Meteorological Society of Japan*, *70*(6), 1071-1084.

Molion, L. C. B. (1990), CLIMATE VARIABILITY AND ITS EFFECTS ON AMAZONIAN HYDROLOGY, *Interciencia*, *15*(6), 367-372.

Monteith, J. L. (1965), Evaporation and environment, *Symp Soc Exp Biol*, *19*, 205-234.

Mu, Q., F. A. Heinsch, M. Zhao, and S. W. Running (2007), Development of a global evapotranspiration algorithm based on MODIS and global meteorology data, *Remote Sensing of Environment*, *111*, 519-536.

Nemani, R. R., and S. W. Running (1989), ESTIMATION OF REGIONAL SURFACE-RESISTANCE TO EVAPOTRANSPIRATION FROM NDVI AND THERMAL-IR AVHRR DATA, *J. Appl. Meteorol.*, *28*(4), 276-284.

Nishida, K., R. R. Nemani, J. M. Glassy, and S. W. Running (2003), Development of an evapotranspiration index from aqua/MODIS for monitoring surface moisture status, *Ieee Transactions on Geoscience and Remote Sensing*, *41*(2), 493-501.

Norman, J. M., W. P. Kustas, and K. S. Humes (1995), SOURCE APPROACH FOR ESTIMATING SOIL AND VEGETATION ENERGY FLUXES IN OBSERVATIONS OF DIRECTIONAL RADIOMETRIC SURFACE-TEMPERATURE, *Agricultural and Forest Meteorology*, *77*(3-4), 263-293.

Papa, F., C. Prigent, and W. B. Rossow (2008a), Monitoring Flood and Discharge Variations in the Large Siberian Rivers From a Multi-Satellite Technique, *Surveys in Geophysics*, *29*(4-5), 297-317.

Papa, F., A. Guntner, F. Frappart, C. Prigent, and W. B. Rossow (2008b), Variations of surface water extent and water storage in large river basins: A comparison of different global data sources, *Geophys. Res. Lett.*, *35*(11).

Papa, F., C. Prigent, F. Aires, C. Jimenez, W. B. Rossow, and E. Matthews (2010a), Interannual variability of surface water extent at the global scale, 1993-2004, *Journal of Geophysical Research-Atmospheres*, *115*.

Papa, F., C. Prigent, F. Aires, C. Jimenez, W. B. Rossow, and E. Matthews (2010b), Interannual variability of surface water extent at the global scale, 1993-2004, *J. Geophys. Res.-Atmos.*, *115*, 17.

Perry, G. D., P. B. Duffy, and N. L. Miller (1996), An extended data set of river discharges for validation of general circulation models, *J. Geophys. Res.-Atmos.*, *101*(D16), 21339-21349.

Priestlr.Ch, and R. J. Taylor (1972), ASSESSMENT OF SURFACE HEAT-FLUX AND EVAPORATION USING LARGE-SCALE PARAMETERS, *Monthly Weather Review*, *100*(2), 81-&.

Prigent, C., F. Papa, F. Aires, W. B. Rossow, and E. Matthews (2007), Global inundation dynamics inferred from multiple satellite observations, 1993-2000, *J. Geophys. Res.-Atmos.*, *112*(D12).

Rabus, B., M. Eineder, A. Roth, and R. Bamler (2003), The shuttle radar topography mission - a new class of digital elevation models acquired by spaceborne radar, *Isprs Journal of Photogrammetry and Remote Sensing*, *57*(4), 241-262.

Rao, V. B., I. F. A. Cavalcanti, and K. Hada (1996), Annual variation of rainfall over Brazil and water vapor characteristics over South America, *J. Geophys. Res.-Atmos.*, *101*(D21), 26539-26551.

Rasmusso.Em (1968), Atmospheric Water Vapor Transport and Water Balance of North America .2. Large-Scale Water Balance Investigations, *Monthly Weather Review*, *96*(10), 720-&.

Richey, J. E., R. H. Meade, E. Salati, A. H. Devol, C. F. Nordin, and U. Dossantos (1986), WATER DISCHARGE AND SUSPENDED SEDIMENT CONCENTRATIONS IN THE AMAZON RIVER 1982-1984, *Water Resour. Res.*, *22*(5), 756-764.

Roads, J., M. Kanamitsu, and R. Stewart (2002), CSE water and energy budgets in the NCEP-DOE Reanalysis II, *J. Hydrometeorol.*, *3*(3), 227-248.

Roads, J. O., S. Chen, A. K. Guetter, and K. P. Georgakakos (1994), Large-Scale Aspects of the United-States Hydrologic-Cycle, *Bulletin of the American Meteorological Society*, *75*(9), 1589-1610.

Rodell, M., and J. S. Famiglietti (1999), Detectability of variations in continental water storage from satellite observations of the time dependent gravity field, *Water Resour. Res.*, *35*(9), 2705-2723.

Rodell, M., J. S. Famiglietti, J. Chen, S. I. Seneviratne, P. Viterbo, S. Holl, and C. R. Wilson (2004a), Basin scale estimates of evapotranspiration using GRACE and other observations, *Geophys. Res. Lett.*, *31*(20).

Rodell, M., et al. (2004b), The global land data assimilation system, *Bulletin of the American Meteorological Society*, *85*(3), 381-+.

Salati, E., J. Marques, and L. C. B. Molion (1978), ORIGIN AND DISTRIBUTION OF RAIN IN AMAZON BASIN, *Interciencia*, *3*(4), 200-205.

Salati, E., A. Dallolio, E. Matsui, and J. R. Gat (1979), RECYCLING OF WATER IN THE AMAZON BASIN - ISOTOPIC STUDY, *Water Resour. Res.*, *15*(5), 1250-1258.

Seneviratne, S. I., P. Viterbo, D. Luthi, and C. Schar (2004), Inferring changes in terrestrial water storage using ERA-40 reanalysis data: The Mississippi River basin, *J. Climate*, *17*(11), 2039-2057.

Seo, K. W., and C. R. Wilson (2005), Simulated estimation of hydrological loads from GRACE, *J. Geodesy*, *78*(7-8), 442-456.

Sheffield, J., E. F. Wood, and F. Munoz-Arriola (2010), Long-Term Regional Estimates of Evapotranspiration for Mexico Based on Downscaled ISCCP Data, *J. Hydrometeorol.*, *11*(2), 253-275.

Sheffield, J., C. R. Ferguson, T. J. Troy, E. F. Wood, and M. F. McCabe (2009a), Closing the terrestrial water budget from satellite remote sensing, *Geophys. Res. Lett.*, *36*, 5.

Sheffield, J., C. R. Ferguson, T. J. Troy, E. F. Wood, and M. F. McCabe (2009b), Closing the terrestrial water budget from satellite remote sensing, *Geophysical Research Letters*, *36*.

Sorooshian, S., et al. (2010), Advanced Concepts on Remote Sensing of Precipitation at Multiple Scales, *Bulletin of the American Meteorological Society*.

Su, Z. (2002), The Surface Energy Balance System (SEBS) for estimation of turbulent heat fluxes, *Hydrology and Earth System Sciences*, *6*(1), 85-99.

Swenson, S., and J. Wahr (2006), Post-processing removal of correlated errors in GRACE data, *Geophys. Res. Lett.*, *33*(8).

Swenson, S., J. Wahr, and P. C. D. Milly (2003), Estimated accuracies of regional water storage variations inferred from the Gravity Recovery and Climate Experiment (GRACE), *Water Resour. Res.*, *39*(8).

Syed, T. H., J. S. Famiglietti, and D. P. Chambers (2009), GRACE-Based Estimates of Terrestrial Freshwater Discharge from Basin to Continental Scales, *J. Hydrometeorol.*, *10*(1), 22-40.

Syed, T. H., J. S. Famiglietti, J. Chen, M. Rodell, S. I. Seneviratne, P. Viterbo, and C. R. Wilson (2005), Total basin discharge for the Amazon and Mississippi River basins from GRACE and a land-atmosphere water balance, *Geophys. Res. Lett.*, *32*(24).

Tang, Q. H., H. L. Gao, P. Yeh, T. Oki, F. G. Su, and D. P. Lettenmaier (2010), Dynamics of Terrestrial Water Storage Change from Satellite and Surface Observations and Modeling, *J. Hydrometeorol.*, *11*(1), 156-170.

Villar, J. C. E., J. Ronchail, J. L. Guyot, G. Cochonneau, F. Naziano, W. Lavado, E. De Oliveira, R. Pombosa, and P. Vauchel (2009,b), Spatio-temporal rainfall variability in the Amazon basin countries (Brazil, Peru, Bolivia, Colombia, and Ecuador), *Int. J. Climatol.*, *29*(11), 1574-1594.

Villar, J. C. E., J. L. Guyot, J. Ronchail, G. Cochonneau, N. Filizola, P. Fraizy, D. Labat, E. de Oliveira, J. J. Ordonez, and P. Vauchel (2009,a), Contrasting regional discharge evolutions in the Amazon basin (1974-2004), *J. Hydrol.*, *375*(3-4), 297-311.

Vorosmarty, C. J., C. J. Willmott, B. J. Choudhury, A. L. Schloss, T. K. Stearns, S. M. Robeson, and T. J. Dorman (1996), Analyzing the discharge regime of a large tropical

river through remote sensing, ground-based climatic data, and modeling, *Water Resour. Res.*, *32*(10), 3137-3150.

Wahr, J., S. Swenson, V. Zlotnicki, and I. Velicogna (2004), Time-variable gravity from GRACE: First results, *Geophys. Res. Lett.*, *31*(11).

Wang, K., R. E. Dickinson, M. Wild, and S. Liang (2010), Evidence for Decadal Variation in Global Terrestrial Evapotranspiration between 1982 and 2002, Part 1: Model Development, *J. Geophys. Res.*, *in review*.

Willmott, C. J., C. M. Rowe, and Y. Mintz (1985), CLIMATOLOGY OF THE TERRESTRIAL SEASONAL WATER CYCLE, *J. Climatol.*, *5*(6), 589-606.

Yirdaw, S. Z., K. R. Snelgrove, and C. O. Agboma (2008), GRACE satellite observations of terrestrial moisture changes for drought characterization in the Canadian Prairie, *J. Hydrol.*, *356*(1-2), 84-92.

Zeng, N. (1999), Seasonal cycle and interannual variability in the Amazon hydrologic cycle, *J. Geophys. Res.-Atmos.*, *104*(D8), 9097-9106.

Zeng, N., J. H. Yoon, A. Mariotti, and S. Swenson (2008a), Variability of basin-scale terrestrial water storage from a PER water budget method: The Amazon and the Mississippi, *J. Climate*, *21*(2), 248-265.

Zeng, N., J. H. Yoon, J. A. Marengo, A. Subramaniam, C. A. Nobre, A. Mariotti, and J. D. Neelin (2008b), Causes and impacts of the 2005 Amazon drought, *Environmental Research Letters*, *3*(1).

Zhang, K., J. S. Kimball, R. R. Nemani, and S. W. Running (2010), A continuous satellite-derived global record of land surface evapotranspiration from 1983 to 2006, *Water Resour. Res.*, *46*.